UNIVERSITÉ DE MONTRÉAL

DEVELOPMENT OF POLYMER NANOCOMPOSITES FROM RENEWABLE CELLULOSE NANOCRYSTALS

DAVOOD BAGHERIASL

DÉPARTEMENT DE GÉNIE CHIMIQUE

ÉCOLE POLYTECHNIQUE DE MONTRÉAL

THÈSE PRÉSENTÉE EN VUE DE L'OBTENTION

DU DIPLÔME DE PHILOSOPHIAE DOCTOR

(GÉNIE CHIMIQUE)

JANVIER 2016

UNIVERSITÉ DE MONTRÉAL

ÉCOLE POLYTECHNIQUE DE MONTRÉAL

Cette thèse intitulée:

DEVELOPMENT OF POLYMER NANOCOMPOSITES FROM RENEWABLE CELLULOSE NANOCRYSTALS

présentée par : BAGHERIASL Davood

en vue de l'obtention du diplôme de : Philosophiae Doctor

a été dûment acceptée par le jury d'examen constitué de :

M. TAVARES Jason-Robert., Ph. D., président

M. CARREAU Pierre, Ph. D., membre et directeur de recherche

M. DUBOIS Charles, Ph. D., membre et codirecteur de recherche

M. RIEDL Bernard, Ph. D., membre et codirecteur de recherche

M. AJJI Abdellah, Ph. D., membre

M. HUNEAULT Michel, Ph. D., membre

DEDICATION

To my beloved spouse Fatemeh

ACKNOWLEDGEMENTS

I would like to express my deep gratitude to my supervisor, Professor Pierre J. Carreau, and my co-supervisors, Professors Charles Dubois and Bernard Riedl. Success of this project was impossible without their extensive supports, encouragements, knowledge, patience and experiences.

Besides my supervisors, I would like to thank the rest of my thesis committee, namely Professor Abdellah Ajji, Professor Michel Huneault and Professor Jason-Robert Tavares for accepting to evaluate my thesis.

A sincere appreciation goes to Professor Marie-Claude Heuzey and Dr. Wadood Y. Hamad, and all the student members of the Rheology Group who have generously shared their knowledge and experiences with me during the productive discussions.

I acknowledge the help and kind cooperation of technical and administrative staffs of Chemical Engineering Department of Polytechnique Montréal during my PhD, especially Mélina Hamdine, Guillaume Lessard, Martine Lamarche, Gino Robin and Valerie Baudart.

I would like to thank Mrs. Mounia Arkoun for her kind help in translating abstract of this thesis to French.

I would like to thank Professor Hossein Nazockdast, my supervisor in Amirkabir University of Technology (Tehran Polytechnic), who taught me great scientific and life lessons.

I would like to convey my heartfelt thanks to all my friends and colleagues who have supported and helped me during my PhD studies and my life in Montréal.

Definitely, my accomplishments throughout my life would not have been possible without unconditional love and support of my beloved parents and brothers.

Finally, my deepest gratitude goes to my lovely spouse, Fatemeh. There will never be a right word to express my feeling of appreciation for everything she has done. With all my heart, I would like to express my undying gratitude and love to her for the overwhelming support she has provided and for sacrifices she has made throughout the past eight years of my life. Thank you for being my best friend. I owe you everything.

RÉSUMÉ

L'utilisation de la cellulose nanocristalline (CNC) comme agent de renfort dans les polymères est en croissance; toutefois, cela reste limité à quelques polymères hydrosolubles ou sous forme de latex. La plupart des polymères industriels communs étant insolubles dans l'eau, par conséquent, la CNC hydrophile ne peut être dispersée dans des matrices polymères hydrophobes. Une compatibilisation ou une modification de surface sont donc nécessaires pour obtenir une bonne dispersion et, de ce fait, améliorer les propriétés des polymères.

Dans ce projet de recherche, notre objectif était de développer des nanocomposites polymère-CNC avec une structure bien dispersée et des propriétés améliorées, comparativement aux polymères non modifiés ou avec de faibles charges de CNC. À cet effet, nous avons choisi le polypropylène (PP), une des polyoléfines les plus communément utilisées dans l'industrie, et le polylactide (PLA), le biopolymère ayant suscité le plus d'intérêt dans l'industrie. Par conséquent, notre étude a été divisée en deux grandes parties.

La première phase du projet portait sur le développement des nanocomposites PP-CNC. Pour favoriser une meilleure dispersion et mouillage des CNC hydrophiles dans la matrice de PP hydrophobe, un poly(éthylène-co-vinyle alcool) a été utilisé comme compatibilisant via une méthode de préparation d'un mélange maître (masterbatch). Deux mélanges maîtres différents ont été préparés, l'un en solution et l'autre à l'état fondu, avec un rapport CNC/compatibilisant de 1/3. Les nanocomposites ont été ensuite préparés par homogénéisation à l'état fondu des mélanges maîtres avec le PP, et avec une teneur en CNC de 5% en poids. Un mélangeur interne a été utilisé à cet effet. Pour des fins de comparaison, du PP contenant 15% en poids d'agent compatibilisant et du PP contenant 5% en poids de CNC ont également été préparés par mélange direct à l'état fondu.

Par la suite, l'effet de la CNC sur les propriétés rhéologiques, mécaniques et thermiques du PP a été étudié. Les observations en microscopie électronique à balayage ont montré la disparition de gros agglomérats après ajout du compatibilisant. La viscosité complexe et le module de conservation des échantillons nanocomposites compatibilisés et obtenus avec la méthode en solution ont été augmentés à basses fréquences, comparativement aux nanocomposites non compatibilisés. De plus, un maximum suivi d'une décroissance (overshoot) prononcé de la viscosité transitoire, dans un test de croissance de la contrainte en cisaillement a été observé pour

le nanocomposite compatibilisé. Le module d'Young a augmenté jusqu'à près de 47% par rapport au PP seul; la résistance à la rupture en traction est restée inchangée et l'allongement à la rupture a diminué pour le nanocomposite compatibilisé. Le module de conservation du PP à température ambiante dans une analyse thermique mécanique dynamique (DMTA) a augmenté jusqu'à près de 60%, quand une bonne dispersion a été atteinte en utilisant l'agent compatibilisant. L'effet de nucléation de la CNC sur la cristallisation du PP a été confirmé par l'augmentation de la cristallinité du nanocomposite PP et par l'augmentation de la température de cristallisation après l'ajout du compatibilisant. Ces observations ont été attribuées à l'efficacité du poly(éthylène-co-vinyle alcool) comme un agent de compatibilisation et ce, en particulier lorsque le mélange maître a été préparé en solution.

La deuxième phase du projet a focalisé sur le développement de bio-nanocomposites PLA-CNC à haute performance. Une simple et nouvelle méthode de coulée utilisant un solvant polaire (N,N-diméthylformamide) a été utilisée pour favoriser une bonne dispersion de la CNC hydrophile dans une matrice PLA à différentes charges de CNC, sans toutefois la nécessité de modifier la CNC ni d'utiliser un compatibilisant. Par la suite, l'effet de la CNC sur les propriétés du PLA a été étudié à l'état fondu et à l'état solide. La microscopie électronique à transmission a révélé l'existence d'une structure bien dispersée de la CNC dans la matrice de PLA. La viscosité complexe et les modules de conservation et de perte ont augmenté de manière significative par l'incorporation de 1% en poids et plus de CNC, en particulier à basses fréquences. Ces améliorations ont été attribuées à la formation d'un réseau interconnecté de la CNC dans la matrice PLA. Le seuil de percolation rhéologique a été établi à 0,68% en poids de CNC. En outre, la viscosité en régime permanent, la contrainte de cisaillement et la première différence des contraintes normales ont augmentés. Le seuil apparent des contraintes a également augmenté avec la teneur en CNC, aussi bien en SAOS qu'en cisaillement en régime permanent. La règle de Cox-Merz n'était pas valable pour les nanocomposites PLA-CNC; Toutefois, pour les nanocomposites à contenu élevé en CNC, la règle de Cox-Merz étendue était applicable. Des maxima prononcés suivis d'une décroissance (overshoots) ont été observés en cisaillement transitoire et pour des écoulements dans un sens et le sens inverse. Ces maxima suivis d'une décroissance (overshoots) ainsi que la reprise de structure suite à des pré-cisaillements ont été expliqués par la formation d'un réseau et par le rôle important du mouvement Brownien pour

rétablir la structure. Les nanocomposites moins concentrés pré-cisaillés à des taux plus élevés ont nécessité des temps plus longs pour rétablir leur structure initiale, après l'arrêt du cisaillement.

Les propriétés rhéologiques ont démontré l'efficacité de la sonication pour disperser la CNC et par conséquent, pour former un réseau interconnecté de CNC dans la matrice PLA. Le module d'Young des nanocomposites a augmenté jusqu'à environ 23% comparativement au PLA seul; cependant, la déformation à la rupture a légèrement diminué et la contrainte en traction quant à elle est demeurée inchangée. En DMTA, le module de conservation des nanocomposites PLA-CNC a augmenté jusqu'à près de 74% dans la région vitreuse et jusqu'à près de 490% dans la région caoutchoutique. L'augmentation de la cristallinité du PLA dans les nanocomposites et le déplacement de la température de cristallisation vers des valeurs plus élevées ont été attribués à l'effet de nucléation de la CNC sur la cristallisation du PLA.

A notre connaissance, il s'agit de la première fois qu'une aussi bonne dispersion de la CNC dans un polymère non hydrosoluble est obtenue et que de telles améliorations dans les propriétés des nanocomposites à l'état solide et fondu sont atteintes, sans aucun changement dans la structure morphologique de la CNC ou l'utilisation de compatibilisants. En outre, au meilleur de notre connaissance, ceci est la première étude fondamentale du comportement rhéologique des nanocomposites PLA-CNC dans différents modes d'écoulement en cisaillement.

ABSTRACT

The application of cellulose nanocrystals (CNCs) as reinforcing agents in polymers have grown, but limited to a few water-soluble polymers or polymers in latex form. However, most of the common polymers in industry are non water-soluble. Therefore, the hydrophilic CNCs cannot be dispersed in hydrophobic polymer matrices and surface modification or compatibilization are necessary to achieve a good dispersion and, consequently, to enhance the properties of polymers.

In this research project our objective was to develop polymer-CNC nanocomposites with a dispersed structure and enhanced properties, relative to the neat polymers, at low CNC loadings. To this end, we selected as matrices polypropylene (PP), which is one the most commonly polyolefins, and polylactide (PLA), which has attracted the largest interest among the biopolymers in industry. The research project was conducted in two phases.

The first phase of the project dealt with the development of the PP-CNC nanocomposite. To favor a better dispersion and wetting of hydrophilic CNCs within the hydrophobic PP matrix a poly(ethylene-co-vinyl alcohol) was used as a compatibilizer via a masterbatch preparation method. Two different masterbatches were prepared, one in solution and the other in molten state, with the CNC to compatibilizer ratio of 1/3. Then, the nanocomposites were prepared by melt-mixing of the masterbatches with PP using an internal mixer at a CNC content of 5 wt%. For sake of comparison, PP containing 15 wt% compatibilizer and PP containing 5 wt% CNCs were also prepared via direct melt mixing. Then, the effect of the CNCs on the rheological, mechanical and thermal properties of PP was investigated. Scanning electron microscopy showed the disappearance of large agglomerates when the compatibilizer was employed. The complex viscosity and storage modulus of the nanocomposite sample containing the compatibilizer prepared by a solution method were increased at low frequencies, compared to those of the non-compatibilized nanocomposite samples. Moreover, a pronounced overshoot for the transient viscosity in a shear stress growth experiment was observed for the compatibilized nanocomposite. The Young modulus was enhanced, up to ca. 47 % compared to the neat PP; the tensile strength remained unchanged and strain at break was decreased for the compatibilized nanocomposite. The storage modulus of the PP at room temperature in dynamic mechanical thermal analysis (DMTA) was increased up to ca. 60% when a good state of dispersion was achieved using the compatibilizer. The nucleation effect of the CNCs on the crystallization of the

PP was confirmed by the enhanced crystalline content of the PP nanocomposites and increased crystallization temperature using the compatibilizer. These observations were ascribed to the efficiency of the poly(ethylene-co-vinyl alcohol) as a compatibilizer, especially when the masterbatch was prepared in solution.

The second phase focused on the development of high performance PLA-CNC bionanocomposites. A simple and novel solution casting method with a polar solvent (i.e. N,N-dimethylformamide) was used to favor a good dispersion of hydrophilic CNCs within a PLA matrix at different CNC loadings without the need of CNC modification or use of any compatibilizer. Then, the effect of the CNCs on the properties of the PLA for both molten and solid states was investigated. Transmission electron microscopy revealed the existence of well-dispersed structure of CNCs within the PLA matrix. The complex viscosity and the storage and loss moduli were increased significantly, especially at low frequencies, by the incorporation of 1 wt% CNCs and larger contents. These enhancements were ascribed to the formation of an interconnected network of CNCs within the PLA matrix. The rheological percolation threshold was determined to be 0.68 wt% CNC. Furthermore, the steady-state viscosity, shear stress and first normal stress difference were increased. The apparent yield stress increased with CNC content, for both SAOS and steady-shear experiments. The Cox-Merz rule was not valid for the PLA-CNC nanocomposites; however, for nanocomposites at large CNC contents the extended Cox-Merz rule was applicable. Pronounced overshoots in transient shear for forward and reverse flows and the structure build-up of samples after pre-shearing were explained by a network formation and the important role of the Brownian motion for structure recovery. The less concentrated nanocomposites pre-sheared at larger rates needed longer times after the cessation of the shear flow to recover their initial structure.

The rheological properties demonstrated the efficiency of the sonicator in solution mixing to disperse the CNCs with the consequent formation of an interconnected network of CNCs within the PLA matrix. The Young modulus of the nanocomposites increased up to ca. 23% compared to the neat PLA; however, the strain at break slightly decreased and tensile strength remained unchanged. In DMTA, the storage modulus of the PLA-CNC naonocomposites increased up to ca. 74% in glassy region and up to ca. 490% in the rubbery region. The observation of increased crystalline content of the PLA in the nanocomposites and shift in the crystallization temperature

towards higher temperatures, were attributed to the nucleation effect of the CNCs on the crystallization of PLA.

To our knowledge, this is the first time that a very good dispersion of CNCs in a non-hydrosoluble polymer together with huge increases in the properties of the corresponding solid and molten state nanocomposite is achieved, without any change in the morphological structure of the CNCs or use of any compatibilizer. Moreover, to the best of our knowledge, this is the first systematic investigation of the rheological behavior of PLA-CNC nanocomposites in different shear flow fields.

TABLE OF CONTENTS

LIST OF TABLES

LIST OF FIGURES

CHAPTER 1 INTRODUCTION

Cellulose nanocrystals (CNCs) are rod-like nanoparticles that are obtained by acid hydrolysis of cellulose from cell walls of different plants, some sea animals, for example tunicin, cotton and bacteria. CNCs provide several interesting properties such as low density, abundance in nature, renewability, biodegradability, high reactivity, very large surface area per unit weight and very high strength and modulus. CNC was discovered in 1949; however, it did not attract huge attention at that time. In 1992, colloidal suspensions of CNCs showed liquid crystalline properties. A few years after, the high strength and stiffness of CNCs created a great interest for their potential use as reinforcing agents in polymers. In 1995, the first use of the CNCs as reinforcing agents in polymer composites was reported by Favier et al. [1] who could enhance the mechanical properties of solution-cast films of poly(styrene-co-butyl acrylate) latex. In the past decade there has been a great interest and need to lower the CO_2 emission by substituting the petroleum-based products with the bio-based materials. Following this thought, employing the renewable and bio-based CNC as a proper alternative for inorganic and non-renewable counterparts used as reinforcing agents in the preparation of composite materials would be a great success [2].

Recently, there has been increasing interest to incorporate CNCs into biopolymers to expand their applications by improving their mechanical and thermal properties over wide range of temperature. Among different biopolymers, polylactide (PLA) is already commercialized and finds applications in numerous fields (e.g. medical, packaging and automotive industries). The incorporation of CNCs can improve the mechanical and thermal properties of PLA while maintaining its unique properties such as biocompatibility, biodegradability and transparency. This would create fully biobased, biocompatible and biodegradable composite materials that can replace petroleum-based polymeric products, especially in packaging and automotive industries. The combination of such features opens wide application prospects and, for these reasons, CNCs have attracted significant interest from both academic and industrial investigators. However, strong hydrogen bonds between the CNC particles result in to the formation of big agglomerates when they are introduced to non water-soluble polymers. Consequently, the use of CNCs, in their pristine form, to enhance the properties of polymers has grown, but it nevertheless remains

limited to a few water-soluble polymers and polymers in latex form [1, 3-8]. However, most of the common polymers in industry, such as polypropylene (PP), polyethylene (PE), polystyrene (PS), polyethylene terephthalate (PET) and recently PLA, are non water-soluble. Therefore, in most cases either surface modification or compatibilization are necessary to achieve a good dispersion of CNCs, and minimum requirement to achieve a significant enhancement of the properties of polymers [9-15]. In some instances, in spite of having good dispersion, mechanical property enhancement has not been observed due to the plasticization effect of the modifiers or compatibilizers. The formation of an interconnected network of particles plays an important role on both melt and solid properties of nanocomposites. Therefore, in this research we tried to find an efficient preparation method to incorporate CNCs in PP or PLA, which both have considerable interests for many applications.

The main contributions of this research are found in three scientific articles; the first has been published in the journal of Composite Science and Technology, the second and third have been submitted to the journal of Cellulose.

This thesis consists of the following chapters:

• Chapter 1: Introduction

• Chapter 2: Literature review

• Chapter 3: Objectives

• Chapter 4: Organization of the articles

• Chapters 5 to 7: The three articles reporting the main results of this project

• Chapter 8: General discussion

CHAPTER 2 LITERATURE REVIEW

2.1 Overview

The term “biocomposite” refers to composite materials made of a matrix and a biobased reinforcing agent. The matrix can also be biobased, which results in completely biobased composites called green composites. Therefore, the combination of both polypropylene (PP) and polylactide (PLA) with CNCs would fall into the category of biocomposites and when a nano-dispersed structure is achieved the term “bionanocomposite” can be used to describe the systems. The combination of biopolymers like PLA and polyhydroxyalcanoates (PHAs) and synthetic fibers also come under biocomposites.

For many years glass fibers were the first choice as a reinforcing agent in polymer composite industry, especially for PP. However, natural reinforcements have emerged as lightweight, low cost and environmentally superior alternatives to glass fibers, mainly due to lower greenhouse gas emissions, less environmental impacts, reduced dependence on non-renewable energy/materials and lower pollutant emissions in production phase. Moreover, the use of natural reinforcements improves fuel efficiency due to the lightweight products in the end use phase, compared to glass fiber. The recovered energy and carbon credits in incineration of the end of life phase can be another advantage of using natural reinforcements. Such superior environmental performances offered by biocomposites are convincing enough for changing the trend of the market towards the use of the natural reinforcements and biocomposites, especially for automotive applications [16]. In this research project we investigated the possibility of employing CNCs as the finest natural reinforcing agents to enhance the properties of commonly used polymers such as PP and PLA.

2.2 CNCs: Preparation and Structure

Cellulose nanocrystals (CNCs) can be extracted from different organic sources from wood and pulp to sea animals, tunicate, etc., by acid hydrolysis, usually sulfuric acid. Depending on the cellulose source, the dimensions of the CNCs will be different. Table 2.1 shows the diversity of CNC’s aspect ratios obtained from different cellulose sources [17]. CNCs are 3-50 nm in diameter and 50 nm to few μm in length, which result in a range of aspect ratio from 2 to 167.

Figure 2.1 schematically illustrates the molecular structure of the smallest part of plants cell walls. Cellulose fibers consist of many cellulose fibrils, each containing many sequential crystalline and amorphous parts. After acid hydrolysis the crystals can be separated from the amorphous parts to yield the CNCs. In the molecular structure of cellulose, there are many hydroxymethyl groups, which are considered more reactive than the hydroxyl groups in conjunction with the cycle of the β(1-->4) linked D-glucose units. Strong hydrogen bonding between the hydroxyl groups is responsible for interesting properties such as very high crystallinity and mechanical strength of CNC particles. Also, hydroxymethyl groups are generally the first sites that can be attacked by the chemical reagents.

Table 2.1: Dimensions of cellulose nanocrystals from various sources obtained by different techniques (adapted from Ref. [17])

Cellulose source	*L* (nm)	*W* (nm)	Aspect ratio (*L/w*)	Technique
Bacterial	100-1000	10-50	2-100	TEM
Cotton	100-150	5-10	10-30	TEM
	150-210	5-11	15-42	E-SEM
MCC	~500	10	50	AFM
Ramie	50-150	5-10	5-30	TEM
Sisal	100-500	3-5	20-167	TEM
Tunicate	1160	16	73	DDLS
	100-several 1000	15-30	3-67	TEM
Valonia	>1000	10-20	50-100	TEM
Wood	100-300	3-5	20-100	AFM

The specific area of CNCs is estimated to be 250-260 m^2/g, approximately, via AFM dimension measurements [18]. However, a more precise specific area, closer to reality, can be obtained by the maximal adsorption of Congo red using UV measurements [19]. The specific surface area, then, can be calculated by the following equation

$$SSA = \frac{A_{max} \times N \times SA}{M_w \times 10^{21}} \quad (2.1)$$

where Amax, N, SA and MW are the maximum absorbed amount, Avogadro's constant, surface area of a single dye molecule (1.73 nm2), and molecular weight of Congo red (696 g/mol), respectively [19]. The specific surface area together with the number of hydroxyl groups per gram of CNCs are among the most important parameters affecting the amount of chemical reagents that should be used for surface treatment.

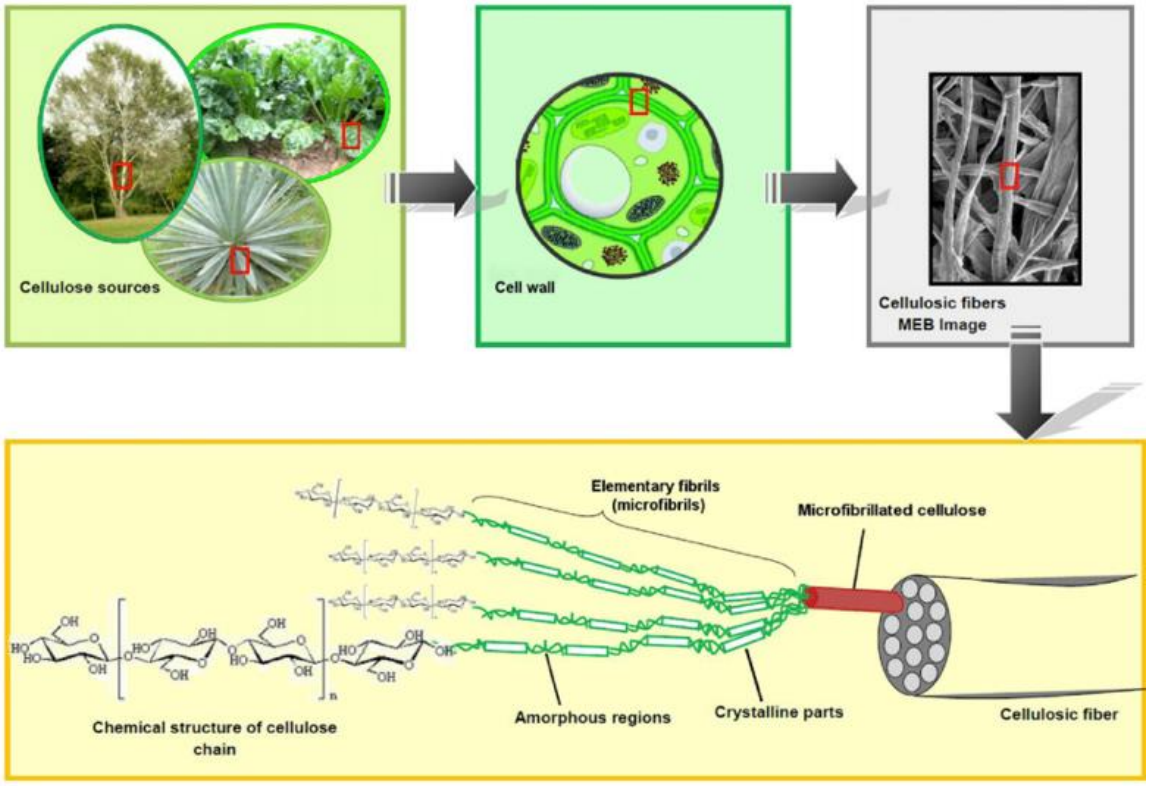

Figure 2.1: Cellulose from plants to molecular structure (from Ref. [20])

2.3 Polylactide (PLA)

The term PLA stands for both polylactide, which is the product of the ring opening polymerization of lactide monomer, and poly lactic acid, that is polymerized from the polycondensation of lactic acid. PLA now commercialized for commodity applications is from lactide. In this dissertation, we refer to polylactide when the term PLA is mentioned. PLA is a biobased, biocompatible and biodegradable aliphatic thermoplastic polyester with interesting properties such as high modulus, and strength at moderate temperature range (sub-zero up to 40-60 °C depending on the glass transition temperature (T_g)) and good clarity. Therefore, it has been emerging as a potential replacement of petroleum-based polymers. However, slow crystallization rate and poor thermal resistance are limiting its applications [21].

2.3.1 PLA structure

Figure 2.2 presents different stereoisomers of lactide. Lactide can be found in two main diastereomeric forms: *meso*-lactide and D,L-lactide, that is also called *rac*-lactide. D-lactide is

more expensive than the other forms and that is the main reason the commercially available PLA grades are usually made from L-lactide or *meso*-lactide monomers. Depending on the type of monomer, initiator and catalyst employed for polymerization reaction polylactides exhibit different microstructures, namely isotactic, syndiotactic and heterotactic. Isotactic PLA constitutes sequential stereocenters of the D- or L-lactide monomers, and poly(L-lactide) and poly(D-lactide) belong to this category. Syndiotactic PLA or poly(*meso*-lactide) is obtained by the sequential stereocenters of the opposite relative configuration. The alternative structure of D- and L-lactide units produces heterotactic PLA and, finally, the random structure of D- and L-lactide units leads to atactic PLA, which is basically an amorphous polymer [22]. Figure 2.3 presents different structures of polylactide. The physical properties of polylactides such as melting point, crystalline content and glass transition temperature strongly depend on their stereochemical composition. For example, if pure poly(L-lactide), a highly crystalline material with a T_m around 180 °C, is contaminated with *meso*-lactide, the crystallinity and melting point decrease [22]. As mentioned earlier, PLA suffers from slow crystallization rate; however, by annealing or changing the stereochemical composition the degree of crystallinity and, consequently, properties of PLA may significantly change. Table 2.2 reports the effects of stereochemistry and crystallinity on the properties of polylactides [23]. When, pure poly(L-lactide) is annealed its mechanical properties are enhanced; however, by the addition of *meso* structure, they are deteriorated.

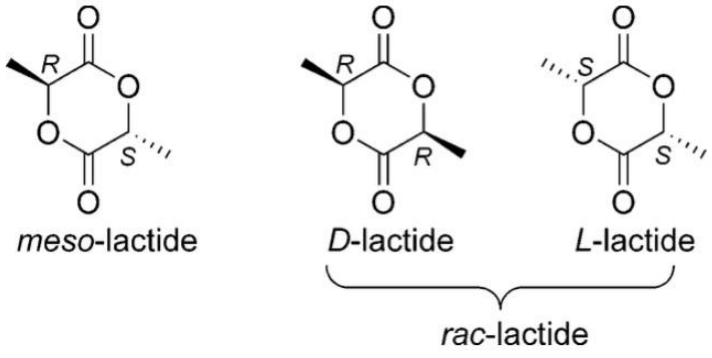

Figure 2.2: Stereoisomers of lactide (from Ref. [22])

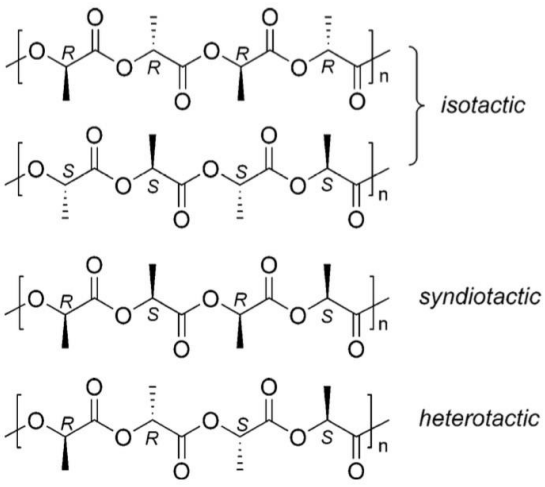

Figure 2.3: Different types of polylactides (from Ref. [22])

Table 2.2: Effects of stereochemistry and annealing on mechanical properties of polylactides (adapted from Ref. [23])

Property	L-PLA	Annealed L-PLA	D,L-PLA
Tensile strength (MPa)	59	66	44
Elongation at break (%)	7.0	4.0	5.4
Tensile Modulus (MPa)	3750	4150	3900
Yield strength (MPa)	70	70	53
Flexural strength (MPa)	106	119	88
Unnotched Izod impact (J/m)	195	350	150
Notched Izod impact (J/m)	26	66	18
Rockwell hardness	88	88	76
Heat deflection temperature (^{0}C)	55	61	50
Vicat penetration (^{0}C)	59	165	52

2.4 Polypropylene (PP)

PP was discovered in the early 1950s by Giulio Natta. Figure 2.4 schematically presents the polymerization of propylene, which is a gaseous by-product of petroleum refining, in presence of a catalyst under careful control on temperature. Propylene is an unsaturated hydrocarbon, composed of only carbon and hydrogen atoms. Depending on the catalyst and the polymerization method employed, three different stereochemical configurations can be produced, namely atactic, isotactic and syndiotactic PP. Figure 2.5 illustrates different configurations of PP. The

development of the Ziegler-Natta catalyst, in the 1950s, made the formation of the isotactic configuration possible with a high level of crystallinity and a wide range of molecular weight [24]. Nowadays, isotactic polypropylene (iPP) is one of the most commonly used polymers in many applications due to its interesting properties, such as low cost, easy processing, good mechanical properties and heat resistance, chemical stability and non-toxicity. Commercially available grades of PP usually show a very high fraction of isotacticity [24]. Isotactic PP has a T_g in the range of -10 to 0 °C, melting point of 165-170 °C and heat deflection temperature (HDT) of 80-90 °C.

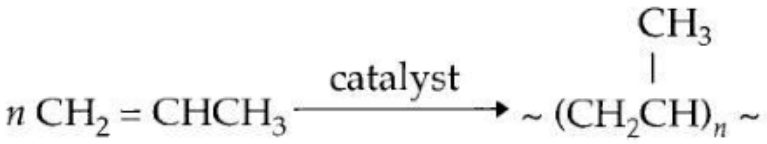

Figure 2.4: Schematic of the polymerization of polypropylene from propylene monomer in the presence of catalyst (from Ref. [24])

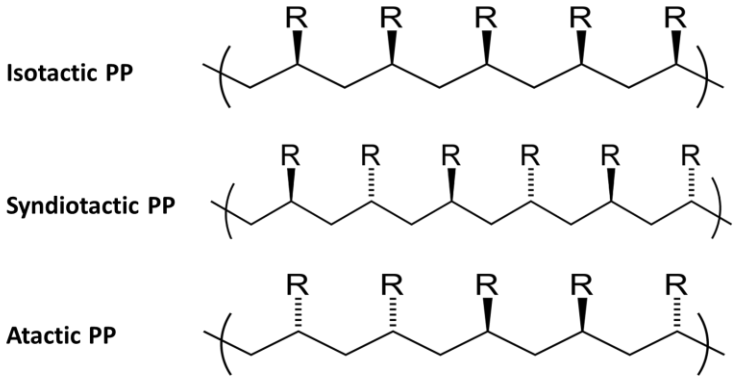

Figure 2.5: Different tacticities of polypropylene. R indicates methyl groups

2.5 CNC Treatments

Apart from interesting properties of CNCs, their application for polymer nanocomposites is limited to only a few hydrophilic polymers such as polyvinyl alcohol (PVOH) [3-5] and polyethylene oxide (PEO) [6] and hydrophobic polymers in latex form [7, 8]. This is due to strong hydrophilicity of CNCs and, consequently, lack of compatibility with more interesting

polymers such as hydrophobic polyolefins, PLA and other hydrophobic polymers. Thus, compatibilization is required to achieve enhanced mechanical properties together with good dispersion of CNCs into polymer matrices [10-14, 25]. To this end, CNC treatments to make it more hydrophobic, functionalization of polymer matrix to make it more hydrophilic or use of compatibilizers needs to be considered. CNC surface treatments can be conducted via a wide variety of plasma [26] and corona [27] treatments and chemical modifications, such as acetylation or esterification [28], tempo-mediated oxidation [29, 30], grafting [11, 12, 15, 31, 32] and cationization [18, 30]. TEMPO-mediated oxidation, acetylation and esterification methods are among the most promising treatments for cellulose nanofibrils (CNFs). By substituting a part of hydroxyl groups on the surface of CNCs these methods can be used to decrease the hydrophilicity of the CNCs. However, due to the lack of sufficient physical or chemical interactions with polymer matrices, for CNCs these methods need to be followed by a post treatment reaction. Therefore, to graft a long hydrophobic chain a grafting agent, usually a surfactant [33, 34], should attach to the carboxylate or carboxylic groups created from the first treatment reaction. This can make the whole process of treatment quite expensive, time consuming and difficult to control, with many sequential steps of washing and re-dispersion in acidic or alkali media. Moreover, there are not many commercially available long chain hydrophobic chemicals that can be grafted to CNCs in the post treatment process. Also, their length are not sufficient to create entanglements with polymer matrix chains and, as a result, these will act as plasticizers when incorporated into the polymer matrix. Coupling agents and compatibilizers have also been used to increase the compatibility between CNCs and polymer matrices. Coupling agents are chemical reagents that can create covalent or hydrogen bonds between the matrix and the dispersed particles. Following an appropriate modification the hydrophilicity of the CNCs becomes lower and the compatibility between CNCs and non polar polymer matrices will increase. This will happen only when long chains are grafted to the surface of CNCs. The use of coupling agents, namely organosilanes and titanates, usually can improve the dispersion of hydrophilic CNCs within hydrophobic matrices [35-37]; however, as short chains are grafted on the surface of CNCs their plasticization effect compromises the reinforcing effect of the CNCs. Thus, among all methods, *in-situ* polymerization and use of functionalized polymers/copolymers may result in increasing the compatibility of CNCs with PP and PLA and, consequently, enhancing the mechanical properties of the nanocomposites. However, in-situ

polymerization is also costly, time consuming and usually does not provide control over the grafting density and length of grafted chains [12, 38].

2.6 PP-CNC (nano)composites

In order to increase the mechanical properties of atactic PP (aPP), which shows very weak properties, Ljungberg et al. [39] utilized tunicin CNCs with an aspect ratio of 67 and diameter of 10-20 nm. To do that, they employed two different modifications; surface modification of CNCs with a phosphoric ester of polyoxyethylene (9) nonylphenyl ether at a weight ratio of BNA/CNC: 4:1, and grafting of maleated PP (PP-g-MA) (Epolene E43 with M_n: 3,900 g/mol and M_w: 9,100 g/mol) onto the CNC, referred to as compatibilized CNC. They prepared the composites via a solvent casting method with toluene as solvent. Figure 2.6 presents SEM micrographs of surface modified (SUCNC), compatibilized (GRCNC) and unmodified CNCs (AGCNC) in aPP. Obviously, there are much finer agglomerates in the surface modified system. However, grafting of PP-g-MA to CNCs seems not to be effective to favor a better dispersion and distribution of CNCs within aPP.

Figure 2.7 reports the storage modulus of the samples for DMTA tests. As expected, unfilled aPP shows very low modulus above T_g, almost 3 orders of magnitude lower than that of iPP. By incorporating 6 wt% surface modified, compatibilized and unmodified CNCs the rubbery-region storage modulus of iPP is enhanced by 1 order of magnitude at room temperature, i.e. 25 °C. However, the addition of unmodified CNCs results in better enhancement compared to the surface modified and compatibilized CNCs (Figure 2.7a). The possible reason could be the plasticization effect of the surfactant and compatibilizer materials on the properties of aPP. The same observations were reported for tensile properties of the samples. Figure 2.8 presents the stress-strain behavior of the samples in tensile tests. Higher Young modulus and tensile strength, but reduced strain at break, are obtained for the aPP-CNC samples (Figure 2.8a). The use of surfactant and compatibilizer does not show any improvement of the mechanical properties of aPP containing unmodified CNCs. In another work they employed the same types of CNCs to enhance the mechanical properties of isotactic PP (iPP) [40]. For iPP-CNC samples, a decrease in the crystalline content of iPP was reported by incorporating 6 wt% of unmodified, surface modified and compatibilized CNC [40].

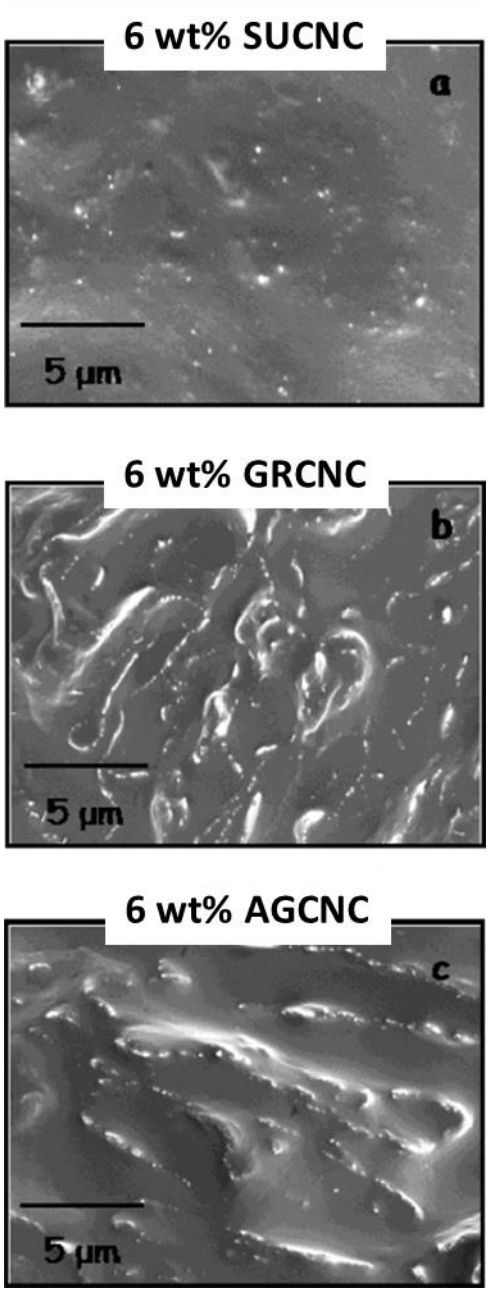

Figure 2.6: SEM micrographs of aPP composite films reinforced with 6 wt % (a) surface modified CNCs (SUCNC), (b) compatibilized CNCs (GRCNC), and (c) unmodified CNCs (AGCNC) (from Ref. [39])

In DMTA tests, the storage moduli for the samples filled with unmodified and surface modified CNCs were identical and higher than those of iPP and iPP filled with compatibilized CNCs in the rubbery region (i.e. temperatures higher than T_g) (Figure 2.7b). However, in the glassy region (i.e.

temperatures lower than T_g), only surface modified CNCs could increase the storage modulus of PP; the other filled samples showed lower storage modulus (Figure 7b). In tensile tests, iPP filled with unmodified CNCs showed a decreased tensile strength, relative to the neat iPP; however, by incorporating compatibilized CNCs into iPP the tensile strength was enhanced, compared to the neat iPP. Better enhancement was observed for iPP filled with surface modified CNCs (Figure 2.8b).

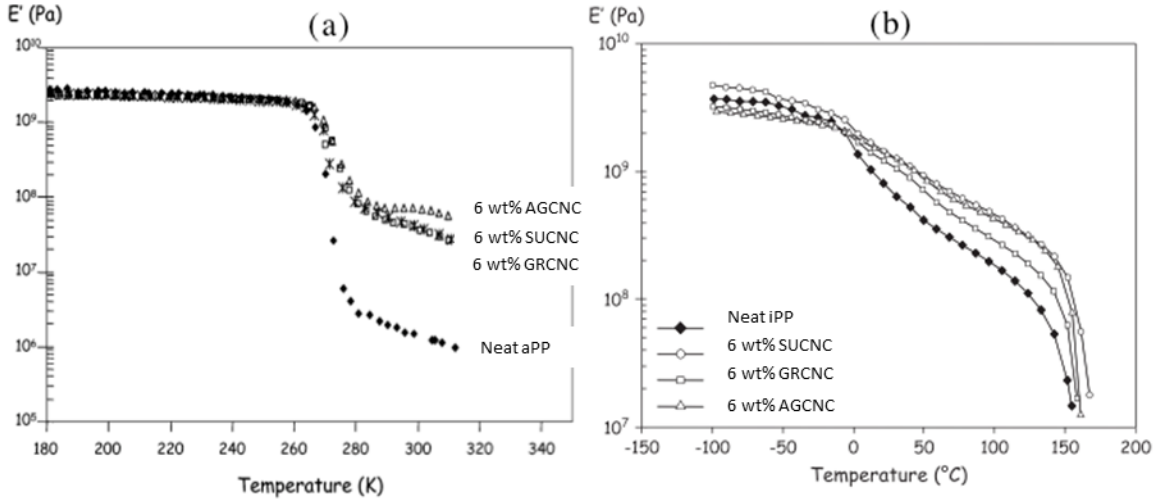

Figure 2.7: Storage modulus vs temperature from DMTA tests comparing (a) neat aPP and (b) neat iPP with composites reinforced with 6 wt% unmodified CNCs (AGCNC), surface modified CNCs (SUCNC), and compatibilized CNCs (GRCNC) (adapted from Ref. [39, 40])

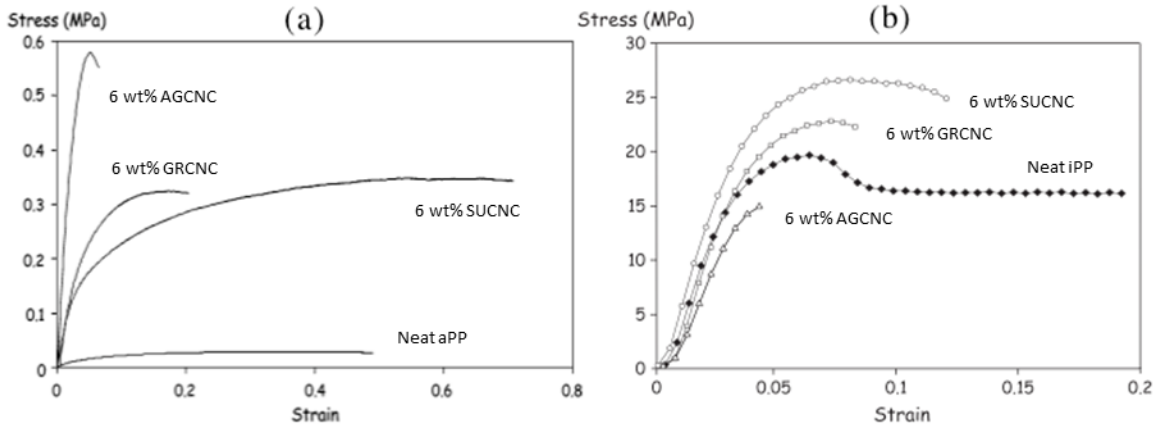

Figure 2.8: Stress vs strain curves for (a) neat aPP and (b) neat iPP and composites reinforced with 6 wt% AGCNC, SUCNC, and GRCNC (adapted from Ref. [39, 40])

Bahar et al. [41] employed the same solvent casting method to prepare PP-CNC composites compatibilized with PP-g-MA (Epolen E 43-Wax, softening point 158 °C, 8 wt% MA, molecular weight M_w: 15,789 and M_n: 7,105). To do that, two different polymer solutions, namely PP in toluene and PP-g-MA in toluene, were prepared at 105-110 °C. Then, the desired amount of CNCs were added into the solution of PP-g-MA and sonication together with stirring applied for 2 h before the addition of this mixture to the solution of PP in toluene. The final mixture was stirred for another 15 min and poured into petri dishes for solvent evaporation, conducted in oven at 90 °C for 24 h. The samples for testing were prepared by compression at 135 °C. The concentration of CNCs in final composites was 5, 10 and 15 wt%. Two sets of samples compatibilized with different contents of PP-g-MA (0.8 and 2 wt% of the systems) were compared in terms of their crystallinity and tensile properties. Figure 2.9 compares the tensile strength of the samples. By incorporating 0.8 wt% PP-g-MA the tensile strength of PP composite increased. However, adding 2 wt% PP-g-MA into PP resulted in to smaller increase (Figure 2.9a). The addition of 5 and 10 wt% CNCs did not enhance the tensile strength of the blends, while for 15 wt% CNCs enhanced tensile strength as shown in Figure 2.9b. The main reason behind this trend is probably the change in the crystalline content of the composites. A reduced crystalline content for filled blend with 5 wt% CNCs, no significant changes for 10 wt% CNCs and ca. 50% increase in crystalline content at 15 wt% CNCs are reported, relative to the value of the PP and PP-g-MA blend. A better comparison is possible via Table 2.3. For all of the filled blends, a reduced tensile modulus is observed, compared to the unfilled blends. Interestingly, the strain at break for the blends is increased by the addition of CNCs, although compared to the neat PP it is reduced. The results do not show the efficiency of PP-g-MA as a compatibilizer except for the system containing 15 wt% CNCs. This contrasts the advantage of nanocomposites as usually a concentration of less than 10 wt% is desired. Moreover, the results of uncompatibilized systems were not presented in the work of Bahar et al. [41] to check the efficiency of the compatibilizer.

Hassanabadi et al. [42] designed more systematic experiments to investigate the effect of five different PP-g-MA compatibilizers[1], varying in acid number and molecular weight, on the

[1] In Ref. [42] refered to as coupler. See the reference for mor information about different couplers.

mechanical properties of PP through a melt preparation method. The composites were prepared via a twin screw extruder and direct melt mixing. The PP and PP-g-MA compatibilizers were dry mixed and introduced from the first feeder; CNC powder was added through a second feeder to reach the final concentration of 1 wt% CNCs with different CNC to compatibilizer ratios. The product was pelletized and introduced into the extruder for a second run. The samples were characterized by tensile, impact and flexural tests. For all of the compatibilizers the optimum ratio of CNC to compatibilizer was determined at 7.5/1, regardless of the molecular weight and acid number. Table 2.4 reports the Young modulus of the samples with different compatibilizers and CNC to compatibilizer ratios. The highest Young modulus improvement (47% compared to the neat PP) was achieved for the compatibilizer with M_w: 15 kDa, acid number of 41 mg KOH/g; the highest flexural modulus enhancement (32% relative to the neat PP) was obtained for the compatibilizer with M_w: 51 kDa and acid number of 15 mg KOH/g. However, the impact strength slightly decreased for all samples. Therefore, they concluded that the most important parameter when using PP-g-MA as a compatibilizer is the CNC/compatibilizer ratio. However, the results of PP filled with uncompatibilized CNC were not reported and all compatibilizers had different values of molecular weight and acid number making the comparison difficult; but the acid number seemed to be more effective than the molecular weight to enhance the mechanical properties. A higher acid number value would favor better wetting of CNCs by the compatibilizer and a higher value of molecular weight would lead to stronger entanglements with PP matrix, although for both parameters there are optimum values.

Khoshkava and Kamal [43] determined the effects of CNC drying process, initial concentration of the CNC aqueous suspensions and final concentration in the nanocomposites on the properties of PP-CNC systems. They obtained a porous morphology for the CNC agglomerates by employing a spray-freeze drying process, which led to property enhancements of PP without the need of a third component. Figure 2.10 presents the SEM micrographs of spray-freeze dried CNCs (CNCSFD) with different initial concentrations in water and final concentrations in PP. Figure 2.10a,b show agglomerates obtained after spray-freeze drying process of aqueous suspensions of CNCs with different concentrations prior to the drying process. Large agglomerates with a very porous structure and low strength are obtained that can be broken down easily when introduced into PP at molten state thereafter. Also there is high potential for PP melt infiltration into these porous agglomerates. Therefore, a uniform dispersion of the CNCs into PP

was achieved (Figure 2.10c,d). The small holes in Figure 2.10c−e are considered spray-freeze dried CNCs that were pulled out during sample preparation for SEM by microtoming. However, the holes could be micro-voids caused by partial polymer melt infiltration into the porous structure of the CNC agglomerates. It seems that a lower initial concentration, i.e. 1 wt%, by providing a more open structure, resulted in easier polymer melt infiltration and, consequently, more dispersed CNCs into PP.

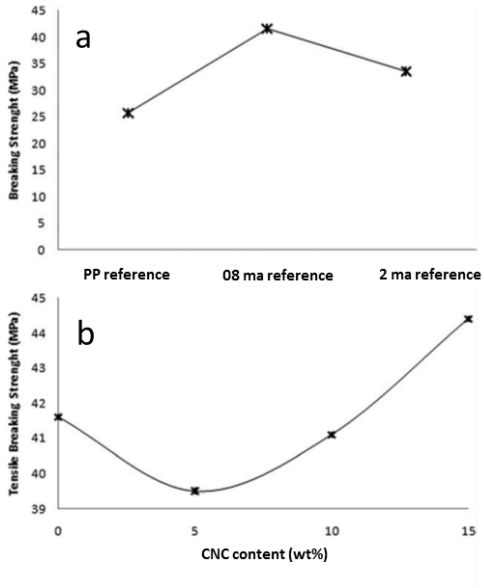

Figure 2.9: Tensile strength of: (a) neat PP, PP with 0.8 wt% PP-g-MA, and PP with 2 wt% PP-g-MA; (b) PP-PP-g-MA blend with 0.8 wt% PP-g-MA and different CNC contents (from Ref. [41])

Table 2.3: Tensile properties of neat PP, PP and PP-g-MA blends, and filled blends (adapted from Ref. [41])

Sample	Tensile strength (MPa)	Elongation at break (%)	Modulus (MPa)
PP reference	25.7	24.9	1258.5
08 ma* reference	41.6	5.2	1534.0
08 ma 5 CNC	39.5	5.5	1498.2
08 ma 10 CNC	41.1	9.76	990.0
08 ma 15 CNC	44.4	7.38	1258.4
08 ma 15 CNC 30 son	40.9	5.61	1129.7
08 ma 15 CNC 60 hyd	46.6	7.4	1295.6
2 ma reference	33.5	2.17	1777.4
2 ma 5 CNC	32.8	4.3	1417.5
2 ma 10 CNC	36.4	5.4	1013.5
2 ma 15 CNC	39.0	4.8	1336.1

* ma stands for PP-g-MA

Table 2.4: Young modulus of the samples prepared with different compatibilizers and CNC to compatibilizer ratios. The concentration of CNC is fixed at 1 wt% (adapted from Ref. [42])

Sample	*F/C* = 5/1		*F/C* = 7.5/1		*F/C* = 10/1	
	Modulus (MPa)	Change compare to PP (%)	Modulus (MPa)	Change compare to PP (%)	Modulus (MPa)	Change compare to PP (%)
PP	450 (17)	-	450 (17)	-	450 (17)	-
PP CNC 1%	508 (10)	13	508 (10)	13	508 (10)	13
PP CNC 1% coupler A	584 (37)	29	599 (21)	33	565 (13)	26
PP CNC 1% coupler B	550 (18)	22	663 (50)	47	573 (32)	27
PP CNC 1% coupler C	495 (10)	10	556 (45)	24	519 (40)	15
PP CNC 1% coupler D	566 (27)	25	572 (50)	27	553 (38)	23
PP CNC 1% coupler E	509 (13)	13	574 (40)	28	528 (29)	17

Numbers in parentheses represent standard deviations. *F/C* is the filler/coupler ratio.

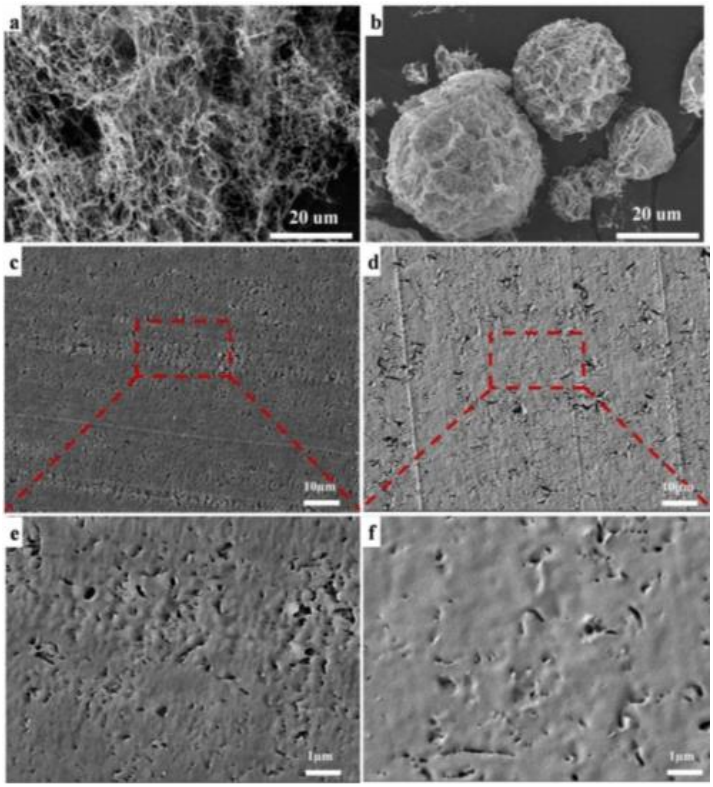

Figure 2.10: SEM images of: (a) spray-freeze dried CNC obtained from 1 wt% CNC aqueous suspension (CNCSFD1), (b) spray-freeze dried CNC obtained from 2 wt% CNC aqueous suspension (CNCSFD), (c, e) PP containing 5 wt% CNCSFD1 and (d, f) PP containing 5 wt% CNCSFD2 at (c, d) low and (e, f) high magnification (from Ref. [43])

The rheological behavior in small-amplitude oscillatory shear (SAOS) was also investigated. Figure 2.11 presents the complex viscosity, storage and loss moduli versus frequency in SAOS tests for PP filled with spray dried, freeze dried and spray-freeze dried CNCs. It seems that almost insignificant polymer melt infiltration took place within the compact structures of CNC agglomerates, obtained from spray and freeze drying; that resulted into no rheological property increases (Figure 2.11a). However, with the porous structure of spray-freeze dried CNCs polymer melt infiltration happened and, as a result, the complex viscosity and storage and loss moduli increased, especially at low frequencies (Figure 2.11b,c). Observation of a high shear-thinning behavior for the complex viscosity and frequency-independency behavior for the storage and loss moduli at low frequencies are ascribed to a CNC network formation. With further rheological characterization, a value of 2.5 wt% was reported as the rheological percolation threshold in the best case, i.e. when the initial concentration of CNCs in the aqueous suspension was 1 wt% prior to spray-freeze drying [43].

To compare the mechanical performance of PP and PP filled with spray died and spray-freeze dried CNCs, DMTA data for the samples were presented [43]. Figure 2.12 reports the variation of storage modulus for a wide range of temperature. The addition of spray dried CNC decreased the storage modulus of PP for the whole range of temperature due to poor dispersion and existence of large agglomerates. However, by incorporating 5 wt% spray-freeze dried CNCs enhanced storage modulus, up to ca. 60% at room temperature, is observed. The nanoparticles were less efficient to improve the properties when the initial concentration of CNC was larger, i.e. at 2 wt% compared to 1 wt%.

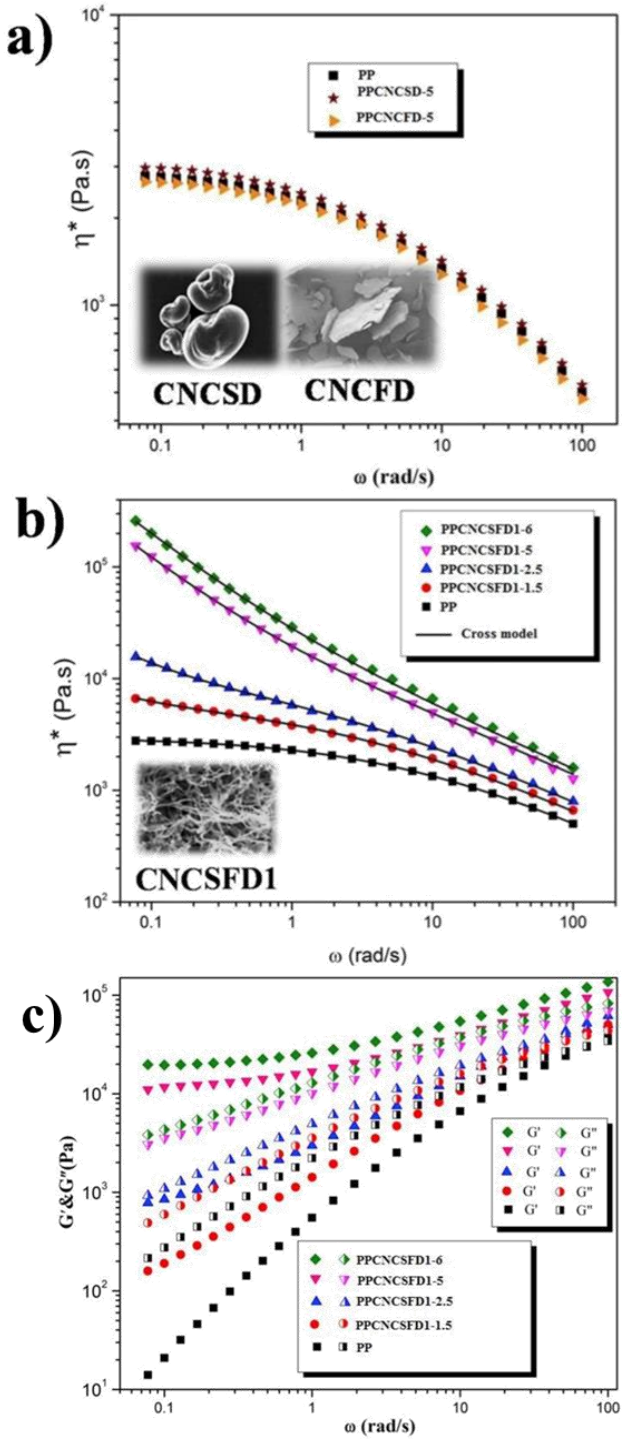

Figure 2.11: Plots of (a,b) complex viscosity vs angular frequency for (a) PP, PP with 5 wt% spray-dried (CNCSD) and freeze-dried (CNCFD) CNC, and (b) PP and PP containing CNCSFD1 agglomerates, and (c) storage and loss moduli vs angular frequency of samples. The insets show SEM images of spray-dried (CNCSD), freeze-dried (CNCFD), and spray-freeze-dried (CNCSFD) CNC agglomerates (adapted from Ref. [43])

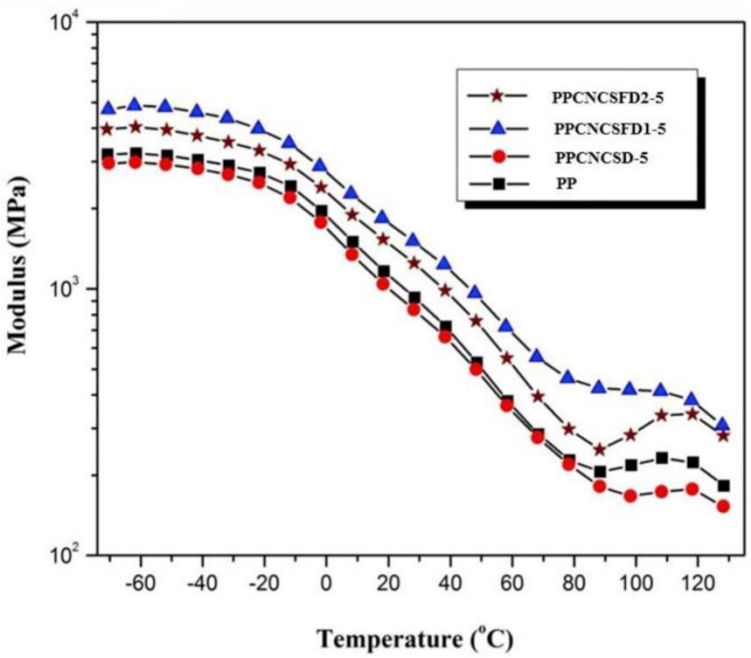

Figure 2.12: Storage modulus vs temperature for PP and PP containing 5 wt% CNCSD, CNCSFD1, and CNCSFD2 (from Ref. [43])

2.7 PLA-CNC (nano)composites

Kamal and Khoshkava [44] used the same idea of spray-freeze drying employed for PP-CNC systems [43] to prepare PLA-CNC nanocomposites with a dispersed structure and enhanced properties. Figure 2.13 illustrate the quality of the dispersion when 7 wt% of spray dried CNCs (CNCSDs) and spray-freeze dried CNCs (CNCSFDs) were melt-compounded with molten PLA via an internal mixer. Very large agglomerates were formed with poor dispersion and distribution for PLA filled with CNCSDs (Figure 2.13a), while a uniform and dispersed structure was obtained when CNCSFDs were added to PLA (Figure 2.13b). Figure 2.14 presents the complex viscosity, storage and loss moduli versus frequency for PLA and PLA-CNC nanocomposites with different CNC contents. Significant increases of the complex viscosity, storage and loss moduli for PLA containing spray-freeze dried CNCs at concentration of 3 wt% and larger are observed, relative to the neat PLA. As discussed earlier, the formation of a CNC network within the PLA is responsible for this huge increase in rheological properties. Moreover, Kamal and Khoshkava [44] performed DMTA tests to compare the mechanical properties of the samples. Figure 2.15 illustrates the variations of the storage modulus and tan δ over a wide range of temperature. The storage modulus is increased up to ca. 27% in the glassy region and up to ca. 20% in the rubbery

region for PLA containing 7 wt% CNCs (Figure 2.15a). Figure 2.15b reports a reduction in the area under tan δ peak, which is usually ascribed to the restriction effect of the CNCs on the segmental motion of the polymer chains at T_g. These observations clearly demonstrate the reinforcing effect of the CNCs on the properties of PLA. Again, there would be a concern that the holes observed in Figure 2.13b are micro-voids rather than pulled out CNCs.

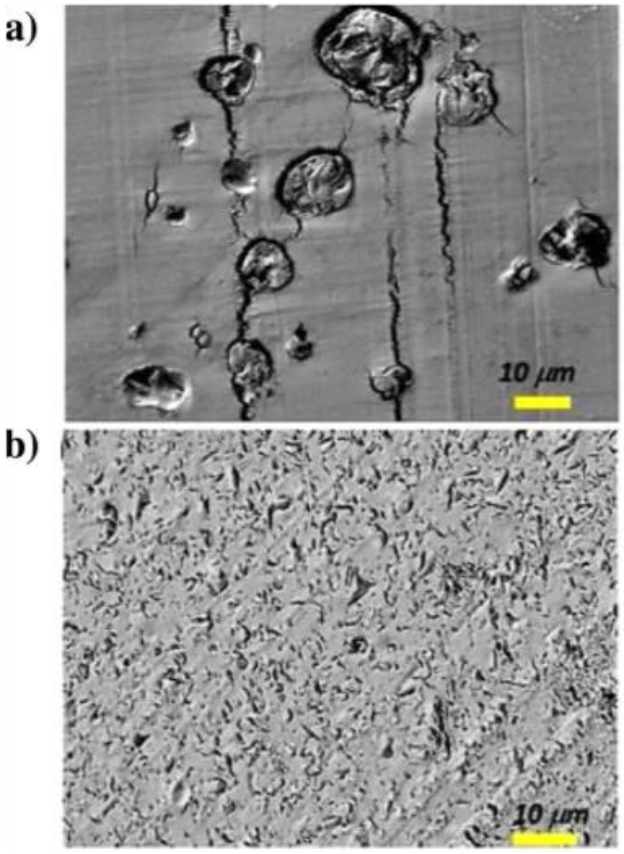

Figure 2.13: SEM micrographs of PLA containing 7 wt% of (a) spray dried CNC (CNCSD) and spray-freeze dried CNC (CNCSFD) (Scale bars: 10 μm) (from Ref. [44])

Pei et al. [45] extracted CNCs from cotton and partially modified them with a silane coupling agent, namely *n*-dodecyldimethylchlorosilane, in a toluene medium. Partially silylated CNCs could form stable suspensions in tetrahydrofuran and chloroform revealing the hydrophobic surface of silylated CNCs. PLA-CNC films were prepared via a solvent casting method in a chloroform medium. For the sake of comparison PLA films with unmodified CNCs were also prepared. Figure 2.16 reports DSC data from cooling cycle for the samples at a rate of 10 °C/min.

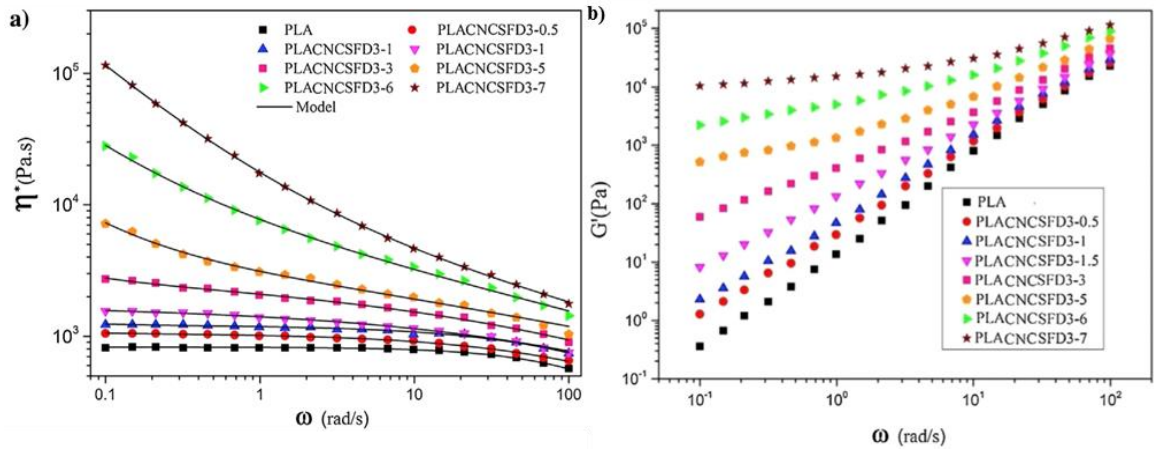

Figure 2.14: Complex viscosity, storage and loss moduli vs frequency for PLA and PLA-CNC nanocomposites. The initial concentration of CNC in the aqueous suspensions was 3 wt% prior to spray-freeze drying (adapted from Ref. [44])

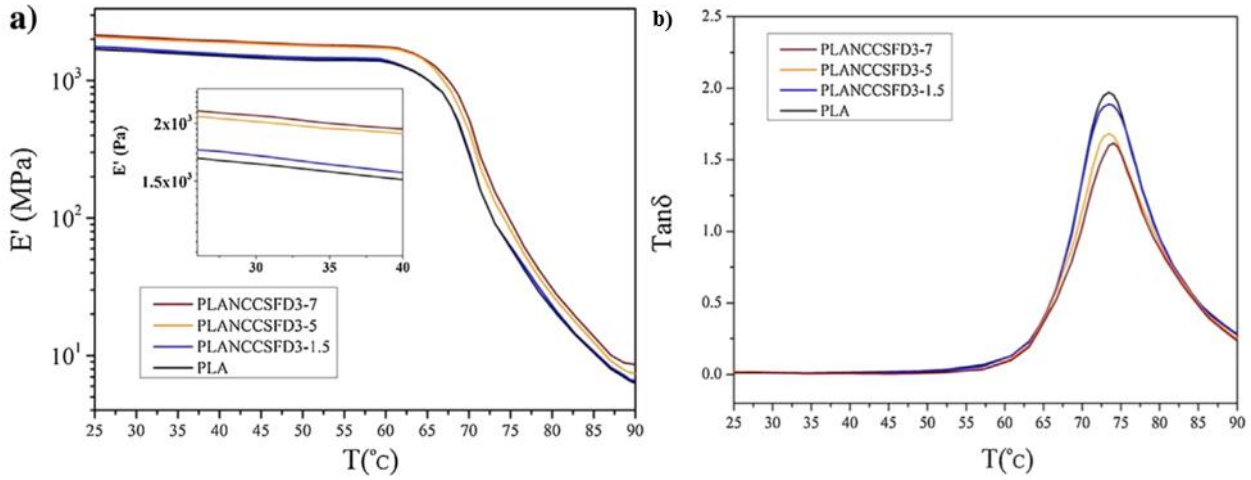

Figure 2.15: The DMTA data for neat PLA and PLA-CNC nanocomposites with 1.5, 3 and 7 wt% spray-freeze dried CNCs: (a) storage modulus and (b) tan δ vs temperature (from Ref. [44])

One of the main industrial problems of PLA is its slow crystallization. Therefore, under fast and even moderate cooling rates PLA does not undergo crystallization. The incorporation of unmodified CNCs did not solve the problem. However, by the addition of silylated CNCs the crystallization took place.

Table 2.5 provides details from heating cycles. The addition of 1 wt% modified CNCs resulted into the highest crystalline content, almost 100% increase relative to the neat PLA and PLA filled with unmodified CNCs. However, by the addition of more modified CNCs, a lower enhancement in the total crystalline content of PLA was achieved. Moreover, they reported reduced half-time of crystallization for PLA samples filled with modified CNCs, especially when isothermal crystallization took place at higher temperatures. These observations definitely confirm the nucleation effect of the CNCs on the crystallization of PLA and the efficiency of the silane coupling agent to yield a better wetting of CNCs with the PLA matrix.

Table 2.6 reports the tensile properties of the PLA and PLA-CNC samples. The Young modulus and tensile strength were increased by ca. 27 and 21%, respectively, by incorporating 1 wt% of silylated CNCs. The main reason for these enhancements was ascribed to the increases in the crystalline content of PLA for modified CNC-filled samples. However, the strain at break significantly decreased by more than 70 % relative to the neat PLA. The addition of larger content of silane modified CNCs resulted in to lower enhancements, probably due to the plasticization effect of the silane modifier.

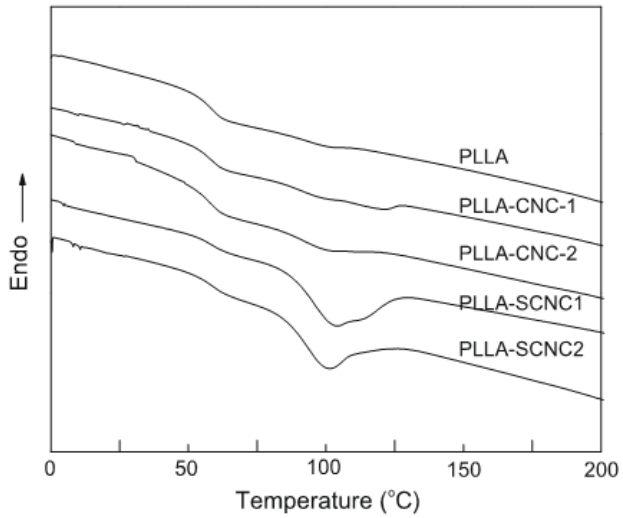

Figure 2.16: DSC runs in cooling cycles for PLLA and PLLA containing partially silylated (SCNC) and unmodified CNCs with final concentration of 1 and 2 wt% (from Ref. [45])

Fortunati et al. [46] investigated the effect of unmodified and surface modified CNCs, with an acid phosphate ester of ethoxylatednonylphenol, on the tensile properties of PLA. The composites were prepared by a solvent casting process in a chloroform medium. Table 2.7 reports

the tensile properties of the samples. By the addition of unmodified CNCs the tensile strength was increased. However, by surface modification the properties were decreased compared to the unmodified systems due to the plasticization effect of the surfactant on the properties of PLA, although it might favor a better dispersion of the particles within PLA matrix. However, the reported values are not typical of PLA, especially elongation at break which has been extensively reported smaller than 10%.

Table 2.5: Thermal parameters of PLLA and PLLA containing partially silylated (SCNCs) and unmodified CNCs with final concentrations of 1 and 2 wt%. Data derived from the heating DSC scans (adapted from Ref. [45])

Sample	T_m (^{0}C)	ΔH_m (J/g)[a]	ΔH_{cc} (J/g)[a]	X_c (%)
PLLA	171.4	25.8	12.5	14.3
PLLA-CNC-1	171.4	28.2	12.9	16.4
PLLA-CNC-2	171.8	30.3	16.0	15.0
PLLA-SCNC-1	171.8	32.3	4.0	30.4
PLLA-SCNC-2	171.4	29.4	10.1	20.7

[a] Data corrected for the percentage of PLLA in the nanocomposites.

Table 2.6: Tensile properties of PLLA and PLLA-CNC composite films at room temperature (adapted from Ref. [45])

Sample	Tensile modulus (GPa)	Tensile strength (MPa)	Elongation at break (%)
PLLA	1.1 ± 0.01	48.3 ± 2.9	31.1 ± 3.0
PLLA-CNC-1	1.0 ± 0.02	49.2 ± 0.4	10.5 ± 2.0
PLLA-CNC-2	1.2 ± 0.03	48.3 ± 0.4	12.2 ± 0.2
PLLA-SCNC-1	1.4 ± 0.08	58.6 ± 3.1	8.3 ± 0.6
PLLA-SCNC-2	1.4 ± 0.04	53.8 ± 2.1	7.1 ± 1.8

Table 2.7: Tensile properties of PLA and PLA containing surface modified (s-CNCs) and unmodified CNCs. The numbers in the formulation represent the concentration of CNCs in the systems, namely 1 and 3 wt% (adapted from Ref. [46])

Sample	Yield stress (MPa)	Elongation at yield (%)	Tensile strength (MPa)	Elongation at break (%)	Young modulus (MPa)
PLA	14.7 ± 5.1	2.3 ± 0.5	16.5 ± 3.1	277.9 ± 33.6	1205 ± 100
PLA-1CNC	31.3 ± 1.6	3.0 ± 0.5	27.1 ± 6.3	200.1 ± 53.3	1330 ± 90
PLA-1s-CNC	22.9 ± 4.2	2.6 ± 0.6	22.9 ± 1.2	286.1 ± 25.2	993 ± 190
PLA-3CNC	42.1 ± 2.0	2.7 ± 0.6	21.9 ± 3.5	100.9 ± 27.9	1930 ± 170
PLA-3s-CNC	25.7 ± 4.8	3.1 ± 0.1	20.2 ± 1.9	210.4 ± 48.1	800 ± 100

Raquez et al. [13] utilized different organosilanes to modify the surface of CNCs for a better compatibility with a PLA matrix. They investigated the effect of CNC surface modification and annealing on mechanical properties of a poorly crystallizable PLA matrix. The surface modified CNCs were melt-compounded with PLA in a mini extruder. The samples for DMTA testing were prepared by injection molding followed by annealing at 110 °C for 90 min. Table 2.8 reports the storage modulus values for the neat PLA and PLA containing different silane-surface modified CNCs at the final CNC concentration of 3 wt%. Significant enhancements were observed for annealed PLA samples. The main reason was ascribed to the increases in the crystalline content of PLA caused by adding modified CNCs. However, the results of unmodified and unannealed samples were not reported to assess the effect of the modification and annealing separately.

Table 2.8: Storage modulus, *E'*, of annealed PLA and PLA filled with silane-surface modified CNCs (adapted from Ref. [13])

Sample	Storage modulus at 25 ^{0}C (MPa)
PLA	1300
Amino-based CNCs	3740
n-Propyl-based CNCs	4250
Methacrylic-based CNCs	4360
Acrylic-based CNCs	4130

Arias et al. [47] reported that when uncompatibilized CNCs are added into PLA via a direct melt mixing large agglomerates were formed. Figure 2.17 depicts the effect of PEO as a compatibilizer on the CNC dispersion within the PLA matrix. Figure 2.17a presents a SEM micrograph of PLA containing 3 wt% CNCs prepared via direct melt mixing. The presence of very large agglomerates as large as few tens of μm is observed. To favor a better dispersion and wetting of CNCs within PLA, Arias et al. [47] initially prepared masterbatches of PEO-CNC with different PEO/CNC ratios by solvent casting in an aqueous medium. Thereafter, they melt mixed the freeze-dried mastrebatches with PLA using an internal mixer. The addition of PEO as a compatibilizer did not show any improvement in the quality of the dispersion; contradictory, a coarser morphology was observed by the incorporation of PEO (Figure 2.17b). However, when the ratio of PEO/CNC in the masterbatch increased a finer and well-distributed morphology was achieved (Figure 2.17c). Therefore, they demonstrated that the ratio of compatibilizer to CNC plays an important role in the quality of dispersion. Despite fine and well-distributed dispersion

of CNCs within PLA, Arias et al. [47] observed slight decreases in the complex viscosity of the PEO compatibilized PLA-CNC samples. Moreover, the employment of PEO as a compatibilizer of PLA-CNC system did not result in enhancing the tensile properties from tensile and DMTA tests. Probably, the reinforcement effect of CNCs was compromised by the plasticization effect of PEO.

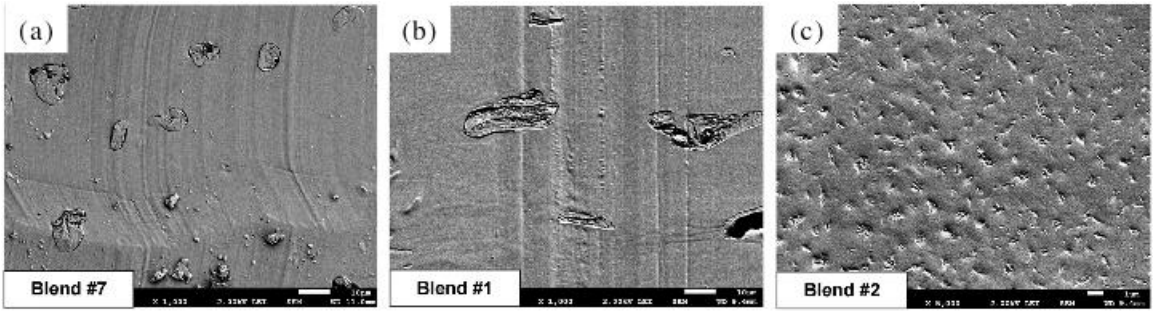

Figure 2.17: Effect of PEO as a compatibilizer on CNC dispersion in a PLA matrix: (a) PLA-CNC prepared via direct melt mixing (scale bar: 10 μm), (b) and (c) PLA containing PEO-CNC masterbatch with high molecular weight PEO and PEO/CNC: 0.25 and 1 (scale bars: 10 (a,b) and 1 μm for (c)), respectively. All samples contain 3 wt% CNC (adapted from Ref. [47])

2.8 Rheological behavior of polymer nanocomposites

For many years rheology has been employed as a powerful tool to understand the interactions between the components of polymer nanocomposites. The formation of an interconnect network of particles plays an important role on the rheological behavior of a nanocomposite system that can reveal whether the preparation method was efficient in leading to nano dispersion. Therefore, in this section we will summarize the possible effects of different nanoparticles on the melt rheological behavior of polymer nanocomposites. Moreover, some of the useful rheological measurements that are sensitive to interactions between the nanoparticles will be introduced. In this section, we review the effects of other commonly used nanoparticles, namely carbon nanotubes (CNT) and nanoclays, on the melt rheological behavior of polymer matrices. The effect of CNCs on some rheological properties, i.e. complex viscosity and loss and storage moduli, for polymer-CNC systems are discussed in the previous sections.

2.8.1 SAOS

The effects of CNCs on the SAOS data for polymer-CNC systems were discussed earlier in this chapter. Transition from a liquid-like behavior for polymer matrices to a solid-like behavior for nanocomposites and huge increases of the dynamic rheological properties such as complex viscosity, storage and loss moduli for nanocomposites relative to those of matrices, especially at low frequencies, are among the main effects caused by CNCs. The behavior of polymer nanocomposites in the low-frequency region is governed by the interactions between the nanoparticles and the formation of an interconnected network of nanoparticles. Such a network is formed at concentrations above the rheological percolation threshold and will affect significantly the rheological properties. A rough estimation of the rheological percolation threshold can be obtained when the complex viscosity is plotted versus complex modulus. Figure 2.18 presents the log-log plot of the complex viscosity versus complex modulus for a polycarbonate (PC) and PC-CNT systems obtained from SAOS data. For PC and PC-CNT nanocomposites with 0.2 and 0.5 wt% CNT no viscosity upturn was observed, while at larger CNT loadings, namely 1, 2 and 5 wt%, unbounded viscosity was observed corresponding to an apparent yield stress. It is believed that the observation of an apparent yield stress occurred at concentrations larger than rheological percolation threshold. In fact, the onset of the solid-like behavior was at the rheological percolation threshold. Therefore, the rheological percolation threshold would fall in the range of 0.5-1 wt% CNTs. To have a more precise idea about the rheological percolation threshold, storage modulus data at low-frequency region of SAOS tests can be used. Figure 2.19 reports the storage modulus in the low-frequency region for PC-CNT samples with different CNT loadings. The following empirical power-law equation can be used to fit the data in order to obtain the rheological percolation threshold:

$$G' = \beta_c G \left(\frac{m - m_c G}{m_c G}\right)^n \text{ for } m > m_c G \quad (2.2)$$

where $\beta_c G$ and n are power-law constants, m is the CNC concentration (wt%) and $m_c G$ is the rheological percolation threshold (wt%) [48, 49]. Abbasi et al. [48] obtained a value of 0.66 wt% for the rheological percolation threshold of PC-CNT nanocomposites at 230 °C.

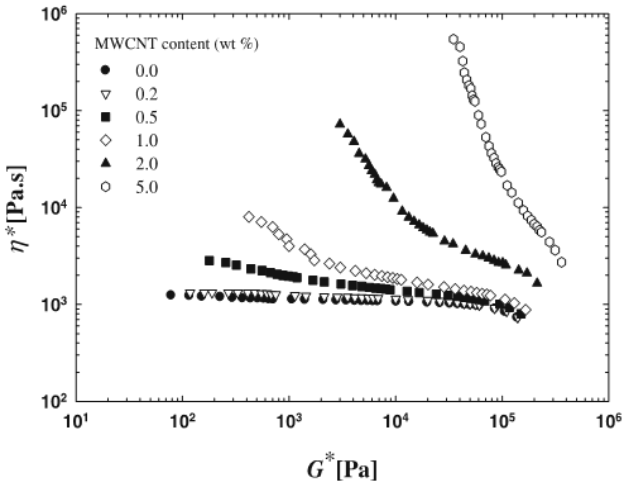

Figure 2.18: Plots of the complex viscosity vs complex modulus for polycarbonate-CNT nanocomposites at 230 °C (from Ref. [48])

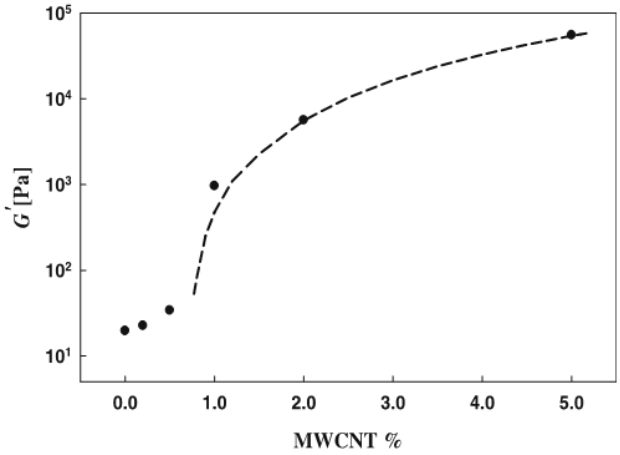

Figure 2.19: Storage modulus as a function of the nanotube loading for PC-CNT nanocomposites at 230 °C (1 rad.s^{-1} data). The line is a fit with the power-law expression (Eq. 2-2) (from Ref. [48])

2.8.2 Steady-shear tests

Similar to the behavior shown previously in SAOS experiments, a shear-thinning behavior without any plateau region and unbounded viscosity at low shear rates for polymer nanocomposites are observed in steady-shear tests while the neat polymer matrices usually exhibit a plateau region at low shear rates. Gupta et al. [50] investigated the effect of nanoclay

(cetyl-dimethyl-ethyl-ammonium bromide-modified sodium-bentonite clay) content on the rheological properties of an ethylene vinyl acetate copolymer (EVA) with 28 wt% vinyl acetate content (EVA28). Figure 2.20 illustrates the steady-shear viscosity versus shear rate for EVA-clay nanocomposites with different nanoclay loadings. A long plateau region for the matrix is observed, as expected, while by the addition of the nanoclay the plateau region disappears and a shear-thinning behavior is observed. The interactions between clay layers become stronger at higher clay contents as the distance between layers becomes smaller. Therefore the possibility of network formation increases and as a result increased viscosity with a more pronounced shear-thinning behavior is observed for larger nanoclay loadings.

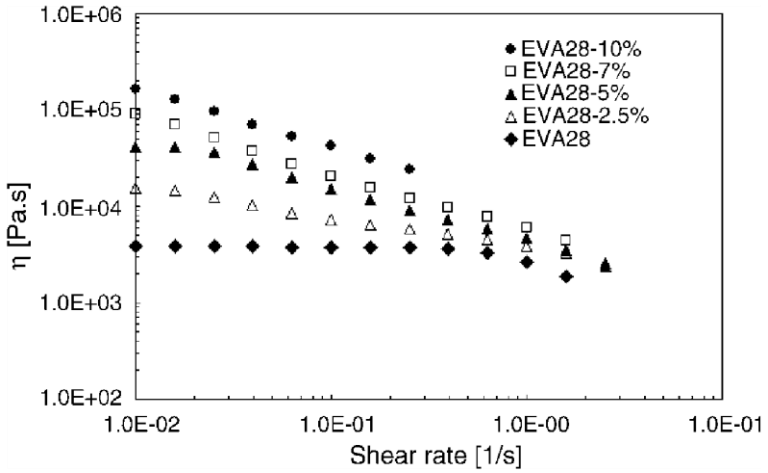

Figure 2.20: Steady-shear viscosity for EVA28-nanoclay nanocomposites as a function of shear rate at 130 °C (from Ref. [50])

2.8.3 Transient tests

Figure 2.21 presents shear stress-strain curves from transient tests for PP/PP-g-MA as matrix and PP/PP-g-MA/Cloisite 20A (a modified nanoclay) (80/15/5) [51]. The matrix does not show any overshoot and immediately after the test starts a plateau behavior for the stress versus strain is observed. However, in the filled sample at the beginning of the test an overshoot is observed revealing that the systems is structured. In fact, an interconnected network of nanoparticles is responsible for that overshoot. These transient tests are destructive; consequently, when the structure is broken down sample exhibits a plateau (Figure 2.21a). The network will be rebuilt

under rest, partially or completely depending on the rest time. If the rest time is sufficient long the structure can be rebuilt completely and the same overshoot as the forward flow will be observed. Figure 2.21b depicts the behavior of the samples for the reverse transient flow. No overshoot is observed when the reverse test is performed right after the forward flow. Small overshoots are seen after 300 s rest time while after a longer rest time (600 s) a larger overshoot is observed; after 1200 s rest time almost the same overshoot as for the forward flow is observed, meaning that the initial structure is completely rebuilt. In fact in the forward flow, the structure in the sample is broken down and the nanoparticles orient themselves in the flow direction. When the flow is immediately reversed the nanoparticles do not have the time to form any structure, exhibiting no overshoot. However, after sufficient rest time particle-particle interactions increase and, consequently, the structure is gradually rebuilt and finally the same structure as before the shear test is formed after 1200 s rest time (Figure 2.21b).

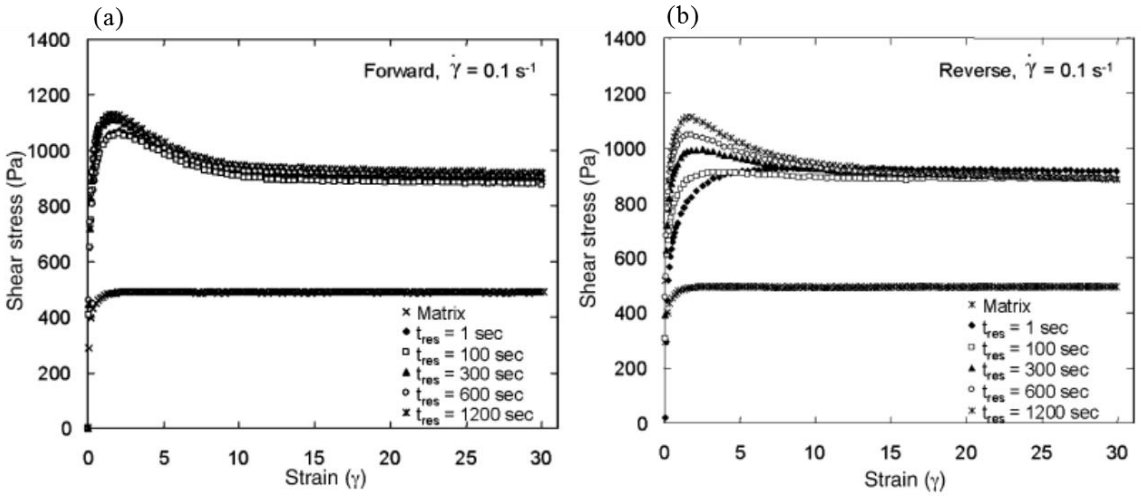

Figure 2.21: (a) Shear stress growth as a function of strain for PP/PP-g-MA/Cloisite 20A (80/15/5) at T = 180 °C and shear rate of 0.1 s^{-1} for: (a) repeated forward flow tests and (b) reverse flow tests after various rest times. The rest times of the legend correspond to those for the reverse transient experiments (adapted from Ref. [51])

2.8.4 Structure build-up tests

The reformation of the broken structure for polymer nanocomposites can also be monitored by structure build-up tests. Basically, the initial structure of the nanoparticles within a polymer matrix is broken down by a shear flow and the behavior of the storage modulus as a function of

time right after the cessation of the shear flow is monitored. Figure 2.22 presents a structure build-up test conducted on a blend of two miscible polybutenes filled with nanoclay (Cloisite 15A). Steady-shear tests at different shear rates were performed to break down the structure of the system, each time on a fresh sample (Figure 2.22a). Right after the cessation of shear flows a time sweep test in SAOS mode was conducted and the evolution of storage modulus was monitored (Figure 2.22b). The storage modulus of the sample increased regardless of the magnitude of the initial shear rate. Observation of increased storage modulus is an indication of reformation of the structure in the system (Figure 2.22b). For the test performed after an applied shear rate of 25×10^{-3} s^{-1} more than a three-fold increase is observed for the storage modulus compared with that obtained after the applied shear rate of 10^{-3} s^{-1}. Obviously, the resulting structures are dependent on the initial shear flow test. Moreover, for larger pre-shear rates the initial structure of the systems was more destroyed and a larger recovery can be observed after the cessation of shear flow and of course in a longer time.

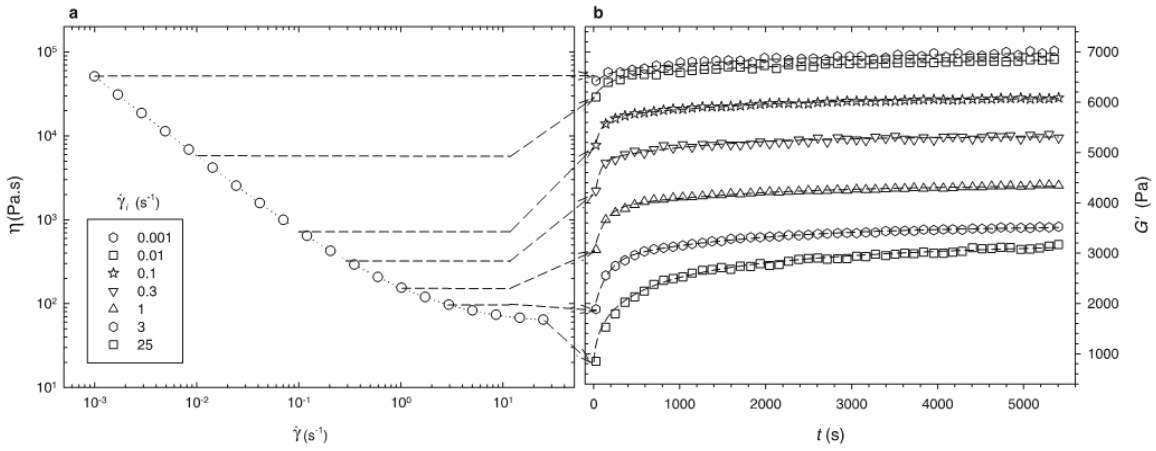

Figure 2.22: Structure changes under preconditioning: (a) steady viscosity vs shear rate and (b) evolution of the storage modulus in time sweep tests at a frequency of 125.6 rad.s^{-1} right after cessation of the steady-shear test carried out in (a). Symbols correspond to the values of the initial shear rates (from Ref. [52])

2.9 Summary

Different methods that can be employed to enhance the compatibility of CNCs with PP and PLA in order to promote the dispersion of the CNCs and enhance the properties of the matrices were briefly discussed. There are very few investigations that employed an efficient method of

preparation that led to the development of PP-CNC or PLA-CNC nanocomposites with a dispersed structure and enhanced properties. However, CNCs used in those investigations had large aspect ratios (more than 70). Moreover, no systematic investigation on the effect of CNCs and their network on the rheological and thermomechanical properties of PP-CNC and PLA-CNC systems has been performed yet. Therefore, this research is planned to fill this gap in the literature by using a low aspect ratio CNC. Therefore, in this research only the use of functionalized polymers/copolymers was investigated to develop PP-CNC nanocomposites. The molecular weight of the compatibilizer should not be lower than that of matrix to avoid the plasticization effect. Also the functional groups of the compatibilizer should be sufficient to partially cover the numerous hydroxyl groups of the CNC surface; otherwise the hydrophilic nature of CNCs remains intact and would cause aggregation/agglomeration when these particles are introduced into PP or PLA matrices. For developing PLA-CNC nanocomposites a simple preparation method was employed in this work that avoids the use of any surface modification or compatibilization.

CHAPTER 3 OBJECTIVES

Taking into account the current knowledge on biocomposites based on non water-soluble polymers and cellulose nanocrystals, the main objective of this research is **to develop polymer nanocomposites from renewable cellulose nanocrystals (CNCs) with dispersed structure and enhanced mechanical properties**.

To reach the main objective, two thermoplastic polymer matrices will be used: a biobased polymer, a polylactide, and a petroleum-based polymer, a polypropylene, and the specific objectives are defined as

1. To enhance the properties of PP by incorporating cellulose nanocrystals. To do this, use of a functionalized polymer/copolymer as a compatibilizer is investigated. A masterbatch preparation method is used to favor the dispersion of the CNCs within PP and the behavior of the systems in melt and solid states is studied.

2. To develop well-dispersed PLA-CNC bionanocomposite and investigate the effect of the dispersed structure on the melt rheological behavior of the composites. Moreover, the efficiency of the melt and solution preparation methods is investigated by means of rheology.

3. To enhance the thermomechanical properties of PLA by incorporation of CNCs without the need of compatibilization.

CHAPTER 4 ORGANIZATION OF THE ARTICLES

The main results from this research are presented in the form of three articles, which are the subject of chapters 5, 6 and 7.

In chapter 5, the use of poly(ethylene-co-vinyl alcohol) as a compatibilizer to promote the dispersion of CNCs within the system and enhance the properties of PP is studied. First, two masterbatches consisting of poly(ethylene-co-vinyl alcohol) and CNCs via two different approaches, namely solution and melt preparation, are prepared. Then, these masterbatches are melt-compounded with PP using a batch internal mixer. The efficiency of each masterbatch to enhance the melt and solid properties of PP is studied. This chapter was published as a scientific article in Composite Science and Technology (2014 impact factor: 3.569) in 2015.

Chapters 6 and 7 deal with the development of PLA-CNC bionanocomposites without need of any modification or compatibilization through a simple method of solution preparation that results in a dispersed structure. In chapter 6, the bionanocomposites are characterized in terms of their rheological behavior in different shear flows to understand the effect of the dispersed structure and CNC content on the melt behavior of PLA composites. This chapter was submitted as a scientific article to the journal of Cellulose (2014 impact factor: 3.573) in November 2015. In chapter 7, the effect of the CNCs on thermomechanical properties of PLA is investigated. This chapter as a scientific article was submitted to the journal of Cellulose in December 2015.

CHAPTER 5 ARTICLE 1 : PROPERTIES OF POLYPROPYLENE AND POLYPROPYLENE/POLY(ETHYLENE-CO-VINYL ALCOHOL) BLEND/CNC NANOCOMPOSITES[2]

D. Bagheriasl[a], P.J. Carreau[a*], C. Dubois[a], B. Riedl[b]

[a]Research Center for High Performance Polymer and Composite Systems (CREPEC), Chemical Engineering Department, Polytechnique Montreal, PO Box 6079, Stn Centre-Ville, Montreal, QC H3C 3A7, Canada

[b]Département des sciences du bois et de la forêt, Faculté de foresterie, géographie et géomatique, Université Laval, Quebec, QC G1V 0A6, Canada

Abstract

Rheological, mechanical and thermal properties of polypropylene (PP)/cellulose nanocrystal (CNC) nanocomposites were compared with those of nanocomposites containing poly(ethylene-co-vinyl alcohol) used as a compatibilizer (CO). The nanocomposites were prepared by an internal mixer at a CNC content of 5 wt%. The complex viscosity and storage modulus of the nanocomposite sample containing the compatibilizer prepared by a solution method were increased at low frequencies, compared to those of the non-compatibilized nanocomposite samples. Moreover, a pronounced overshoot of the transient viscosity in a shear stress growth experiment was observed for the compatibilized nanocomposite. Scanning electron microscopy (SEM) showed the disappearance of large agglomerates when using the compatibilizer. The Young modulus of the nanocomposite samples containing the compatibilizer was increased up to ca. 47 % compared to the neat PP. The elongation at break was decreased in all PP/CNC nanocomposite samples, but less for those containing the compatibilizer. The crystallinity of the PP in the nanocomposites and the crystallization temperature were increased after

[2] Published in Composites Science and Technology. 2015;117:357-363.

compatibilization. These results show that the poly(ethylene-co-vinyl alcohol) is an efficient compatibilizer that favors a better dispersion and wetting of the hydrophilic CNCs within the hydrophobic PP phase.

Keywords: A.Nano composites; A.Cellulose nanocrystals (CNCs); A.Polymers; B.Thermomechanical properties; D.Rheology

5.1 Introduction

In spite of the interesting properties of cellulose nanocrystals (CNCs), such as abundance in nature, biodegradability, low density, high strength, etc. [1], their applications as a reinforcing agent in polymer nanocomposites remain limited to only a few hydrophilic polymers such as polyvinyl alcohol (PVOH) [2-4] and polyethylene oxide (PEO) [5] and hydrophobic polymers in latex form [6, 7]. Strong inter-particle interactions due to hydrogen bonds lead CNCs to form agglomerates, sometimes as large as few tens of micrometers, when introduced into nonpolar matrices [8]. Consequently due to a lack of strong interface between the matrix and substrate, achieving enhanced mechanical properties with more widespread polymers such as hydrophobic polyolefins is challenging. Thus, compatibilization is a key issue to improve the properties of CNC-hydrophobic polymer composites [9-14]. To this end, surface treatments of CNCs, functionalization of polymer matrices and the use of a third component as a compatibilizer or a coupling agent are possible methods that could be used.

CNC surface treatments can be achieved via a wide variety of plasma [15] and corona [16] treatments and chemical modifications, such as acetylation or esterification [17], tempo-mediated oxidation [18, 19], grafting [11, 12, 20-22] and cationization [19, 23]. With surface modification of cellulose nanocrystals (CNCs), stable suspensions in nonpolar solvents such as toluene and cyclohexane can be obtained, but the mechanical properties of the resultant nanocomposites may remain unchanged or even reduced, compared to the unmodified polymer/CNC nanocomposites [24-26]. The possible reasons could be either desulfonation of sulfonate groups during processing conditions or a decrease in the thermal degradation temperature of the modified CNCs during the nanocomposite preparation [27].

To enhance the mechanical properties and dispersion of the cellulosic particles, coupling agents and compatibilizers have also been used. Coupling agents are chemical reagents that can create

covalent or hydrogen bonds between the matrix and the dispersed particles. Among commercially available coupling agents, two classes showed good results in terms of increasing compatibility. They are organosilanes and titanates [28-30]. A better state of dispersion will be achieved when these chemicals are used. However, due to plasticization effects the mechanical properties of the treated composites will not be affected significantly, if not reduced.

Another approach to obtain a fairly good dispersion and, consequently, acceptable mechanical properties for composites reinforced by micro- or nanoparticles is the use of functionalized polymers such as polypropylene graft maleic anhydride (PP-g-MA), polypropylene graft acrylic acid (PP-g-AA), polylactide graft maleic anhydride (PLA-g-MA), poly(ethylene-co-vinyl acetate) (EVAc) or poly(ethylene-co-vinyl alcohol) (EVOH). Ljungberg et al. [26] used PP-g-MA (7.5 wt% MA) as a compatibilizer for atactic polypropylene (aPP) reinforced with CNCs. They observed a reduction in mechanical properties in the compatibilized system compared to the uncompatibilized one. Arias et al. [31] also reported no significant improvement in Young modulus in tensile tests and elastic modulus in DMTA and reduced tensile strength for PEO compatibilized PLA/CNC systems compared to uncompatibilized systems. However, Sojoudiasli et al. [32] showed enhanced tensile properties for PP-g-MA and PP-g-AA compatibilized polypropylene/flax fiber composites. They concluded that the efficiency of the employed compatibilizers depended on their melt flow index (MFI) and grafted maleic anhydride or acrylic acid content. Therefore, Epolene E43 with the highest content of maleic anhydride was found to be the most efficient in improving both the dispersion of the fibers and tensile properties of the resulting composite. Sonia et al. [33] investigated the mechanical properties and thermal aging of poly(ethylene-co-vinyl acetate) (18 % vinyl acetate content) reinforced with different cellulose micro fiber (CMF) loadings from 0 to 15 wt%. The microcomposites containing 7.5 wt% CMFs had the best mechanical properties. Tensile and tearing strength, elongation at break and dynamic storage modulus of the reinforced systems increased with CMF loading up to a concentration of 7.5 wt%; however, above that concentration, the properties decreased and the mechanical properties of microcomposites containing 15 wt% CMFs were almost the same as those of the unfilled system. A comparison of SEM images of EVA/CMF composites containing 5 wt% and 10 wt% showed a more uniform dispersion of fibers at 5 wt% loading compared to the composite containing 10 wt% CMFs. Copolymers with a hydrophilic moiety, usually vinyl acetate and vinyl alcohol, were used by Sonia et al. [33] and, to our knowledge, there is no other similar

investigations in the literature. However, the properties of PVA (polyvinyl alcohol) reinforced by cellulose nanocrystals (CNCs) had been previously investigated by other researchers [2, 4]. Abitbol et al. [4] prepared PVA/CNC hydrogels and observed that the elastic modulus of the PVA/CNC nanocomposites was increased relative to those of the neat PVA hydrogel. A decrease in the degree of the crystallinity for the reinforced hydrogels was observed compared to the neat PVA hydrogel, probably due to the increased interactions between CNCs and PVA chains and, consequently, the hindrance effect of CNCs on the mobility of PVA chains. In another work, Peresin et al. [2] produced PVAs reinforced with cellulose nanocrystals via an electrospinning technique. Two PVAs having approximately the same molecular weight (125 000 and 127 000 Daltons) but differing in the residual acetyl content (2 and 12 %) were used. For nonwoven mats of PVA/CNCs a 3-fold increase was observed at 15 wt% CNC content for the storage modulus of the samples prepared with fully hydrolyzed PVA compared to the neat PVA. This could be due to the strong interactions between the CNCs and the fully hydrolyzed PVA matrix, which results in an efficient stress transfer between the CNCs and PVA matrix. This effect was not observed for the partially hydrolyzed PVA/CNC electrospun nanocomposites.

In this work the effect of the CNCs on the rheological, mechanical and thermal properties of polypropylene was investigated. To this end, poly(ethylene-co-vinyl alcohol) was used as a compatibilizer to favor a better dispersion and wetting of hydrophilic CNCs within the hydrophobic polypropylene (PP) matrix via two different masterbatch preparation methods, in molten and solution states. Our objective is to develop PP/CNC nanocomposites with enhanced mechanical properties at low CNC loadings.

5.2 Experimental

5.2.1 Materials

A commercial grade polypropylene (PP) (Pro-fax 6323) with MFR of 12 g/10 min (230 °C/2.16 kg) and melting point of 166 °C was provided from LyondellBasell (Houston, TX, USA) and used as the matrix. A poly(ethylene-co-vinyl alcohol) with ethylene content of 27 mol% (CO) and MFI= 3.9 g/10 min (210 °C/2.16 kg) and N,N-dimethylformamide (DMF), anhydrous 99.8 %, were purchased from Sigma-Aldrich Canada Co. (Oakville, Ontario, Canada) and, finally, the spray-dried CNCs were kindly provided by FPInnovations (Pointe-Claire, QC, Canada). Based

on the information provided by the supplier, the average length and diameter of individual CNCs are about 100 and 15 nm, respectively.

5.2.2 Sample preparation

Two types of masterbatches of the CNCs and the compatibilizer (CO) were produced via melt mixing and solution mixing. To prepare the masterbatch via melt mixing, the CNCs and CO were introduced in an internal mixer (C.W. Brabender Plasticorder) and melt-compounded at 210 °C, 100 rpm for 7 min under N_2 atmosphere. Then, the product was grinded into small granules. To prepare the masterbatch via solution mixing, the CNCs were first dispersed in DMF using a water-bath sonicator, then the desired amount of CO was added and the mixture was heated up to 60 °C while stirring with a magnetic stirrer until the complete dissolution of the CO. The mixture was then poured on a tray and dried in a vacuum oven at 80 °C for 24 h. The product was grinded into powder and/or small granules that were kept in the oven at 50 °C overnight. The ratio of CO to the CNCs in both masterbatches was 3/1 wt/wt. In the final step, to produce PP/CO/CNCs nanocomposite samples, the masterbatches were melt-compounded with PP via the internal mixer at 210 °C, 100 rpm for 10 min under N_2 atmosphere. Thereafter, the samples were compression molded for 14 min at 205 °C in the presence of N_2 to prepare the test specimens.

5.2.3 Characterization

The rheological properties of PP and the nanocomposites were measured using a stress-controlled Anton Paar MCR 301 rheometer. The experiments were conducted under nitrogen to avoid oxidation of the samples. A parallel plate geometry was used with a gap of 1 mm and a plate diameter of 25 mm. Frequency sweeps in small-amplitude oscillatory shear (SAOS) at a strain amplitude of 5 % and shear stress growth experiments were carried out on the samples at 195 °C.

Tensile properties of the samples were measured using an Instron 3365 at room temperature according to standard ASTM D638. Tensile specimens, of dog-bone shape type V, were stretched at room temperature with a crosshead speed of 5 mm/min using a load cell of 500 N. For each sample a minimum of 6 specimens were tested.

Differential scanning calorimetry (DSC) of PP and the nanocomposites was performed on a DSCQ1000 (TA Instruments, New Castle, DE, USA) on typically 10 mg of material, under a nitrogen atmosphere. The samples were heated from room temperature to 250 °C at a constant

rate of 10 °C/min and held at that temperature for 5 min, then cooled to -30 °C with the same rate. The DSC tests were performed twice for each sample with a fresh specimen.

Dynamic mechanical thermal analysis (DMTA) was performed on compression-molded samples using a DMA 2980 analyzer (TA Instruments, New Castle, DE, USA). The specimens were tested in the dual cantilever bending mode at an amplitude of 30 μm, a frequency of 1 Hz, and a heating rate of 3 °C/min from −70 to 140 °C.

Scanning electron microscopy (SEM) analysis was carried out on ultra-microtomed surfaces, coated with Platinum. The microscope was a JEOL JSM 7600TFE Scanning Electron Microscope (SEM) (JEOL USA Inc., Peabody, MA, USA) operated at a voltage of 2 kV.

5.3 Results and discussion

5.3.1 SEM analysis

Figure 5.1 compares SEM micrographs of PP/5CNC and PP/15SCO/5CNC. In Figure 5.1a and b, a few micron size agglomerates of CNCs together with some smaller fibrillated agglomerates are observed, which reveal the incompatibility of the CNCs with PP. However, in Figure 5.1c and d, we see how the compatibilization could lead a better state of dispersion with the absence of agglomerates. We observe also in Fig. 5.1c the presence of the dispersed phase (copolymer) as droplets of diameter ranging from 1-3 μm, showing that the poly(ethylene-co-vinyl alcohol) and the PP used are immiscible. Our efforts to localize the CNC particles using transmission electron microscopy (TEM) were unsuccessful for these composites. However, we could get clear TEM images for similar nanocomposites based on a larger molecular weight PP and the same poly(ethylene-co-vinyl alcohol) (see supplementary Figures 5.S1 and 5.S2). These images show individual CNCs dispersed into the PP matrix and the formation of a network. For the systems discussed here, we assume that initially the CNCs are well dispersed in the solution of the copolymer in the DMF solution and, then, when mixed at high temperature the nanoparticles diffuse in a large quantity to the PP matrix. According to Khoshkava and Kamal [8] the surface energy of CNCs is reduced at high temperatures compared to that of PP and become close to the value of PP; the interfacial tension between CNCs and PP is lowered at high temperatures. Therefore, the compatibility of PP and CNCs enhanced at high temperatures.

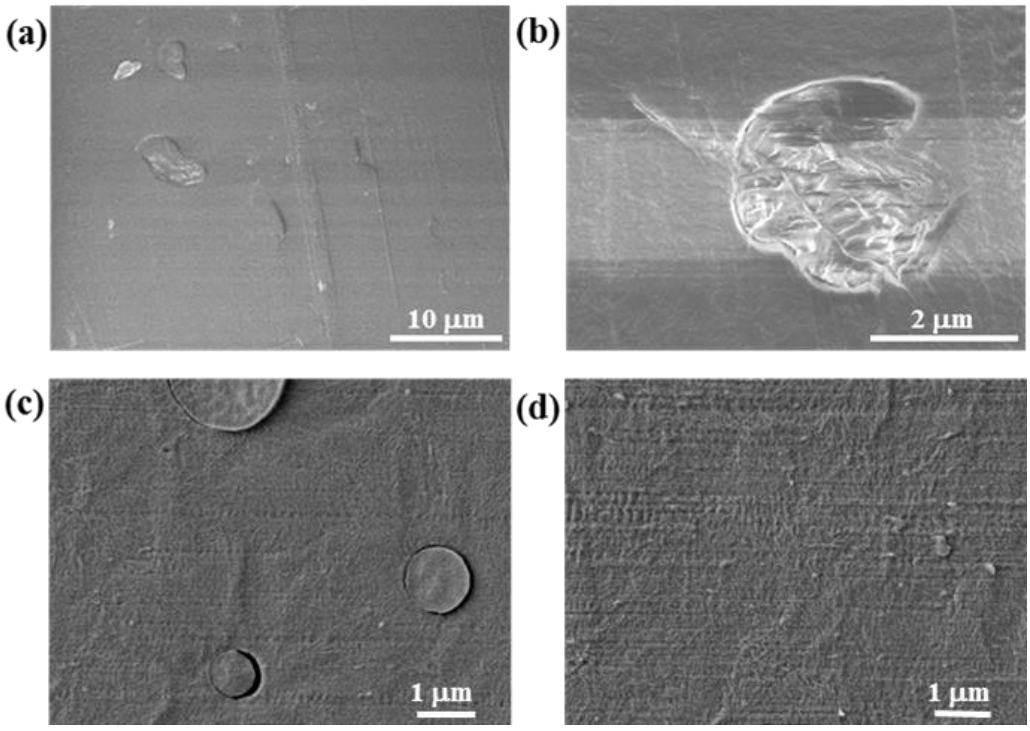

Figure 5.1: SEM micrographs of two different locations of PP/5CNC (a) and (b), and PP/15SCO/5CNC (c) and (d)

5.3.2 Rheology

All the samples exhibited stable rheological properties in time-sweep experiments, with changes less than 10 %. The results for the complex viscosity, η^*, and storage modulus, G', versus frequency, ω, of all samples are illustrated in Figure 5.2. The behavior of the neat PP and PP containing 15 wt% compatibilizer is typical of that of molten polymers, exhibiting a plateau for η^* at low frequencies and a shear-thinning behavior at large frequencies (Figure 5.2a) and a terminal zone with a slope of 2 on the log-log plot of G' vs. ω (Figure 5.2b). Slight increases for both η^* and G' of PP containing 15 wt% compatibilizer (PP/15CO) and PP and PP/15CO containing 5 wt% CNC (PP/5CNC, PP/15CO/5CNC) are observed in Fig. 5.2, compared to the neat PP. With the use of CO, η^* of PP/15CO is slightly increased in comparison with that of PP. With the addition of the CNCs no differences are observed when the masterbatch was prepared via melt mixing. Surprisingly, the nanocomposite sample for which the CO/CNC masterbatch was prepared via solution mixing (PP/15SCO/5CNC) exhibits a shear-thinning behavior for η^* without any plateau region at low frequencies and G' that tends towards a plateau at low

frequencies. This is the indication of the formation of a network and a transition from liquid- to solid-like behavior as observed for many polymer nanocomposites, attributed to the more efficient dispersion of the CNCs in the copolymer in solution with sonication. Similar rheological behavior in SAOS has been reported for other polymer nanocomposites containing CNCs, clays or carbon nanotubes [34-36]. It is well known that an interconnected structure of nanoparticles in a polymeric matrix can result in an apparent yield stress with an unbounded viscosity and a plateau in G' at low frequencies. Strangely enough as seen in Fig. 5.2 the viscosity and storage modulus for the solution-based nanocomposite (PP/15SCO/5CNC) are lower at high frequencies than the based matrix (PP of PP/15CO). That could have been due to the presence of traces of solvent left into the nanocomposite; however, the complex viscosity of the PP/15CO was found to be identical to that of the solution prepared matrix (PP/15SCO).

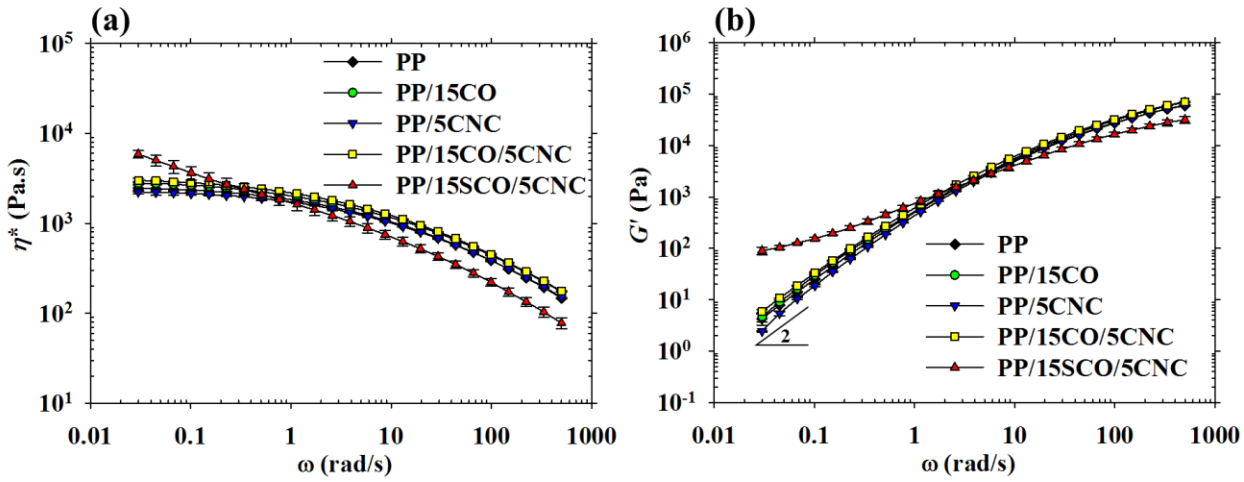

Figure 5.2: Complex viscosity (a) and storage modulus (b) versus frequency of the neat PP, PP containing 15 wt% compatibilizer and nanocomposites in SAOS at 195 °C (strain = 5 %)

Figure 5.3 presents the variations of the transient viscosity with time in a shear stress growth experiment. No overshoots are observed for the neat PP and PP/15CO and a very small one (barely visible in the figure) is depicted for PP/5CNC, probably due to a poor dispersion of the CNCs and the presence of large agglomerates, as large as few μm as shown above. For the sample in which the masterbatch was prepared via melt mixing (PP/15CO/5CNC), a larger overshoot is observed, but to a lesser extent than what is seen for the nanocomposite prepared via

the solution method (PP/15SCO/5CNC). This very large overshoot is again an indication of a strong network made by the nanoparticles, confirming the behavior observed in SAOS (Fig. 5.2). We note that this stress growth experiment is destructive and the rapid decrease following the peak is the result of the network destruction. The rheological properties reported in this section are in good agreement with the SEM micrographs and show the efficiency of the sonicator in solution mixing to disperse the CNCs with the consequent formation of an interconnected network of CNCs.

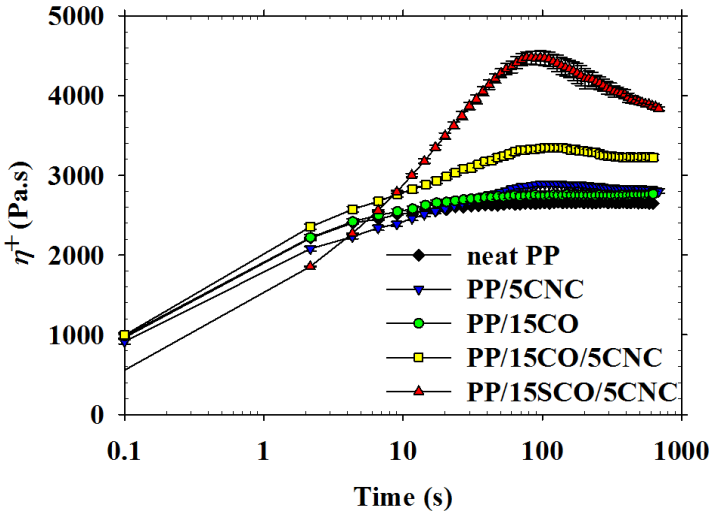

Figure 5.3: Variations of the transient viscosity with time for a shear stress growth experiment at $\dot{\gamma}$ = 0.02 s^{-1} and T = 195 °C

5.3.3 Mechanical and thermal properties

5.3.3.1 Tensile properties

The Young modulus, maximum tensile strength and elongation at break of the samples are compared to those of the neat PP in Figure 5.4. The Young modulus of PP is increased with the addition of CNCs and the compatibilizer (CO) by ca. 13 % and 26 %, respectively, as seen in Figure 5.4 a. A synergistic effect is observed in the nanocomposite samples containing both the CNCs and CO as the Young modulus increased by ca. 36 % when the masterbatch was prepared via melt mixing and ca. 47 % when the masterbatch was prepared via solution mixing. Here again

one can see another proof that the solution mixing method was more efficient for preparing the masterbatch, leading to a finer dispersion of the CNCs in the matrix.

In Figure 5.4b, the tensile strength of the nanocomposites does not show any enhancement compared to that of the neat PP, whereas by comparing the two compatibilized nanocomposite samples, i.e. PP/15SCO/5CNC and PP/15CO/5CNC, a 24 % larger tensile strength is observed for the sample in which the masterbatch was prepared via solution mixing. A similar tensile behavior, enhanced Young modulus but unchanged tensile strength, has also been observed for other nanocomposites [9, 22, 24]. The investigators ascribed this behavior to the lack of stress transfer from the matrix to the filler. Therefore, the composite is not able to show its potential. This happens usually when the polarity of the matrix and the filler is different and there is no strong bonds between the filler and the matrix, which would interfere with the stress distribution throughout the composite when a load is applied [28]. Finally, as shown by Figure 5.4c the elongation at break decreases significantly when CNCs are added to PP, which is generally the case of composite materials due to the reduction of chain mobility by the fillers.

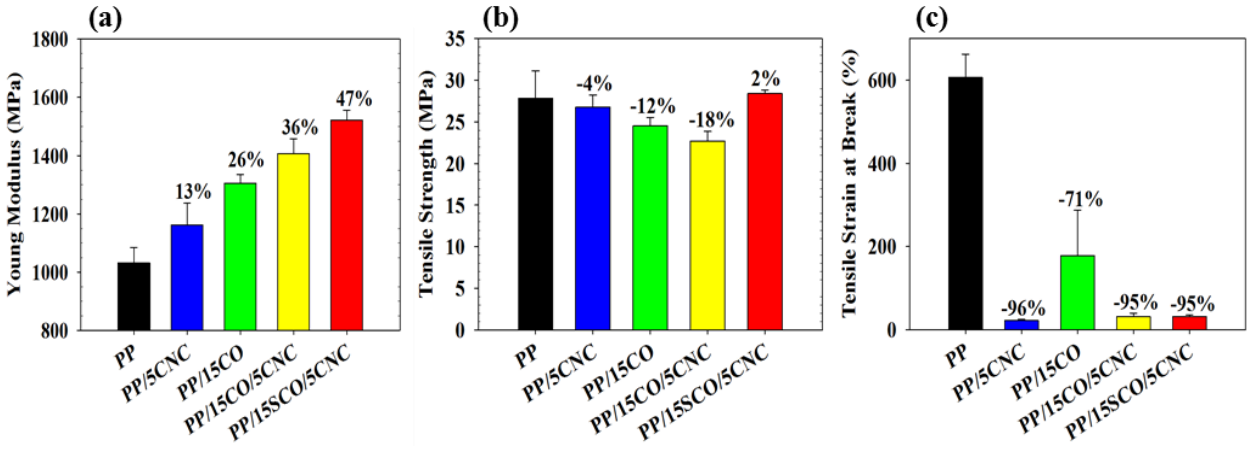

Figure 5.4: Comparison of the tensile properties: Young modulus (a), tensile strength (b) and tensile strain at break (c) of the samples. The numbers above the bars represent the changes in percent with respect to the neat PP

5.3.3.2 DMTA properties

The variations of tan δ and the storage modulus obtained from DMTA for the samples over a wide range of temperature are displayed in Figure 5.5. Two characteristic peaks in tan δ are observed for all samples (Figure 5.5a). The peak observed at high temperature is the α-transition, which is related to the relaxation of trapped PP amorphous chains in the crystalline structure of the PP. It can also be ascribed to the local mobility in crystalline lamellae, which affects the trapped chains in the crystalline phase [37, 38]. It is worth mentioning that this transition in PP sometimes has been observed as a shoulder instead of a peak [39]. The first transition, the β-transition occurring at ca. 0 °C, is related to the unrestricted PP amorphous chains and is considered as the glass transition temperature of PP (T_g) [37-39]; T_g of PP is not affected significantly by the addition of the CNCs nor the compatibilizer. However, the area under the peak of T_g, which is strongly related to the extent of damping or energy dissipation due to the segmental motion of the PP chains at T_g, is decreased by either the CNCs or the compatibilizer within the PP phase. In case of the compatibilized nanocomposite samples this reduction is more significant especially when the masterbatch was prepared via solution mixing (PP/15SCO/5CNC). This motion will be reduced if there is any physical or chemical interaction between the polymer chains and the nanoparticles [38, 39]. A better dispersion of the filler leads to a larger interfacial area, which restricts more the polymer chains. Consequently, less energy is required for segmental motions and damping decreases at T_g.

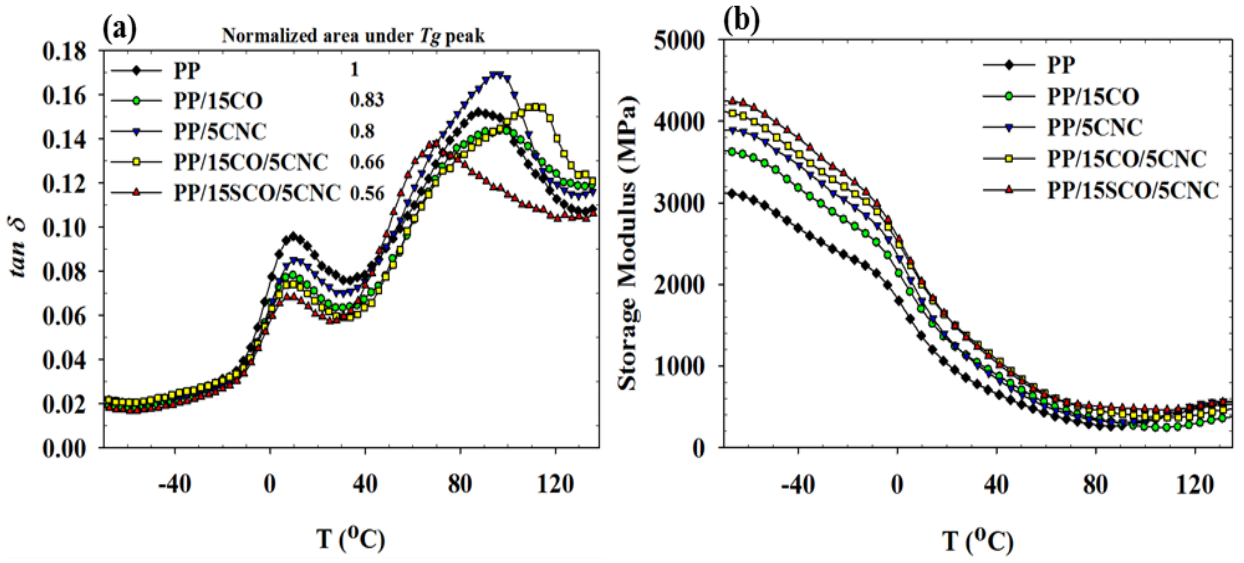

Figure 5.5: DMTA data for the various samples over a large range of temperature, from −70 to 140 °C: (a) tan δ (the numbers in the legend of the figure represent the area under the T_g peak observed for each sample divided by that of the neat PP); (b) storage modulus

Figure 5.5b shows that the storage modulus of PP is enhanced by the addition of the CNCs. This improvement is even better when the masterbatch containing both the nanoparticles and the compatibilizer were mixed to the neat PP, especially using the solution method. In fact, a better state of dispersion of the CNCs in PP/15SCO/5CNC made the material stiffer, with a higher modulus. The storage modulus of PP is enhanced up to ca. 60 % when a good state of dispersion is achieved using the compatibilizer. Similar results were obtained by Khoshkava and Kamal [34].

5.3.3.3 DSC properties

Figure 5.6 illustrates the effect of the CNCs and use of CO on the crystalline content of PP and onset temperature of crystallization during the cooling cycle. The crystalline content of the samples reported in Figure 5.6a was calculated from the enthalpy of melting, ΔH_m, in the first heating cycle according to the following equation:

$$X_c = \frac{\Delta H_m}{w_{pp} \times \Delta H_m^0} \qquad (5.1)$$

where w_{PP} is the weight fraction of the PP phase and ΔH_m^0 is the enthalpy of the 100 % crystalline PP (207 J/g) [40].

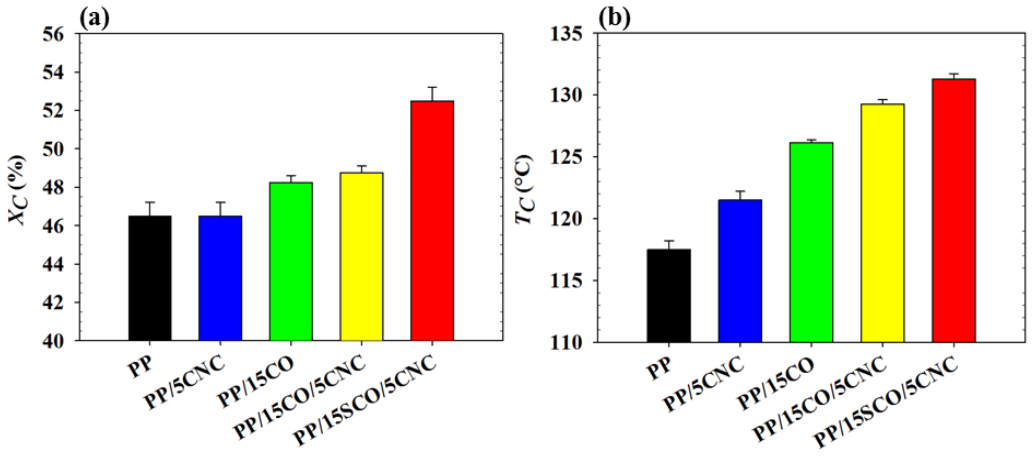

Figure 5.6: Crystalline content of the samples (a), calculated based on the data obtained in the heating cycle using Eq. 1, and comparison of on-set temperature of the crystallization peak of the samples (b), occurring in the cooling cycle

In crystallization of polymers both the total amount of nuclei and the mobility of polymer chains affect the total crystalline content, the former increases whereas the latter decreases with the addition of nanoparticles. Therefore, sometimes no significant changes are observed with the addition of nanoparticles. Here, the addition of the CNCs slightly changed the total crystalline content of PP, up to ca. 13 % increase in PP/15SCO/5CNC. Almost half of this extent of increase in crystalline content was reported for polycaprolactone (PCL) containing 6 wt% unmodified Luffa cylindrica nanocrystals [14] and for polyethylene (PE) containing 5 wt% ramie cellulose whiskers modified with stearoyl chloride [24]. As the specimens for DSC measurements were cut from the dumbbell samples for tensile tests, we can conclude that the changes in the crystalline content of the samples had little effect on the enhancements of the mechanical properties. Figure 5.6b compares the onset temperature of crystallization of samples in cooling cycles, T_c, which is gradually shifted to higher values compared to that of the neat PP. This shift, from ca. 117 °C for

the neat PP up to ca. 131°C for PP/15SCO/5CNC, can be definitely ascribed to the nucleation effect of the CNCs on the crystallization of PP, although a part of this change is due to the presence of CO. Therefore, better dispersed CNCs in PP/15SCO/5CNC compared to the other samples could act as nucleation sites for the crystal growth in PP.

5.4 Conclusion

In this work the effect of the CNCs on the rheological, mechanical and thermal properties of polypropylene was investigated. The addition of the 5 wt% CNCs and the use of poly(ethylene-co-vinyl alcohol) as a compatibilizer resulted in increases in the storage modulus and complex viscosity at low frequencies, a more pronounced overshoot in the transient viscosity, enhancement in the Young modulus and storage modulus in DMTA. A portion of the enhancement in the mechanical properties was due to the higher crystalline content of the samples compared to that of the neat PP. Furthermore, the nucleation effect of the CNCs on the crystallization of PP was observed in the DSC measurements by shifting the crystallization temperature to higher values. SEM micrographs showed that large agglomerates disappeared for samples containing the copolymer and prepared by the solution mixing method. These observations could be ascribed to the efficiency of the poly(ethylene-co-vinyl alcohol) as a compatibilizer, which favored a better dispersion and wetting of the hydrophilic CNCs within the hydrophobic PP. The compatibilizer was more efficient in dispersing the CNCs in the solution mixing mode.

5.5 Acknowledgments

The authors acknowledge the financial support from the Natural Sciences and Engineering Research Council of Canada (NSERC). The authors are also grateful to FPInnovations for providing the CNCs and wish to thank Dr. Wadood Hamad for helpful discussions.

5.6 Supplementary Information

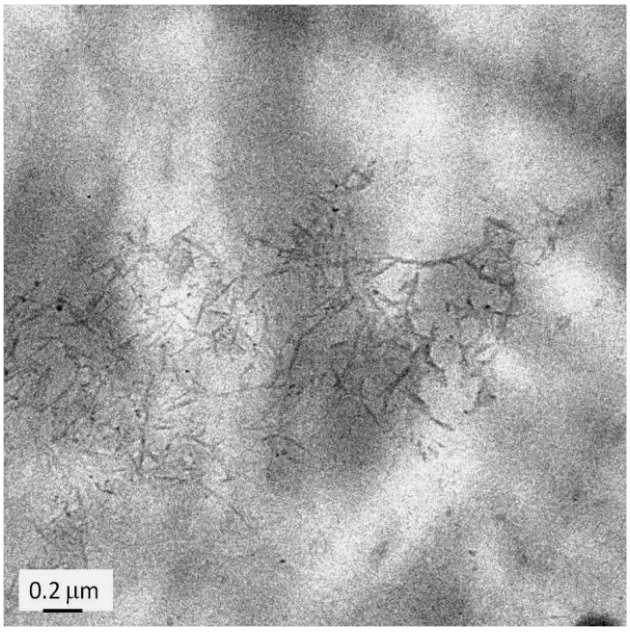

Figure 5.S1: TEM image of PP6523/9SCO/3CNC (a nanocomposite containing 3 wt % of CNCs, but based on a larger molecular weight PP)

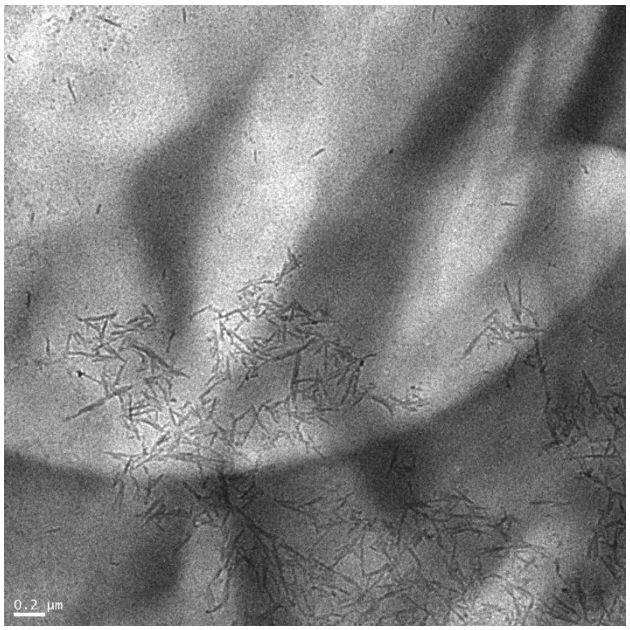

Figure 5.S2: TEM image of PP6523/9SCO/3CNC (a nanocomposite containing 3 wt % of CNCs, but based on a larger molecular weight PP)

5.7 References

[1] D. Klemm, F. Kramer, S. Moritz, T. Lindstrom, M. Ankerfors, D. Gray, and A. Dorris, "Nanocelluloses: A new family of nature-based materials," Angew Chem Int Ed Engl, vol. 50, no. 24, pp. 5438-5466, 2011.

[2] M. S. Peresin, Y. Habibi, J. O. Zoppe, J. J. Pawlak, and O. J. Rojas, "Nanofiber composites of polyvinyl alcohol and cellulose nanocrystals: Manufacture and characterization," Biomacromolecules, vol. 11, no. 3, pp. 674-661, 2010.

[3] W. Zhang, X. He, C. Li, X. Zhang, C. Lu, X. Zhang, and Y. Deng, "High performance poly (vinyl alcohol)/cellulose nanocrystals nanocomposites manufactured by injection molding," Cellulose, vol. 21, no. 1, pp. 485-494, 2014.

[4] T. Abitbol, T. Johnstone, T. M. Quinn, and D. G. Gray, "Reinforcement with cellulose nanocrystals of poly(vinyl alcohol) hydrogels prepared by cyclic freezing and thawing," Soft Matter, vol. 7, no. 6, pp. 2373-2379, 2011.

[5] W.-I. Park, M. Kang, H.-S. Kim, and H.-J. Jin, "Electrospinning of poly(ethylene oxide) with bacterial cellulose whiskers," Macromolecular Symposia, vol. 249-250, no. 1, pp. 289-294, 2007.

[6] G. Siqueira, H. Abdillahi, J. Bras, and A. Dufresne, "High reinforcing capability cellulose nanocrystals extracted from syngonanthus nitens (capim dourado)," Cellulose, vol. 17, no. 2, pp. 289-298, 2010.

[7] A. Bendahou, H. Kaddami, and A. Dufresne, "Investigation on the effect of cellulosic nanoparticles' morphology on the properties of natural rubber based nanocomposites," European Polymer Journal, vol. 46, no. 4, pp. 609-620, 2010.

[8] V. Khoshkava, and M. R. Kamal, "Effect of surface energy on dispersion and mechanical properties of polymer/nanocrystalline cellulose nanocomposites," Biomacromolecules, vol. 14, no. 9, pp. 3155-3163, 2013.

[9] G. Siqueira, J. Bras, and A. Dufresne, “Cellulose whiskers versus microfibrils: Influence of the nature of the nanoparticle and its surface functionalization on the thermal and mechanical properties of nanocomposites,” Biomacromolecules, vol. 10, no. 2, pp. 425-432, 2009.

[10] H. Nakatani, K. Iwakura, K. Miyazaki, N. Okazaki, and M. Terano, “Effect of chemical structure of silane coupling agent on interface adhesion properties of syndiotactic polypropylene/cellulose composite,” Journal of Applied Polymer Science, vol. 119, no. 3, pp. 1732-1741, 2011.

[11] A. L. Goffin, J. M. Raquez, E. Duquesne, G. Siqueira, Y. Habibi, A. Dufresne, and P. Dubois, “Poly(ε-caprolactone) based nanocomposites reinforced by surface-grafted cellulose nanowhiskers via extrusion processing: Morphology, rheology, and thermo-mechanical properties,” Polymer, vol. 52, no. 7, pp. 1532-1538, 2011.

[12] A. L. Goffin, J. M. Raquez, E. Duquesne, G. Siqueira, Y. Habibi, A. Dufresne, and P. Dubois, “From interfacial ring-opening polymerization to melt processing of cellulose nanowhisker-filled polylactide-based nanocomposites,” Biomacromolecules, vol. 12, no. 7, pp. 2456-2465, 2011.

[13] J. M. Raquez, Y. Murena, A. L. Goffin, Y. Habibi, B. Ruelle, F. DeBuyl, and P. Dubois, “Surface-modification of cellulose nanowhiskers and their use as nanoreinforcers into polylactide: A sustainably-integrated approach,” Composites Science and Technology, vol. 72, no. 5, pp. 544-549, 2012.

[14] G. Siqueira, J. Bras, N. Follain, S. Belbekhouche, S. Marais, and A. Dufresne, “Thermal and mechanical properties of bio-nanocomposites reinforced by luffa cylindrica cellulose nanocrystals,” Carbohydrate Polymers, vol. 91, no. 2, pp. 711-717, 2013.

[15] B. Couturaud, A. Baldo, A. Mas, and J. J. Robin, “Improvement of the interfacial compatibility between cellulose and poly(l-lactide) films by plasma-induced grafting of l-lactide: The evaluation of the adhesive properties using a peel test,” Journal of Colloid and Interface Science, vol. 448, pp. 427-436, 2015.

[16] M. N. Belgacem, P. Bataille, and S. Sapieha, "Effect of corona modification on the mechanical properties of polypropylene/cellulose composites," Journal of Applied Polymer Science, vol. 53, no. 4, pp. 379-385, 1994.

[17] B. Braun, and J. R. Dorgan, "Single-step method for the isolation and surface functionalization of cellulosic nanowhiskers," Biomacromolecules, vol. 10, no. 2, pp. 334-341, 2009.

[18] S. Montanari, M. Roumani, L. Heux, and M. R. Vignon, "Topochemistry of carboxylated cellulose nanocrystals resulting from tempo-mediated oxidation," Macromolecules, vol. 38, no. 5, pp. 1665-1671, 2005.

[19] M. Salajková, L. A. Berglund, and Q. Zhou, "Hydrophobic cellulose nanocrystals modified with quaternary ammonium salts," Journal of Materials Chemistry, vol. 22, no. 37, pp. 19798-19805, 2012.

[20] G. Morandi, L. Heath, and W. Thielemans, "Cellulose nanocrystals grafted with polystyrene chains through surface-initiated atom transfer radical polymerization (SI-ATRP)," Langmuir, vol. 25, no. 14, pp. 8280-8286, 2009.

[21] W. Y. Hamad, and C. Miao, Nanocomposite biomaterials of nanocrystalline cellulose (NCC) and polylactic acid (PLA), U.S. Patent 8,829,110, 2014.

[22] Y. Habibi, A.-L. Goffin, N. Schiltz, E. Duquesne, P. Dubois, and A. Dufresne, "Bionanocomposites based on poly(ε-caprolactone)-grafted cellulose nanocrystals by ring-opening polymerization," Journal of Materials Chemistry, vol. 18, no. 41, pp. 5002-5010, 2008.

[23] M. Hasani, E. D. Cranston, G. Westman, and D. G. Gray, "Cationic surface functionalization of cellulose nanocrystals," Soft Matter, vol. 4, no. 11, pp. 2238-2244, 2008.

[24] A. Junior de Menezes, G. Siqueira, A. A. S. Curvelo, and A. Dufresne, "Extrusion and characterization of functionalized cellulose whiskers reinforced polyethylene nanocomposites," Polymer, vol. 50, no. 19, pp. 4552-4563, 2009.

[25] K. G. Nair, and A. Dufresne, “Crab shell chitin whiskers reinforced natural rubber nanocomposites. 3. Effect of chemical modification of chitin whiskers,” Biomacromolecules, vol. 4, no. 6, pp. 1835-1842, 2003.

[26] N. Ljungberg, C. Bonini, F. Bortolussi, C. Boisson, L. Heux, and J. Y. Cavaille, “New nanocomposite materials reinforced with cellulose whiskers in atactic polypropylene: Effect of surface and dispersion characteristics,” Biomacromolecules, vol. 6, no. 5, pp. 2732-2739, 2005.

[27] M. Roman, and W. T. Winter, “Effect of sulfate groups from sulfuric acid hydrolysis on the thermal degradation behavior of bacterial cellulose,” Biomacromolecules, vol. 5, no. 5, pp. 1671-1677, 2004.

[28] T.-W. Kim, S.-Y. Lee, S.-J. Chun, G.-H. Doh, and K.-H. Paik, “Effect of silane coupling on the fundamental properties of wood flour reinforced polypropylene composites,” Journal of Composite Materials, vol. 45, no. 15, pp. 1595-1605, 2011.

[29] H. Kargarzadeh, R. M. Sheltami, I. Ahmad, I. Abdullah, and A. Dufresne, “Cellulose nanocrystal: A promising toughening agent for unsaturated polyester nanocomposite,” Polymer, vol. 56, pp. 346-357, 2015.

[30] J. Lu, P. Askeland, and L. T. Drzal, “Surface modification of microfibrillated cellulose for epoxy composite applications,” Polymer, vol. 49, no. 5, pp. 1285-1296, 2008.

[31] A. Arias, M.-C. Heuzey, M. Huneault, G. Ausias, and A. Bendahou, “Enhanced dispersion of cellulose nanocrystals in melt-processed polylactide-based nanocomposites,” Cellulose, vol. 22, no. 1, pp. 483-498, 2015.

[32] H. Sojoudiasli, M.-C. Heuzey, and P. J. Carreau, “Rheological, morphological and mechanical properties of flax fiber polypropylene composites: Influence of compatibilizers,” Cellulose, vol. 21, no. 5, pp. 3797-3812, 2014.

[33] A. Sonia, K. P. Dasan, and A. Rosamma, “celluloses micro fibres (CMF) reinforced poly(ethylene-co-vinyl acetate) (EVA) composites: Dynamic mechanical, gamma and thermal ageing studies,” Chemical Engineering Journal, vol. 228, pp. 1214–1222, 2013.

[34] V. Khoshkava, and M. R. Kamal, “Effect of cellulose nanocrystals (CNC) particle morphology on dispersion and rheological and mechanical properties of polypropylene/CNC nanocomposites,” ACS Appl Mater Interfaces, vol. 6, no. 11, pp. 8146-8157, 2014.

[35] S. Abbasi, P. J. Carreau, A. Derdouri, and M. Moan, “Rheological properties and percolation in suspensions of multiwalled carbon nanotubes in polycarbonate,” Rheologica Acta, vol. 48, no. 9, pp. 943-959, 2009.

[36] A. Ghanbari, M. C. Heuzey, P. J. Carreau, and M. T. Ton-That, “A novel approach to control thermal degradation of pet/organoclay nanocomposites and improve clay exfoliation,” Polymer, vol. 54, no. 4, pp. 1361-1369, 2013.

[37] B. Wunderlich, "The nature of glass transition and its determination by thermal analysis," Assignment of the glass transition, R. J. Seyler, ed., Philadelphia, Pa: American Society for Testing and Materials, 1994.

[38] V. Hristov, and S. Vasileva, “Dynamic mechanical and thermal properties of modified poly(propylene) wood fiber composites,” Macromolecular Materials and Engineering, vol. 288, no. 10, pp. 798-806, 2003.

[39] A. Amash, and P. Zugenmaier, “Thermal and dynamic mechanical investigations on fiber-reinforced polypropylene composites,” Journal of Applied Polymer Science, vol. 63, no. 9, pp. 1143-1154, 1997.

[40] R. L. Blaine, “Thermal applications note: Polymer heats of fusion,” TA Instruments, New Castle, DE, USA.

CHAPTER 6 ARTICLE 2 : SHEAR RHEOLOGY OF POLYLACTIDE (PLA)-CELLULOSE NANOCRYSTAL (CNC) NANOCOMPOSITES[3]

Davood Bagheriasl[a], Pierre J. Carreau[*, a], Bernard Riedl[b], Charles Dubois[a], Wadood Y. Hamad[c]

[a]*Research Center for High Performance Polymer and Composite Systems (CREPEC), Chemical Engineering Department, Polytechnique Montreal, PO Box 6079, Stn Centre-Ville, Montreal, QC H3C 3A7, Canada*

[b]*Département des sciences du bois et de la forêt, Faculté de foresterie, géographie et géomatique, Université Laval, Quebec, QC G1V 0A6, Canada*

[c]*FPInnovations, 2665 East Mall, Vancouver, BC V6T 1Z4, Canada*

*Corresponding Author: e-mail: pcarreau@polymtl.ca

Abstract

A simple method for the preparation of polymer-cellulose nanocrystal (CNC) nanocomposite is shown to yield good dispersion of CNCs within a polylactide (PLA) matrix, which consequently resulted in the lowest rheological percolation threshold reported so far for polymer-CNC systems. The rheological behavior of the nanocomposites was determined in dynamic, transient and steady-shear flow fields in the molten state. The complex viscosity and storage modulus of the nanocomposites increased markedly with CNC content, particularly at low frequencies; the samples were highly shear thinning and exhibited a transition from liquid- to solid-like behavior as the CNC concentration increased. Larger values for steady-state viscosity, yield stress, shear stress and first normal stress difference were reported for the more concentrated nanocomposites. Also, pronounced overshoots in the transient start-up viscosity of the nanocomposites were observed. These results could be ascribed to the formation of an interconnected CNC network within the PLA matrix.

Keywords: *nanocomposites; cellulose nanocrystals (CNCs); polylactide; rheological properties; dispersion*

---

[3] This chapter was submitted as a scientific article to the journal of Cellulose in November 2015.

6.1 Introduction

Cellulose is the most common biomacromolecule on earth and constitutes the structural matter of all plants. Therefore, there have always been searches for new applications of cellulose due to the low cost, abundance in nature, renewability and biodegradability. Cellulose and its derivatives in different forms have been used for energy source, paper, building material, clothing, foodsutffs, pharmaceuticals, films, coatings and membranes for many years [1, 2]. One form of cellulose that has attracted interest and importance is nano cellulose, especially cellulose nanocrystal (CNC). CNCs are rodlike particles with nanoscale dimensions and provide several interesting properties such as biodegradability, low density, abundance in nature, very large surface area and high strength, which can be of interest for many applications [2]. Over the last years, the combination of these properties has made CNC an interesting reinforcing agent in polymer composite industry. However, some of their features such as strong inter-particle interactions due to hydrogen bonds make it difficult to obtain a good dispersion and, consequently, enhanced properties when incorporated in hydrophobic polymers. That is why obtaining a good dispersion of CNCs in hydrophobic polymers remains a challenge, in particular without the use of any compatibilizer or CNC modification. The first use of CNCs as a reinforcing agent in polymers was reported by Favier et al. who could enhance the mechanical properties of solution-cast films of poly(styrene-co-butyl acrylate) latex [3]. Since then, their applications as reinforcing agents in polymers have grown, but limited to a few hydrophilic polymers or polymers in latex form [3-9]. CNC surface modification or compatibilization was necessary to achieve a good CNC dispersion in most of common polymers [10-16].

Recently, there has been increasing interest to incorporate CNCs into biopolymers to expand their applications by improving their properties. Such combinations of biorenewable, biocompatible and biodegradable components would create a new category in composite materials that can replace petroleum-based polymeric products, especially in packaging and automotive industries. However, obtaining a fairly good dispersion of CNCs within the chosen matrix is necessary in order to achieve enhanced properties for the resulting biocomposites at low nanoparticle concentrations. Among the numerous investigations conducted to achieve fairly good dispersion of CNCs only a few considered the rheological characterization of polymer-CNC systems [12, 17-22]. The formation of an interconnect network of particles plays an important role on the

rheological properties of a nanocomposite system. Therefore, the rheological behavior of the resulting nanocomposites can reveal whether the preparation method is efficient in leading to nano dispersions. Pereda et al. [17]. reported reduced viscosity values for 1 wt% polyethylene oxide (PEO) aqueous solutions with different CNC loadings in steady-shear flow experiments for a wide range of shear rates. Arias et al. [18] could obtain a good dispersion of CNCs in a polylactide (PLA) of a low molecular weight via a PEO-CNC masterbatch preparation. However, the complex viscosity of the resulting nanocomposites did not show any changes compared to those of the neat PLA and PLA filled with CNCs in absence of PEO. The rheological behavior in small-amplitude oscillatory shear (SAOS) and steady-shear flows of polypropylene (PP)-CNC nanocomposites was investigated by Khoshkava and Kamal [19]. They determined the effects of the CNC drying process, initial concentration of the CNC aqueous suspensions and final concentration in the nanocomposites on the properties of PP-CNC systems. A value of 2.5 wt% was reported as the rheological percolation threshold in the best case, where the initial concentration of CNCs in the aqueous suspension was 1 wt% and the CNCs were spray-freeze dried [19]. Kamal and Khoshkava [20] used the same method to prepare PLA-CNC nanocomposites and reported significant increases of the complex viscosity, storage and loss moduli for the PLA filled with spray-freeze dried CNCs compared to the neat PLA. An increased storage modulus in SAOS experiments for a polycaprolactone (PCL) filled with PCL-grafted CNCs was reported by Goffin et al. [12]; the increase was attributed to a better state of dispersion of the CNCs in PCL, obtained by in situ ring-opening polymerization of the lactone in presence of the CNCs. Mabrouk et al. [21] reported increases of the complex viscosity and storage modulus at low frequencies, up to almost 4 and 5 orders of magnitude, respectively, for nanocomposites based on a poly(styrene-co-hexylacrylate) copolymer and cellulose whiskers prepared via in situ polymerization of styrene and 2-ethylhexylacrylate. Increased complex viscosity and storage modulus for blends of PLA and natural rubber (NR) filled with unmodified CNCs and CNCs grafted with C18 alkyl chains were reported by Bitinis et al. [22]. However, their results did not show significant changes for PLA-NR blends filled with PLA grafted CNCs.

In this work the effect of the CNCs on the rheological properties of polylactide was investigated. To this end, a solution casting method with a polar solvent was used to favor a better dispersion of hydrophilic CNCs within a PLA matrix without the need of CNC modification or use of any compatibilizer. To stress the efficiency of the solvent mixing method, the rheological properties

of samples of PLA-CNC at a CNC content of 2 wt% prepared via direct melt mixing and the solution casting method are compared. Our objective is first to develop biobased and biodegradable PLA-CNC nanocomposites with a dispersed structure via a simple method and, second, to characterize the rheological behavior of these nanocomposites for different shear flow fields. To our knowledge, this is the first time that the rheological behavior of polymer-CNC nanocomposites in different shear flow fields is systematically reported.

6.2 Experimental Section

6.2.1 Materials

A commercial grade polylactide (PLA) (Ingeo Biopolymer 3251D) with MFR of 35 g/10 min (190 °C/2.16 kg), crystalline melting temperature of 155-170 °C and glass transition temperature (T_g) of 55-60 °C was purchased from NatureWorks LLC (Minnetonka, MN, USA) and used as the matrix. N,N-dimethylformamide (DMF), anhydrous 99.8%, was purchased from Sigma-Aldrich Canada Co. (Oakville, ON, Canada). Freeze-dried CNCs were kindly provided by FPInnovations (Pointe-Claire, QC, Canada).

6.2.2 Sample Preparation

To prepare the nanocomposites a solution mixing method in DMF medium was used. The desired amount of CNCs were first dispersed in 135 mL of DMF using a water-bath sonicator (FS30 100 Watts Ultrasonic Cleaner, Fisher Scientific, Pittsburg, PA) during 2 h; then, 40 g of PLA was added and the mixture was heated up to ca. 70 °C while stirring during 150 min with a magnetic stirrer until the complete dissolution of the PLA. The mixture was finally poured on a tray and dried in a vacuum oven at 80 °C for 36 h. Using a coffee grinder, the product was ground into powder and kept in the oven at 60 °C for another 36 h. For the sake of comparison, PLA-CNC composite samples were also prepared via melt mixing: the CNCs and PLA were introduced in an internal mixer, DDRV501 Brabender (C. W. Brabender Instruments Inc., NJ, USA), and melt-compounded at 180 °C, 100 rpm for 7 min under N_2 atmosphere. Thereafter, all samples were compression molded for 10 min at 175 °C in the presence of N_2 followed by 5 min at room temperature to prepare the test specimens.

6.2.3 Characterization

6.2.3.1 Microscopy

Transmission electron microscopy (TEM) analysis was conducted on ultra-microtomed samples using a JEOL JEM-2100F microscope (JEOL USA Inc., Peabody, MA, USA), operating at 200 kV. The samples were microtomed into slices with an approximately 50-80 nm thickness at ca. −100 °C using an Ultracut FC microtome (LEICA) with a diamond knife. For a better visualization the samples were stained using a bis(ethylenediamine)copper(II) hydroxide solution (copper(II)-ethylenediamine complex) 1.0 M in H2O purchased from Sigma-Aldrich Canada Co. (Oakville, ON, Canada). To this end, first, the copper(II)-ethylenediamine complex was diluted to 1 wt% solution with deionized (DI) water; then, the ultra-microtomed samples placed on copper grids were immersed in the solution for 150 s. To remove the excess of the absorbed solution the samples were successively immersed in DI water three times, each time in fresh water for 10 s. Finally, the samples were left at room temperature for 24 h to avoid fracture of the stained layer due to fast evaporation, followed by another 24 h in a desiccator before TEM analysis.

Scanning electron microscopy (SEM) analysis was carried out on ultra-microtomed surfaces, coated with gold. The microscope was a JEOL JSM 7600TFE scanning electron microscope (SEM) (JEOL USA Inc., Peabody, MA, USA) operated at 2 kV.

6.2.3.2 Rheology

The rheological properties of the neat PLA and the nanocomposites were measured using a stress-controlled MCR 301 rheometer (Anton Paar, Austria). The experiments were conducted under a nitrogen atmosphere to avoid oxidation of the samples. A cone-and-plate geometry was used with a truncation of 51 μm, cone angle of 1.98°, parallelity of ±1 μm and a diameter of 25 mm. Time-sweep experiments at strain amplitude of 0.05 and frequency of 1 rad.s^{-1} were conducted to verify the thermal stability of samples within the time required to do small-amplitude oscillatory shear (SAOS) experiments. SAOS tests were performed at strain amplitude of 0.05 to ensure the measurements were in the linear viscoelastic regime. Steady-shear experiments were also performed over a wide range of shear rate and shear stress-growth experiments were conducted at a rate of 5 s^{-1} in forward and reverse directions for different rest times between consecutive tests, 0, 200 and 1000 s. Finally, time-sweep tests at strain amplitude

of 0.05 and frequency of 1 rad.s^{-1} were performed right after the stress-growth tests to monitor the structure build-up in samples. All the rheological measurements were performed at 170 °C.

6.3 Results and discussion

6.3.1 Microscopy

Figure 6.1 depicts a TEM image of CNCs and SEM and TEM images of PLA containing 4 wt% CNC (PLA4CNC). The TEM image in Figure 6.1a was obtained for an aqueous suspension containing 0.5 wt% CNCs. It shows individual and bundles of few CNCs; from over 200 measurements via the ImageJ software, the average particle width, length and aspect ratio were found to be 16 ± 3 nm, 90 ± 17 nm and 6 ± 2, respectively. Figure 6.1b presents a SEM image of PLA4CNC (nanocomposite containing 4 wt% CNCs); some agglomerates of CNCs are obviously formed within the PLA and those are fibrillar and of random-shaped size in the range of 1-3 μm. Individual CNCs and bundles of few individual CNCs dispersed into the PLA matrix are observed in the TEM images of Figures 1c and d for two different locations. The nanoparticles seem to have the same dimension size as observed in Fig. 6.1a. These images reveal that the solution preparation method used could lead to a good dispersion of the CNCs, down to the individual size or bundles of few individual CNCs. In fact, initially the CNCs were well dispersed in DMF by means of the sonicator and, then, when the PLA was added and dissolved the individual nanoparticles could be trapped within the PLA chains and this structure remains after solvent casting. The TEM images of Figure 6.1c and d validate our assumption that the solution preparation method is efficient in dispersing the CNCs into the PLA, although some small agglomerates in the range of few (1-3) μm are observed (Fig. 6.1b).

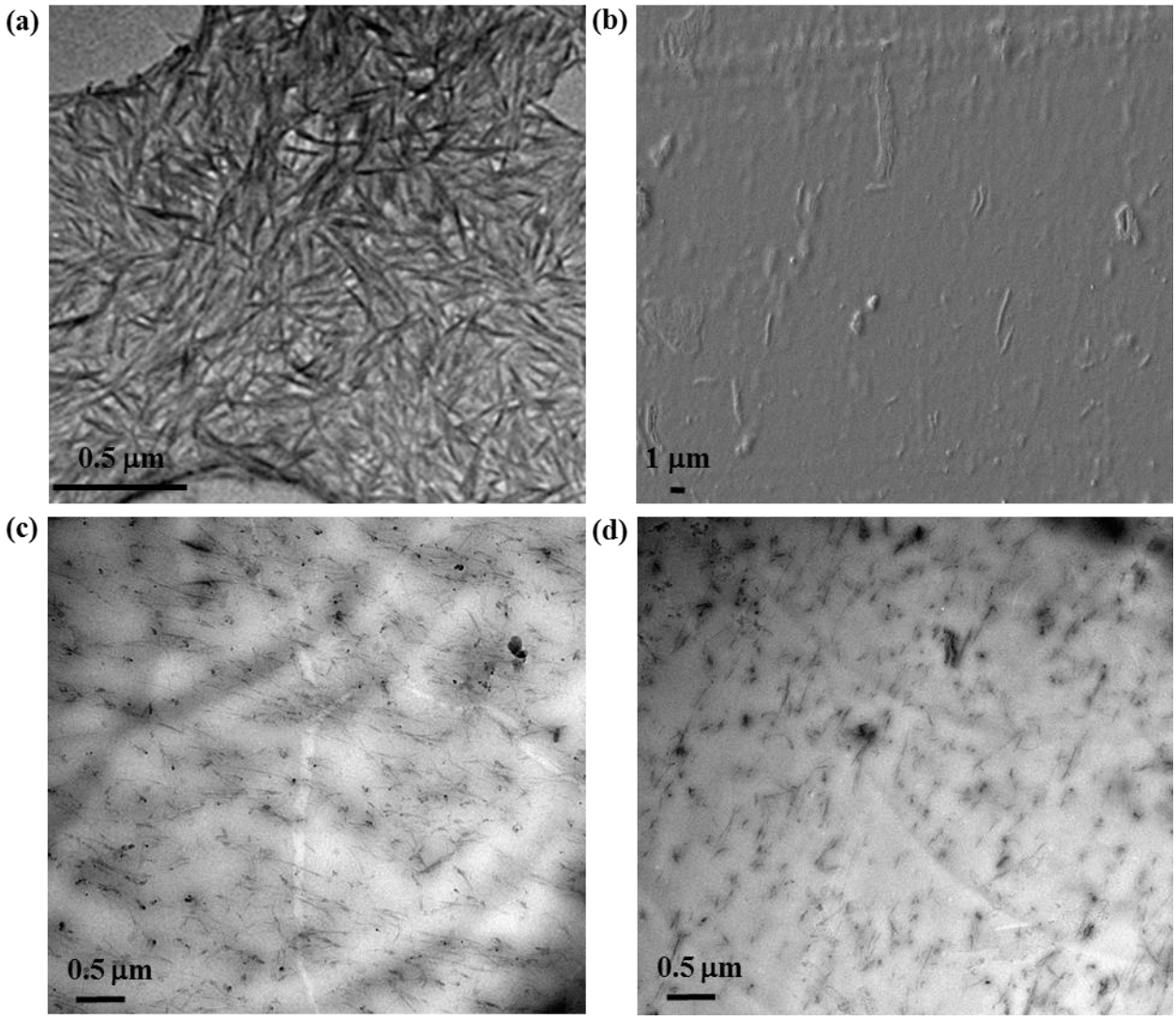

Figure 6.1: TEM image of CNCs taken from an aqueous suspension of 0.5 wt% CNC (a), SEM micrograph (b), and TEM images (c) and (d) of PLA4CNC from two different locations of the sample

6.3.2 Rheology

6.3.2.1 SAOS

All samples exhibited stable rheological properties, with changes of less than 2%, in time-sweep experiments over 15 min. Figure 6.2 presents the complex viscosity, η^*, and storage modulus, G', versus frequency, ω, of the neat PLA and PLA-CNC nanocomposites with CNC loadings varying from 0.5 to 7 wt%. The complex viscosity, η^*, of the neat PLA exhibits a long plateau, with a

slight shear-thinning behavior at high frequencies (Fig. 6.2a) and its storage modulus, G', is typical of molten polymers with a terminal zone of slope equal to 2 on the log-log plot of G' versus ω (Fig. 6.2b). For all nanocomposites, even those with CNC concentration as low as 0.5 wt%, spectacular increases of η^* and G' are observed, mainly at low frequencies, which clearly show the strong effect of CNCs on the rheological properties of PLA. At 1 wt% CNC, η^* and G' increase by 1 and 4 orders of magnitude, respectively relative to the neat PLA (Fig. 6.2). Further increases in both η^* and G', up to 3 and 6 orders of magnitude, respectively, are observed for the nanocomposite samples at larger CNC concentrations. All nanocomposite samples exhibit a shear-thinning behavior for η^* without any plateau region at low frequencies and G' that tends towards a plateau at low frequencies. We can infer that these results indicate the formation of a network and a transition from liquid- to solid-like behavior as observed for many polymer nanocomposites, attributed to the good dispersion of the CNCs in the PLA. Similar rheological behavior in SAOS has been reported for other polymer nanocomposites containing CNCs, clays or carbon nanotubes for which a good dispersion was achieved [12, 19, 23, 24]. It is worth mentioning that the SAOS data of PLA containing 7 wt% CNC are lower than those of the PLA filled with 6 wt%. This can be explained by a significant formation of agglomerates at this high CNC content.

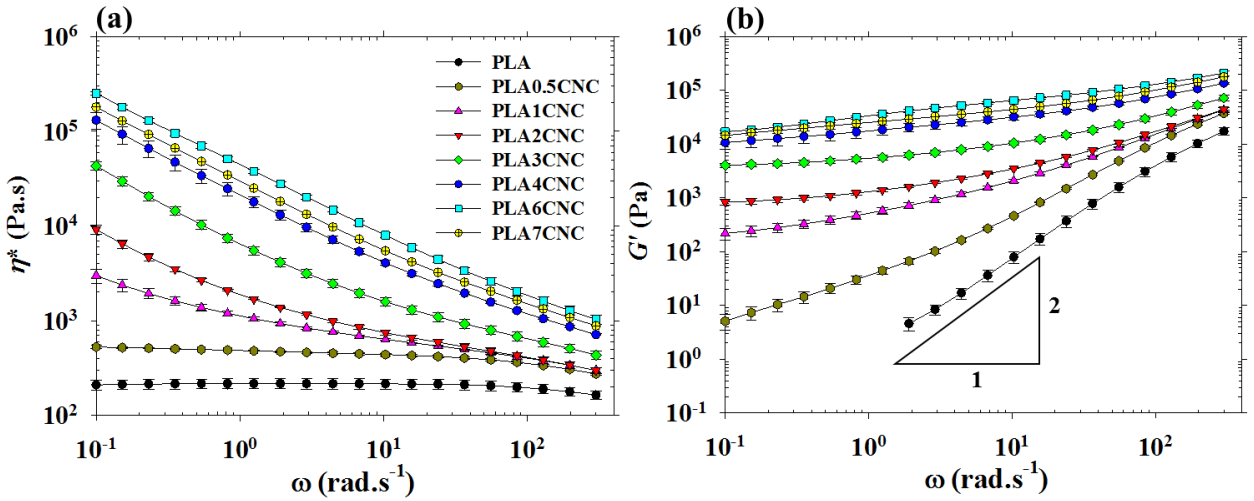

Figure 6.2: Complex viscosity, η^*, (a) and storage modulus, G' (b) vs frequency, ω, of the neat PLA and PLA-CNC nanocomposites at 170 °C (strain = 5%)

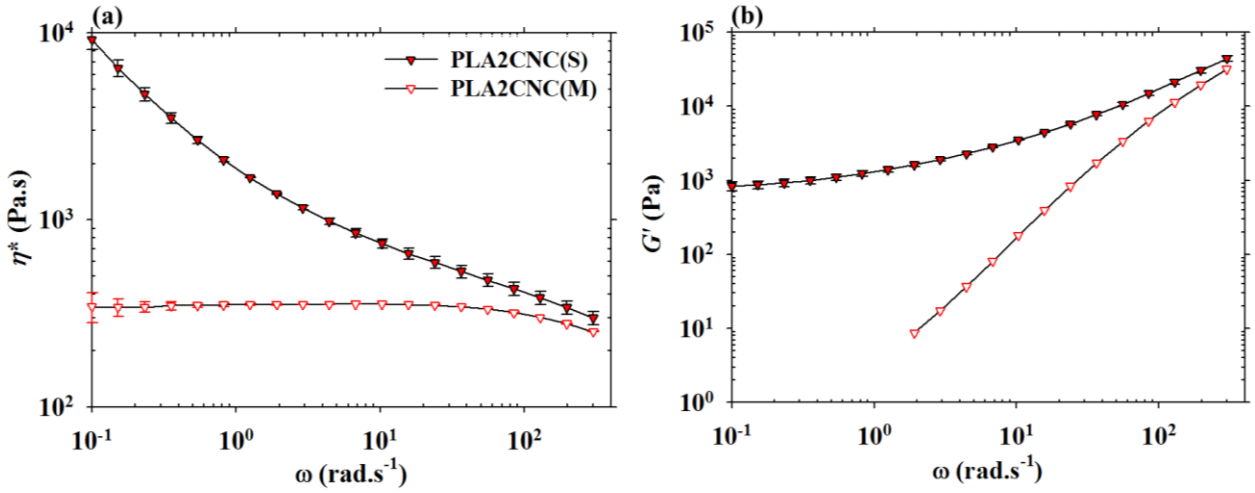

Figure 6.3: Comparison of η^* (a) and G' (b) vs ω of PLA2CNC prepared via solution (S) and melt (M) method

Figure 6.3 compares the efficiency of the solution preparation method utilized in the present work over the melt mixing preparation. Although at high frequencies the values of η^* and G' of all samples are in the same range, huge differences in η^* and G' of the PLA containing 2 wt% CNCs prepared in solution (PLA2CNC(S)) are observed at low frequencies compared to PLA2CNC(M), prepared in melt. This comparison reveals the efficiency of the solution method for preparing PLA-CNC nanocomposites over the melt preparation approach, which does not show significant improvements in the rheological behavior compared to that of the neat PLA shown in Fig. 6.2. We can conclude that the novel and simple method used in this work led to a good dispersion resulting in large increases in viscosity and modulus that have never been reported for polymer-CNC systems.

It is well known that an interconnected structure of nanoparticles in a polymeric matrix can result in a solid-like behavior with an unbounded viscosity, a plateau in G' at low frequencies and an apparent yield stress. To better show the apparent yield stress we have made plots of the complex viscosity as a function of the complex modulus, G^*, in log-log scales as illustrated in Figure 6.4. For the neat PLA and PLA0.5CNC samples no apparent yield stress is observed while for other nanocomposites a viscosity up-turn can be seen as G^* decreases. The apparent yield stress can be easily obtained by using a modified Herschel-Bulkley model:

$$\eta^* = \frac{G_0^*}{\omega} + k(\gamma^0\omega)^{n-1} \qquad (6.1)$$

$$\sigma_0 = G_0^* \gamma^0 \quad (6.2)$$

where G_0^* is the magnitude of the complex modulus at the lowest frequency, γ^0 is the strain amplitude (=0.05), k is a constant and n is the flow index [25]. The fitting parameters for the modified Herschel-Bulkley model are presented in Table 6.1. As expected the apparent yield stress, σ_0, increases with CNC content while n decreases. The increasing σ_0 can be ascribed to stronger particle–particle and polymer–particle interactions, which induce more restriction to chain mobility [25]. For the PLA containing 6 wt% CNCs almost the same σ_0 value was obtained by Kamal and Khoshkava [20]; however, for less concentrated systems they reported much lower values compared to our results. This is an indication of a better dispersion of the CNCs within our systems. Another useful information that can be obtained from Figure 6.4 is the CNC concentration at which rheological percolation occurs. The PLA with 1 wt% CNC shows an apparent yield stress while this is not the case for the 0.5 wt% CNC sample. Therefore, the rheological percolation threshold should be between 0.5 and 1 wt%, as confirmed below.

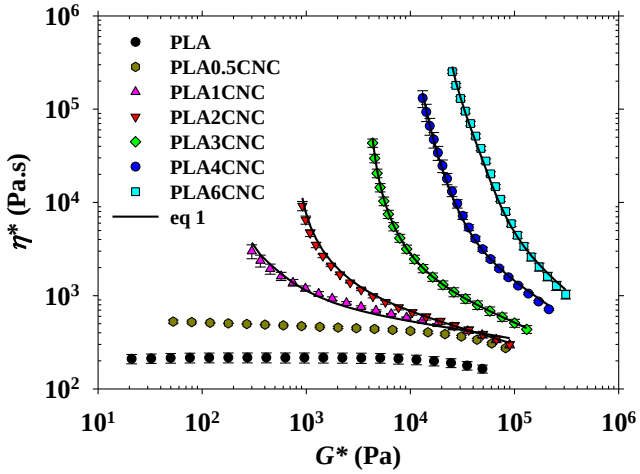

Figure 6.4: Complex viscosity, η^*, vs the complex modulus, G^*, of the neat PLA and PLA-CNC nanocomposites. The lines are the fits of the modified Herschel-Bulkley model (Eq. 6.1)

Table 6.1: Yield stress and melt flow index of the nanocomposites using the Herschel-Bulkley model (Eq. 6.4) and the modified Herschel-Bulkley model (Eqs. 6.1 and 6.2)

CNC Content (wt%)	SAOS			Steady Shear		
	σ_0 (Pa)	k (Pa.s^n)	n	τ_0 (Pa)	a (Pa.s^n)	n
1	15.0	505	0.86	52.7	640	0.73
2	45.9	581	0.76	107	856	0.69
3	217	966	0.70	334	1450	0.60
4	655	2040	0.62	847	2970	0.50
6	1260	3490	0.56	1280	4730	0.38

6.3.2.2 Rheological percolation threshold

The rheological percolation threshold is the content of solid particle above which the rheological properties of suspension increase exponentially and exhibit an apparent yield stress. In the previous section this value was estimated to fall in the range of 0.5-1 wt% CNCs. To have a more precise value, the storage modulus of the samples at the lowest measured frequency in SAOS experiments (here 0.1 rad.s^{-1}) is plotted versus the CNC content in Figure 6.5. The percolation threshold can be obtained by using an empirical power-law relation defined as

$$G' = \beta_c G \left(\frac{m - m_c G}{m_c G}\right)^n \text{ for } m > m_c G \quad (6.3)$$

where $\beta_c G$ and n are power-law constants, m is the CNC concentration (wt%) and $m_c G$ is the rheological percolation threshold (wt%) [23, 26, 27]. A value of 0.68 wt% is obtained from the fit of the data of Figure 6.5 using Eq. 6.3. This is much smaller than the values of 2.5 and 3 wt% reported elsewhere for the rheological percolation threshold of PP and PLA filled CNCs, respectively [19, 20]. This again reveals that a better dispersion is achieved in the present work that results in smaller rheological percolation threshold value.

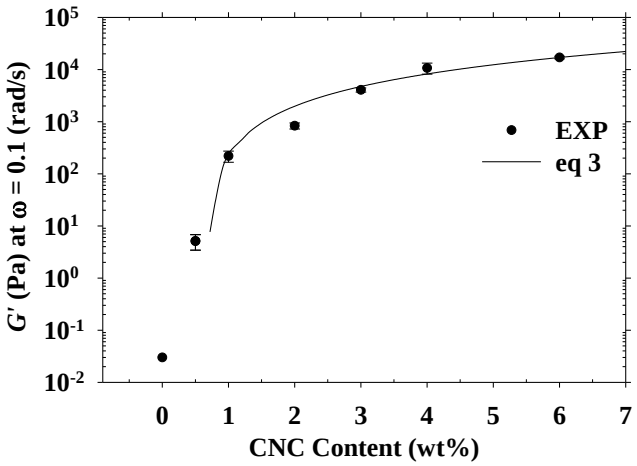

Figure 6.5: Storage modulus of the PLA-CNC nanocomposites as a function of the CNC loading obtained at 170 °C and ω = 0.1 rad.s^{-1}. The line is a fit with the power-law expression of Eq. 6.3. Note that the value of the neat PLA was obtained after extrapolation to ω = 0.1 rad.s^{-1}

6.3.2.3 Steady-shear flow

Figure 6.6 presents the steady-shear viscosity, η, over a wide range of shear rates for the neat PLA and PLA containing 1 and 4 wt% CNCs. Similar to the behavior shown previously in SAOS experiments (Fig. 6.2), a shear-thinning behavior without any plateau region and unbounded viscosity at low shear rates for the PLA containing 1 and 4 wt% CNC are observed while the neat PLA shows a Newtonian behavior. Figure 6.6a compares the shear viscosity of the samples when two consecutive tests were conducted from low-to-high shear rates (filled symbols) with that of high-to-low experiments (open symbols) using the same samples. Clearly higher viscosities for the low-to-high experiments are observed at low shear rates. In fact, when a test is performed from low-to-high shear rates the CNC network within the PLA matrix is gradually destroyed as the shear rate increases. Hence, in the second experiments conducted from high-to-low shear rates on the same sample, lower viscosity values are observed. From this thixotropic behavior of PLA filled CNC samples observed in Fig. 6.6a it can be concluded that the CNC network broken down in a low-to-high shear test cannot be reformed with the same strength in a high-to-low shear test. Figure 6.6b compares the viscosities of fresh samples for two consecutive high-to-low shear tests. Obviously, the data for both tests superpose indicating again that the structure broken down at high shear rates cannot be totally reformed at low shear rates.

The original Herschel-Bulkley model used to fit the steady-shear data of Figure 6.7a is expressed as

$$\tau = \tau_0 + a\dot{\gamma}^n \quad (6.4)$$

where τ_0 is the apparent yield stress in simple shear and , n, is power-law (melt flow) index. The fitting parameters of the Herschel-Bulkley model are presented in Table 6.1. For the neat PLA no yield stress is observed while as CNCs are added to the PLA an apparent yield stress is observed, as reported above for the SAOS data. We note with surprise from Table 6.1 that the apparent yield stress values obtained from steady-shear data are considerably larger than those obtained from SAOS data, except for PLA6CNC. This is difficult to interpret at this stage, but it possibly reflects complexities associated with measuring the yield stress via extrapolation methods or using empirical equations. Figure 7b presents the first normal stress difference N_1 as a function of shear rate for the PLA-CNC nanocomposites. N_1 depicts a plateau at low shear rates and, then, increases with $\dot{\gamma}$ at higher rates. As expected, N_1 increases with increasing CNC concentration in the PLA and these larger normal stress differences are the sign of stronger particle-particle interactions and a more elastic network. Similar behavior has been reported for epoxy and carbon nanotube (CNT) systems by Natale et al. [28]. They developed a model that predicts that the contribution of the particle-particle interactions is a linear function of $\dot{\gamma}$ while that of the network elasticity decreases with shear rate due to the destruction of the network.

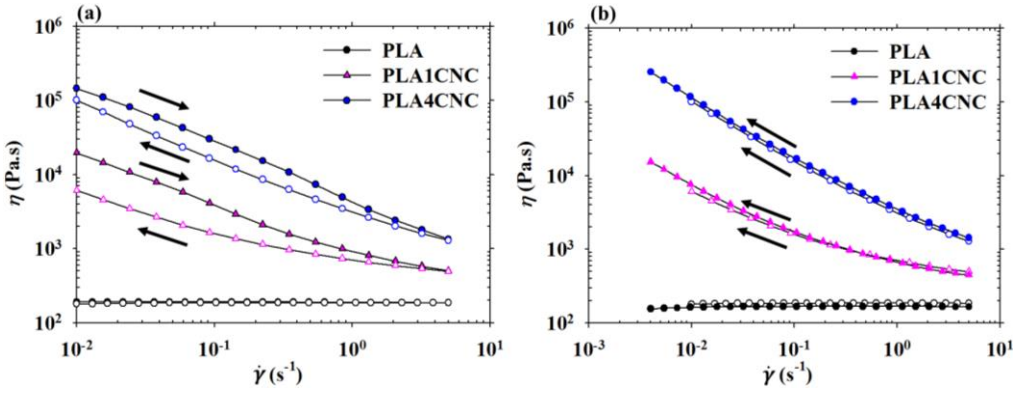

Figure 6.6: Variation of the steady-state viscosity vs shear rate of the neat PLA and nanocomposite samples; (a) filled symbols represent the experiments performed from high-to-low shear rates while the open symbols show the results of measurements from low-to-high on the same samples. (b) The two consecutive experiments were both conducted from high-to-low shear rates; open symbols: first test: filled symbols, second test

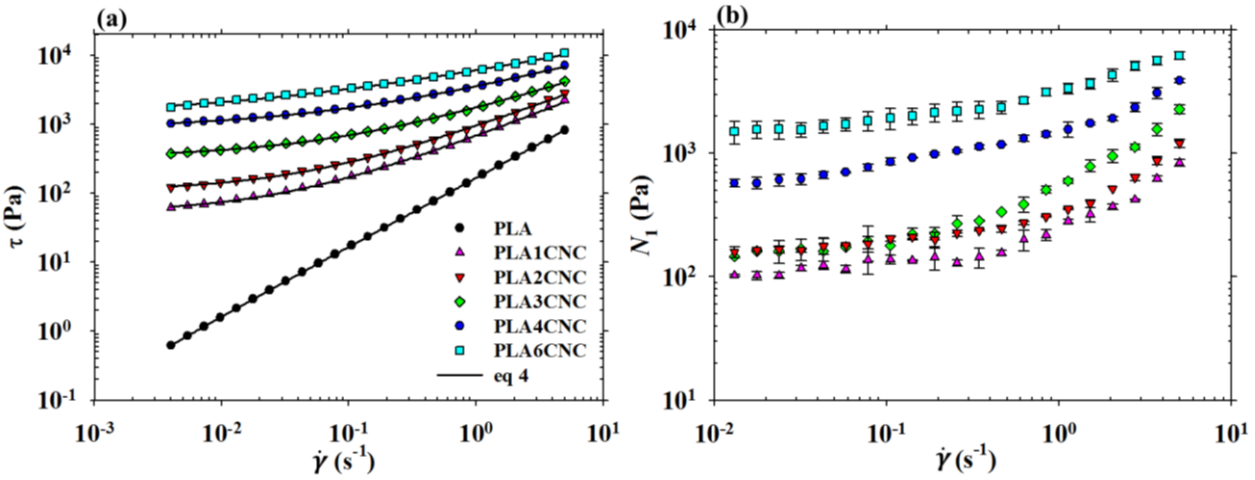

Figure 6.7: Steady-state stress data for the PLA-CNC nanocomposites from high-to-low shear rate measurements; (a) Shear stress vs shear rate. The lines are fits of the Herschel-Bulkley model (Eq. 6.4). (b) First normal stress difference vs shear rate

6.3.2.4 Cox-Merz rule

The Cox-Merz rule states that the steady-state viscosity $\eta(\dot{\gamma})$ and complex viscosity $\eta^*(\omega)$ are equal when compared at $\dot{\gamma} = \omega$ [29, 30]. This rule is not expected to be applicable for filled polymer systems, in particular nanocomposites. To verify this, the complex viscosity versus angular frequency in SAOS experiments is compared to the steady-shear viscosity versus shear rate in Figure 6.8a. As anticipated, the neat PLA follows the Cox-Merz rule. However, the PLA-CNC nanocomposites deviate largely from this rule. For both PLA1CNC and PLA4CNC samples, larger η^* values are observed compared to the η values and the differences are much larger for PLA4CNC relative to PLA1CNC. This can be explained by the structure breakdown in steady-shear flows. In fact, this rule is obeyed by isotropic systems or systems with negligible/minimal structure [30]. For filled systems that show yield stress another correlation is suggested, which is referred to as the extended Cox-Merz rule [31]. According to this relation, if the steady-state viscosity η and the complex viscosity η^* are plotted versus shear rate $\dot{\gamma}$ and $\gamma^0\omega$, respectively, where γ^0 is the strain amplitude of the SAOS experiments, the curves will superimpose [31]. Figure 6.8b compares the two curves. An acceptable agreement of this rule is observed for the neat PLA and PLA4CNC samples. However, for the PLA containing 1 wt% CNC large deviations are seen at low rates.

.

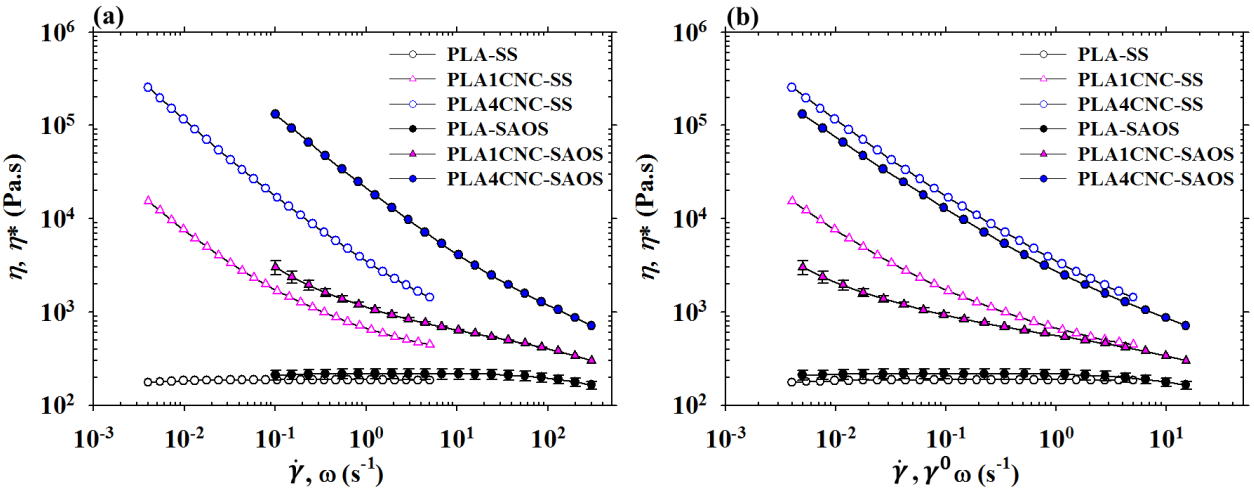

Figure 6.8: Variation of the steady-state and complex viscosities of the neat PLA and nanocomposite samples versus (a) shear rate and frequency, and (b) shear rate and $\gamma^0\omega$, respectively

6.3.2.5 Transient flow

Figure 6.9 compares the rheological behavior of samples for start-up or stress growth experiments in forward (Fig. 6.9a) and reverse (Fig. 6.9b) flows. In the filled systems the observation of an overshoot in transient viscosity, η^+, [32] shear stress, σ^+, [33] and first normal stress difference N_1^+, [32] versus time or strain can be attributed to the structure or networks of particles within the polymer matrices. Here, the variations of the transient viscosity, η^+, with time are presented in Figure 6.9a for the forward flow. As expected, the neat PLA does not show any overshoot due to the absence of any structure and of its low viscoelasticity. However, for the PLA-CNC nanocomposites overshoots at the beginning of the tests, corresponding to a low deformation of about 1, are observed for all concentrations, which can be attributed to the strong CNC network within the PLA. A similar behavior for PP-CNC nanocomposites was reported in our previous work when a good dispersion of the CNCs was achieved [10]. The overshoot becomes larger as the concentration of CNC increases revealing a stronger CNC network. These transient tests are destructive and the structure will be rebuilt under rest. Figure 6.9b depicts the behavior of the samples in the reverse flow right after, 200 and 1000 s after the first forward flow. No overshoot is observed when the reverse test is performed right after the forward flow. Small overshoots for both PLA1CNC and PLA4CNC are seen after 200 s rest time while after a longer rest time (1000 s) a larger overshoot is observed. In fact in the forward flow, the structure

in the samples is broken down and the CNCs possibly orient themselves in the flow direction. When the flow is immediately reversed the nanoparticles need time to form any structure and also due to their short length they cannot tilt over as observed for fiber suspensions [32]. However, with increasing rest time particle-particle interactions increase due to the Brownian motion, which is not negligible in these systems. Calculating the rotary particle diffusivity, D_r, assumed to be related to Brownian motion, [33-36] for rods or nanofibers of length *l* and diameter *d* [34]:

$$D_r = \frac{3K_BT\,(\ln\left(\frac{l}{d}\right) - 0.8)}{\pi\eta_0 l^3} \qquad (6.5)$$

where K_B is the Boltzmann constant (1.38×10^{-23} J.K^{-1}), T is the temperature (443.15 K), η_0 is the polymer viscosity (215 Pa.s), D_r is found to be ca. 0.04 s^{-1}. The Brownian motion in absence of flow can play an important role towards the formation of a network and particle-particle interactions. If the rest time is long enough, a network structure is progressively rebuilt, which results in overshoots in the reverse flow. The magnitude of the overshoot in the reverse flow depends on how much the network is restored during rest [33]. Letwimolnun et al. [33] observed a similar behavior for PP/PP graft maleic anhydride (PP-g-MA)/nanoclay systems.

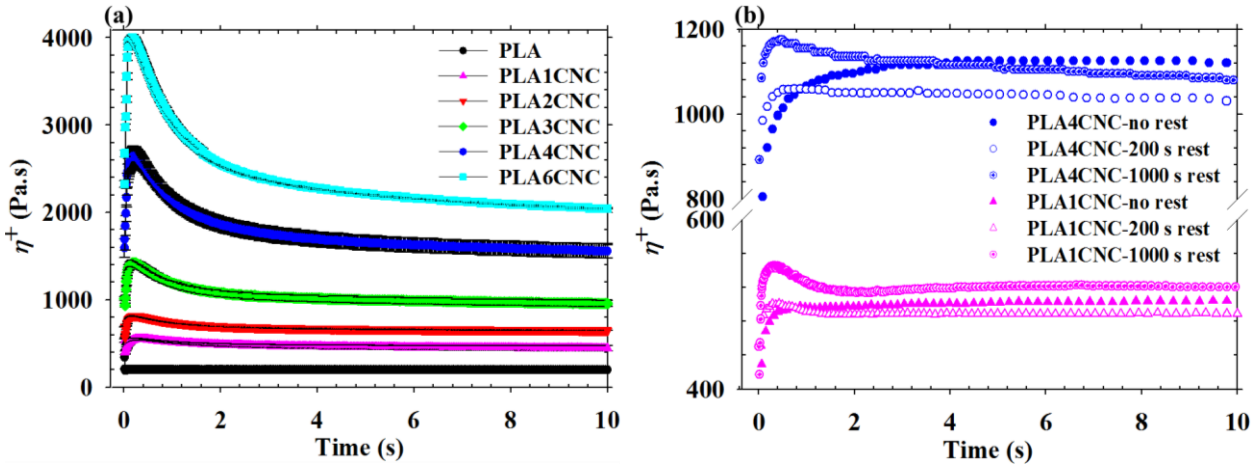

Figure 6.9: Variations of the shear stress growth coefficient, η^+, of the PLA and PLA-CNC nanocomposites as functions of time for an imposed shear rate $\dot{\gamma}$ = 5 s^{-1} in forward (a) and reversed flow after 0, 200 and 1000 s (b)

6.3.2.6 Structure build-up

Following the discussion in the previous section on microstructure build-up after cessation of a shear flow, this section tackles the effect of the flow history on the evolution of the

microstructure in PLA-CNC nanocomposites. The storage modulus, G', in SAOS experiments as a function of time after the cessation of steady-shear is presented in Figure 6.10a for samples pre-sheared at a rate of 5 s^{-1} for 360 s. As expected the neat PLA does not exhibit the formation of any microstructure. However, all PLA-CNC nanocomposites show a structure build-up during the time sweep tests. For each PLA-CNC nanocomposite sample G' grows from an initial value, $G_i^{'}$, to a time-independent value, $G_\infty^{'}$. The following empirical exponential relation can be used to describe the data [37]

$$G_t' = G_i' + (G_\infty' - G_i')\left(1 - \exp\left(-\frac{t}{\tau}\right)\right) \quad (6.6)$$

where τ is the characteristic time of each system representing the rate of structure build-up. A similar relation was used by Mobuchon et al. [38] for nanoclay (Cloisite 15A) in a blend of two miscible polybutenes. The fits of Eq. 6.6 for the data of each sample are shown by the dashed lines in Fig. 6.10. The characteristic time of the samples varies from ca. 647 s for PLA containing 1 wt% CNC to ca. 367 s for the 6 wt% CNC nanocomposite. The decrease in the characteristic time was expected because in a more concentrated sample particle-particle interactions are more pronounced and they can take place soon after cessation of shear flow compared to a less concentrated sample in which the distances between the particles, after the shear flow, are longer. Besides the effect of concentration on the evolution of the structure after cessation of shear flow, the shear rate at which the samples were pre-sheared can affect the structure build-up. Figure 6.10b illustrates the development of G' as a function of time after the cessation of flow for different shear rates in PLA containing 4 wt% CNC (PLA4CNC). No build-up in the structure of the sample, which did not experience a shear flow, is exhibited. However, samples that experienced pre-shearing at different rates exhibit a structure build-up with the same trend as observed in Fig. 6.10a. The larger the pre-shear rate the more destroyed is the initial structure and a larger recovery can be observed after the cessation of shear flow. Using Eq. 6.6, the characteristic times of the samples were obtained as 273, 340 and 450 s for samples pre-sheared at shear rates of 0.05, 0.5 and 5 s^{-1}, respectively. As expected, the sample sheared at the largest rate (i.e. 5 s^{-1}), requires longer time to build-up its structure due to the more destroyed structure. A value of 600 s was reported as the characteristic time of nanoclay filled system [38].

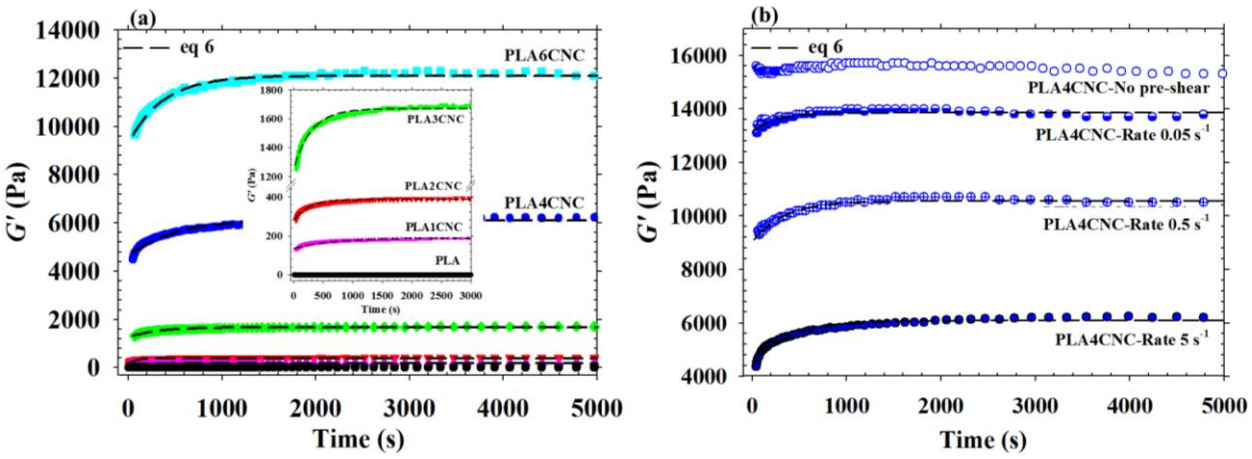

Figure 6.10: Structure evolution of PLA-CNC nanocomposites with time right after the cessation of shear flow at $\dot{\gamma}$ = 5 s^{-1} (a) (the inset shows a magnified part of Fig. 10a); structure development of the PLA4CNC nanocomposite sample not pre-sheared and pre-sheared at $\dot{\gamma}$ of 0.05, 0.5 and 5 s^{-1} (b). G' measured at a frequency of 1 rad.s^{-1} and fits using Eq. 6 (dashed lines)

6.4 Concluding remarks

In this work for the first time the rheological behavior of the well-dispersed PLA-CNC nanocomposites in SAOS, steady-shear, transient and structure build-up experiments has been investigated. SEM and TEM images showed that most of the nanoparticles are well dispersed into the PLA matrix during solution-casting, which favors the wetting of the hydrophilic CNCs within PLA. The addition of CNCs up to 6 wt% resulted in huge increases in the storage modulus and complex viscosity, especially at low frequencies. The rheological percolation threshold was calculated to be as low as 0.68 wt% CNC. Moreover, similar increases in the steady-shear viscosity for all of the nanocomposites were observed. Furthermore, it was found that the PLA-CNC nanocomposites do not obey the Cox-Merz rule. However, for nanocomposites at larger CNC content the extended Cox-Merz rule was applicable. In both SAOS and steady-shear experiments apparent yield stresses were observed for all of the nanocomposites and increased with CNC content. In steady-state experiments, increased viscosity, shear stress and first normal stress difference were observed and ascribed to the importance of the CNC network and particle-particle interactions. Furthermore, overshoots in shear transient for forward and reverse flows and structure build-up of samples after pre-shearing were ascribed to the network formation. The shear history of the nanocomposite samples was found to affect the behavior of the

nanocomposites after cessation of applied shear. The samples pre-sheared at larger rates needed longer time to recover their initial structure. Moreover, structure recovery took place at longer times for less concentrated nanocomposites due to weaker particle-particle interactions.

The rheological properties reported in this work proved the efficiency of the sonicator in solution mixing to disperse the CNCs with the consequent formation of an interconnected network of CNCs within the PLA matrix. To our knowledge, this is the first time that a very good dispersion of CNCs in a non-hydrosoluble polymer is achieved, without any change in the morphological structure of the CNCs or use of any compatibilizer or modified CNCs.

6.5 Acknowledgments

The authors acknowledge the financial support from the Natural Sciences and Engineering Research Council of Canada (NSERC). The authors are also grateful to FPInnovations for providing the CNCs.

6.6 References

[1] Klemm D, Heublein B, Fink HP, Bohn A. Cellulose: fascinating biopolymer and sustainable raw material. Angewandte Chemie. 2005;44(22):3358-3393.

[2] Klemm D, Kramer F, Moritz S, Lindstrom T, Ankerfors M, Gray D, et al. Nanocelluloses: a new family of nature-based materials. Angewandte Chemie. 2011;50(24):5438-5466.

[3] Favier V, Chanzy H, Cavaille JY. Polymer Nanocomposites Reinforced by Cellulose Whiskers. Macromolecules. 1995;28(18):6365-6367.

[4] Peresin MS, Habibi Y, Zoppe JO, Pawlak JJ, Rojas OJ. Nanofiber Composites of Polyvinyl Alcohol and Cellulose Nanocrystals: Manufacture and Characterization. Biomacromolecules. 2010;11(3):674-681.

[5] Zhang W, He X, Li C, Zhang X, Lu C, Zhang X, et al. High performance poly (vinyl alcohol)/cellulose nanocrystals nanocomposites manufactured by injection molding. Cellulose. 2014;21(1):485-494.

[6] Abitbol T, Johnstone T, Quinn TM, Gray DG. Reinforcement with cellulose nanocrystals of poly(vinyl alcohol) hydrogels prepared by cyclic freezing and thawing. Soft Matter. 2011;7(6):2373-2379.

[7] Park W-I, Kang M, Kim H-S, Jin H-J. Electrospinning of Poly(ethylene oxide) with Bacterial Cellulose Whiskers. Macromolecular Symposia. 2007;249-250(1):289-294.

[8] Siqueira G, Abdillahi H, Bras J, Dufresne A. High reinforcing capability cellulose nanocrystals extracted from Syngonanthus nitens (Capim Dourado). Cellulose. 2010;17(2):289-298.

[9] Bendahou A, Kaddami H, Dufresne A. Investigation on the effect of cellulosic nanoparticles' morphology on the properties of natural rubber based nanocomposites. European Polymer Journal. 2010;46(4):609-620.

[10] Bagheriasl D, Carreau PJ, Dubois C, Riedl B. Properties of polypropylene and polypropylene/poly(ethylene-co-vinyl alcohol) blend/CNC nanocomposites. Composites Science and Technology. 2015;117:357-363.

[11] Siqueira G, Bras J, Dufresne A. Cellulose Whiskers versus Microfibrils: Influence of the Nature of the Nanoparticle and its Surface Functionalization on the Thermal and Mechanical Properties of Nanocomposites. Biomacromolecules. 2009;10(2):425-432.

[12] Goffin AL, Raquez JM, Duquesne E, Siqueira G, Habibi Y, Dufresne A, et al. Poly(ε-caprolactone) based nanocomposites reinforced by surface-grafted cellulose nanowhiskers via extrusion processing: Morphology, rheology, and thermo-mechanical properties. Polymer. 2011;52(7):1532-1538.

[13] Goffin AL, Raquez JM, Duquesne E, Siqueira G, Habibi Y, Dufresne A, et al. From interfacial ring-opening polymerization to melt processing of cellulose nanowhisker-filled polylactide-based nanocomposites. Biomacromolecules. 2011;12(7):2456-2465.

[14] Raquez JM, Murena Y, Goffin AL, Habibi Y, Ruelle B, DeBuyl F, et al. Surface-modification of cellulose nanowhiskers and their use as nanoreinforcers into polylactide: A sustainably-integrated approach. Composites Science and Technology. 2012;72(5):544-549.

[15] Siqueira G, Bras J, Follain N, Belbekhouche S, Marais S, Dufresne A. Thermal and mechanical properties of bio-nanocomposites reinforced by Luffa cylindrica cellulose nanocrystals. Carbohydrate Polymers. 2013;91(2):711-717.

[16] Morandi G, Heath L, Thielemans W. Cellulose nanocrystals grafted with polystyrene chains through surface-initiated atom transfer radical polymerization (SI-ATRP). Langmuir : the ACS journal of surfaces and colloids. 2009;25(14):8280-8286.

[17] Pereda M, Kissi NE, Dufresne A. Extrusion of Polysaccharide Nanocrystal Reinforced Polymer Nanocomposites through Compatibilization with Poly(ethylene oxide). ACS applied materials & interfaces. 2014;6(12):9365-9375.

[18] Arias A, Heuzey M-C, Huneault M, Ausias G, Bendahou A. Enhanced dispersion of cellulose nanocrystals in melt-processed polylactide-based nanocomposites. Cellulose. 2015;22(1):483-498.

[19] Khoshkava V, Kamal MR. Effect of cellulose nanocrystals (CNC) particle morphology on dispersion and rheological and mechanical properties of polypropylene/CNC nanocomposites. ACS applied materials & interfaces. 2014;6(11):8146-8157.

[20] Kamal MR, Khoshkava V. Effect of cellulose nanocrystals (CNC) on rheological and mechanical properties and crystallization behavior of PLA/CNC nanocomposites. Carbohydr Polym. 2015;123:105-114.

[21] Mabrouk AB, Magnin A, Belgacem MN, Boufi S. Melt rheology of nanocomposites based on acrylic copolymer and cellulose whiskers. Composites Science and Technology. 2011;71(6):818-827.

[22] Bitinis N, Verdejo R, Bras J, Fortunati E, Kenny JM, Torre L, et al. Poly(lactic acid)/natural rubber/cellulose nanocrystal bionanocomposites part I. Processing and morphology. Carbohydr Polym. 2013;96(2):611-620.

[23] Abbasi S, Carreau PJ, Derdouri A, Moan M. Rheological properties and percolation in suspensions of multiwalled carbon nanotubes in polycarbonate. Rheologica Acta. 2009;48(9):943-959.

[24] Sinha Ray S, Yamada K, Okamoto M, Ueda K. New polylactide-layered silicate nanocomposites. 2. Concurrent improvements of material properties, biodegradability and melt rheology. Polymer. 2003;44(3):857-866.

[25] Ghanbari A, Heuzey M-C, Carreau P, Ton-That M-T. Morphological and rheological properties of PET/clay nanocomposites. Rheologica Acta. 2013;52(1):59-74.

[26] Du F, Scogna RC, Zhou W, Brand S, Fischer JE, Winey KI. Nanotube Networks in Polymer Nanocomposites: Rheology and Electrical Conductivity. Macromolecules. 2004;37(24):9048-9055.

[27] Hu G, Zhao C, Zhang S, Yang M, Wang Z. Low percolation thresholds of electrical conductivity and rheology in poly(ethylene terephthalate) through the networks of multi-walled carbon nanotubes. Polymer. 2006;47(1):480-488.

[28] Natale G, Heuzey MC, Carreau PJ, Ausias G, Férec J. Rheological modeling of carbon nanotube suspensions with rod–rod interactions. AIChE Journal. 2014;60(4):1476-1487.

[29] Cox WP, Merz EH. Correlation of dynamic and steady flow viscosities. Journal of Polymer Science. 1958;28(118):619-622.

[30] Shafiei-Sabet S, Hamad WY, Hatzikiriakos SG. Rheology of nanocrystalline cellulose aqueous suspensions. Langmuir : the ACS journal of surfaces and colloids. 2012;28(49):17124-17133.

[31] Doraiswamy D, Mujumdar AN, Tsao I, Beris AN, Danforth SC, Metzner AB. The Cox–Merz rule extended: A rheological model for concentrated suspensions and other materials with a yield stress. Journal of Rheology. 1991;35(4):647-685.

[32] Sepehr M, Ausias G, Carreau PJ. Rheological properties of short fiber filled polypropylene in transient shear flow. Journal of Non-Newtonian Fluid Mechanics. 2004;123(1):19-32.

[33] Letwimolnun W, Vergnes B, Ausias G, Carreau PJ. Stress overshoots of organoclay nanocomposites in transient shear flow. Journal of Non-Newtonian Fluid Mechanics. 2007;141(2–3):167-179.

[34] Cassagnau P. Linear viscoelasticity and dynamics of suspensions and molten polymers filled with nanoparticles of different aspect ratios. Polymer. 2013;54(18):4762-4775.

[35] Hong JS, Kim YK, Ahn KH, Lee SJ. Shear-induced migration of nanoclay during morphology evolution of PBT/PS blend. Journal of Applied Polymer Science. 2008;108(1):565-575.

[36] Ren J, Casanueva BF, Mitchell CA, Krishnamoorti R. Disorientation Kinetics of Aligned Polymer Layered Silicate Nanocomposites. Macromolecules. 2003;36(11):4188-4194.

[37] Khalkhal F, Carreau PJ, Ausias G. Effect of flow history on linear viscoelastic properties and the evolution of the structure of multiwalled carbon nanotube suspensions in an epoxy. Journal of Rheology. 2011;55(1):153-175.

[38] Mobuchon C, Carreau P, Heuzey M-C. Effect of flow history on the structure of a non-polar polymer/clay nanocomposite model system. Rheologica Acta. 2007;46(8):1045-1056.

CHAPTER 7 ARTICLE 3 : ENHANCED PROPERTIES OF POLYLACTIDE BY INCORPORATING CELLULOSE NANOCRYSTALS[4]

Davood Bagheriasl[a], Pierre J. Carreau[a]*, Bernard Riedl[b], and Charles Dubois[a]

[a]*Research Center for High Performance Polymer and Composite Systems (CREPEC), Chemical Engineering Department, Polytechnique Montreal, PO Box 6079, Stn Centre-Ville, Montreal, QC H3C 3A7, Canada*

[b]*Département des sciences du bois et de la forêt, Faculté de foresterie, géographie et géomatique, Université Laval, Quebec, QC G1V 0A6, Canada*

*Corresponding Author: e-mail: pcarreau@polymtl.ca

Abstract

Polylactide (PLA)-cellulose nanocrystal (CNC) bionanocomposites with different CNC loadings were prepared via a simple solvent casting preparation method. Scanning electron microscopy showed some very fine aggregates with a size of 1-3 μm whereas transmission electron microscopy revealed the existence of a well-dispersed structure of CNCs within the PLA matrix at a nano-scale. The loss and storage moduli of the nanocomposites increased significantly with CNC content, particularly at low frequencies, indicative of a solid-like behavior. The Young modulus of the nanocomposites increased up to 23%, for PLA containing 6 wt% CNCs compared to the neat PLA; however, the strain at break slightly decreased. In dynamic mechanical thermal analysis, the storage modulus of the naonocomposites increased up to 74% in the glassy region and 490% in the rubbery region. The total crystalline content of the PLA in the nanocomposites and the crystallization temperature increased, which were ascribed to the nucleation effect of the CNCs on the crystallization of PLA.

Keywords: *polymer nanocomposites; cellulose nanocrystals (CNCs); polylactide; mechanical properties; dispersion; thermal properties*

[4] Submitted to Cellulose in December 2015.

7.1 Introduction

Cellulose nanocrystals (CNCs) are rodlike nanoparticles obtained by acid hydrolysis of cellulose, which is the most common biomacromolecule on earth. CNC's properties such as high strength, renewability, abundance in nature, biocompatibility, biodegradability, low density and very large surface area per weight unit are of interest for many applications [1, 2]. Over the last years, the combination of these properties has made CNCs interesting alternatives to inorganic reinforcing agents for polymer composites. However, obtaining a good dispersion of CNCs in hydrophobic polymers and, consequently, enhanced properties when incorporated in hydrophobic polymers remains a challenge, in particular without the use of any compatibilizers and CNC modifications. The strong hydrogen bonds between CNC particles favor the formation of large agglomerates. The first use of CNCs as reinforcing agents in polymers was reported by Favier et al. [3] who could enhance the shear modulus of solution-cast films of poly(styrene-co-butyl acrylate) latex by 4 orders of magnitudes in the rubbery region. Since then, their applications as reinforcing agents in polymers have grown, but limited to a few water-soluble polymers or polymers in latex form [3-9]. However, in most common polymers CNC surface modification or compatibilization was necessary to achieve a good CNC dispersion [10-16].

Recently, there has been increasing interest to incorporate CNCs into biopolymers to expand their applications by improving their mechanical and thermal properties over a wide range of temperature [11, 13, 17]. Such combinations of biorenewable, biocompatible and biodegradable components would create green composite materials that can replace petroleum-based polymeric products, especially in packaging and automotive industries.

Polylactide (PLA) as a biorenewable, biocompatible and biodegradable polymer has been commercialized and found applications in tissue engineering, medical, textile, automotive and packaging industries by employing various industrial processing techniques similar to those used for polyolefins (i.e. extrusion, injection molding, film blowing and blow molding) [18-20]. Also it has been used in food industry to produce short shelf life products with applications such as salad containers, drinking cups, water/milk bottles and degradable plastic bags, overwrap and lamination films [18, 21-25]. In the coming years, PLA production and consumption are expected to increase. However, neat PLA exhibits slow crystallization and, consequently, low degree of crystallization upon fast cooling and low heat resistance (low modulus at high temperature),

which limits its use in many applications. To overcome these drawbacks, one solution is the use of reinforcing agents. For this aim, CNCs are suitable candidates for improving the mechanical and thermal properties of PLA, while maintaining its unique properties such as biocompatibility, biodegradability and transparency. However, obtaining a fairly good dispersion of CNCs within PLA is necessary in order to achieve enhanced properties for the resulting biocomposites at low nanoparticle concentrations.

Goffin et al. [26] reported improved morphology and increased storage modulus, G', in small-amplitude oscillatory shear, SAOS, tests for blends of PLA and polycaprolactone (PCL) when the CNCs were added via a semi-solution based method. They initially prepared a masterbatch of p(lactide-co-caprolactone) di-block copolymer-grafted CNC via a two-step in-situ polymerization in solution and, then, introduced the resulting masterbatch into PLA-PCL blends through melt-extrusion. Nucleating effect of the CNCs on the crystallization of PLA was revealed by the differential scanning calorimetry results when 8 wt% PLA-grafted CNCs were added to PLA [13]. Bitinis et al. [27] observed increased values for the complex viscosity, η^*, and storage modulus, G', for blends of PLA and natural rubber (NR) filled with 3 wt% unmodified CNCs and 3 and 5 wt% CNCs grafted with C_{18} alkyl chains. However, their results did not show significant changes when PLA-NR blends were filled with PLA-grafted CNCs. In another work, they reported enhanced storage modulus in dynamic mechanical thermal analysis (DMTA) at temperatures below the glass transition temperature, T_g, of PLA when CNC-g-PLA, CNC-g-C18 and unmodified CNCs were added to PLA-NR blends. However, the tensile properties were decreased, except for PLA-NR filled with 1 wt% CNC-g-C18. Better results were observed for PLA-NR filled with unmodified CNCs for both tensile and DMTA results, compared to the modified CNCs [28]. Enhanced tensile strength and Young modulus were reported, by 27 and 21%, respectively, for PLA containing 1 wt% organosilane modified CNCs prepared via solution casting from a toluene medium, and ascribed to the increased degree of crystallinity. However, the strain at break significantly decreased, by more than 70 % relative to the neat PLA. The addition of a larger content of organosilane modified CNCs resulted in lower enhancements, probably due to the plasticization effect of the organosilane modifier [29]. In some cases achieving good dispersion did not result in enhanced properties [30, 31]. Fortunati et al. [30, 32] obtained a finer dispersion of CNCs in PLA by using a surfactant, but the mechanical properties were deteriorated compared to the PLA and PLA filled with unmodified CNCs, due to a

plasticization effect of the surfactant [30]. Arias et al. [31] could obtain a well-dispersed structure of CNCs in a PLA matrix via a PEO-CNC masterbatch preparation, although no property enhancements were reported for the resulting nanocomposites compared to the neat PLA and PLA filled with uncompatibilized CNCs.

In this work the effect of the CNCs on the rheological, mechanical and thermal properties of PLA was investigated. To this end, a simple solution preparation method and solvent casting was used to favor a better dispersion of the hydrophilic CNCs within the PLA matrix. Our main objective is to develop biobased and biodegradable PLA-CNC nanocomposites with improved mechanical properties. A dispersed structure via a simple method without any modification or compatibilization is achieved leading for the first time to major enhancements of the solid-state properties.

7.2 Experimental Section

7.2.1 Materials

A commercial grade polylactide (PLA) (Ingeo Biopolymer 3251D) with MFR of 35 g/10 min (190 °C/2.16 kg), crystalline melting temperature of 155-170 °C and glass transition temperature (T_g) of 55-60 °C was purchased from NatureWorks LLC (Minnetonka, MN, USA) and used as the matrix. N,N-dimethylformamide (DMF), anhydrous 99.8%, was purchased from Sigma-Aldrich Canada Co. (Oakville, ON, Canada). Freeze-dried CNCs were kindly provided by FPInnovations (Pointe-Claire, QC, Canada).

7.2.2 Sample Preparation

To prepare the nanocomposites a solution mixing method in DMF medium was used. The desired amount of CNCs were first dispersed in 135 mL of DMF using a water-bath sonicator (FS30 100 Watts Ultrasonic Cleaner, Fisher Scientific, Pittsburg, PA) for 2 h, then 40 g of PLA were added and the mixture was heated up to 70 °C while stirring with a magnetic stirrer during 150 min until the complete dissolution of the PLA. The mixture was then poured on a tray and dried in a vacuum oven at 80 °C for 36 h. Using a coffee grinder, the product was ground into powder and kept in the oven at 60 °C for another 36 h. Thereafter, the samples were compression molded for 10 min at 175 °C in the presence of N_2, where the pressure was increased gradually from 0 to 29

kPa, followed by 5 min at room temperature and pressure of 29 kPa to prepare the test specimens. The nanocomposites containing CNCs were coded according to their CNC content on weight percentage basis. For instance, PLA6CNC denotes to PLA containing 6 wt% CNCs.

7.2.3 Characterization

7.2.3.1 Microscopy

Scanning electron microscopy (SEM) was carried out on ultra-microtomed surfaces, coated with gold, using a JEOL JSM 7600TFE microscope (JEOL USA Inc., Peabody, MA, USA) operated at a voltage of 2 kV.

Transmission electron microscopy (TEM) analysis was conducted using a JEOL JEM-2100F microscope (JEOL USA Inc., Peabody, MA, USA), operating at 200 kV. The samples were microtomed into slices of approximately 50-80 nm thick at −100 °C using an Ultracut FC microtome (LEICA) with a diamond knife. For a better visualization the samples were stained using a bis(ethylenediamine) copper(II) hydroxide solution (1.0 M in H_2O) purchased from Sigma-Aldrich Canada Co. (Oakville, ON, Canada). To this end, first the copper(II)-ethylenediamine complex was diluted to a 1 wt% solution with deionized (DI) water, then the ultra-microtomed samples placed on copper grids were immersed in the solution for 150 s. To remove the excess of the absorbed solution the samples were successively immersed in DI water three times, each time in fresh water for 10 s. Finally, the samples were left at room temperature for 24 h to avoid fracture of the stained layer due to fast evaporation, followed by another 24 h in a desiccator before TEM analysis.

7.2.3.2 Rheology

The rheological properties of PLA and the nanocomposites were measured using a stress-controlled MCR 301 rheometer (Anton Paar, Austria). The experiments were conducted under a nitrogen atmosphere to avoid oxidation of the samples. A cone-and-plate geometry was used with a gap of 51 μm, cone angle of 1.98°, parallelity of ±1 μm and a diameter of 25 mm. Small-amplitude oscillatory shear (SAOS) tests were performed at a strain amplitude of 0.05 to ensure that the measurements were in the linear viscoelastic regime. Time-sweep experiments at a

frequency of 1 rad.s^{-1} were conducted over 15 min to check the thermal stability of the samples within the time of the SAOS experiments.

7.2.3.3 Mechanical and thermal properties

7.2.3.3.1 Tensile

Tensile properties of the samples were measured using an Instron 3365 at room temperature according to standard ASTM D638. Tensile specimens, of dumbbell shape type V, were stretched at room temperature with a crosshead speed of 5 mm/min using a load cell of 5 kN. For each sample a minimum of 7 specimens were tested.

7.2.3.3.2 Dynamic mechanical thermal properties (DMTA)

DMTA was performed on compression-molded samples using a DMA 2980 analyzer (TA Instruments, New Castle, DE, USA). The specimens were tested in the dual cantilever bending mode at an amplitude of 30 μm, a frequency of 1 Hz, and a heating rate of 3 °C/min from 24 to 120 °C. Four replicates for each sample were tested.

7.2.3.3.3 Differential scanning calorimetry (DSC)

DSC of the neat PLA and nanocomposites was performed on a DSCQ1000 (TA Instruments, New Castle, DE, USA) on 5-10 mg material, under a nitrogen atmosphere. The samples were heated from 25 to 200 °C at a constant rate of 2 °C/min and held at 200 °C for 3 min, then cooled to 40 °C at the same rate. The DSC tests were performed twice for each sample with a fresh specimen.

7.3 Results and discussion

7.3.1 Microscopy

Figure 7.1a shows a TEM image of individual and bundles of few CNCs that was obtained for a 0.5 wt% aqueous suspension of CNCs. The average particle width, length and aspect ratio over 200 measurements were 16±3 nm, 90±17 nm and 6±2, respectively, measured with ImageJ software. Figure 7.1b and c present SEM and TEM images of PLA4CNC (nanocomposite containing 4 wt% CNCs). Some agglomerates of CNCs, fibrillar and random-shape of sizes

varying from 1 to 3 μm are obviously formed within the PLA (Fig. 7.1b). Individual CNCs and bundles of few CNCs dispersed into the PLA matrix are observed in the TEM images of Figure 7.1c. These images reveal that the solution preparation method used in this study could lead to a good dispersion of the CNCs, down to the individual size or bundles of few CNCs. The TEM image of Fig. 7.1c clearly validates our assumption that the simple solution preparation is efficient in dispersing the CNCs into the PLA, although some small agglomerates in the range of few (1-3) μm are observed (Fig. 7.1b).

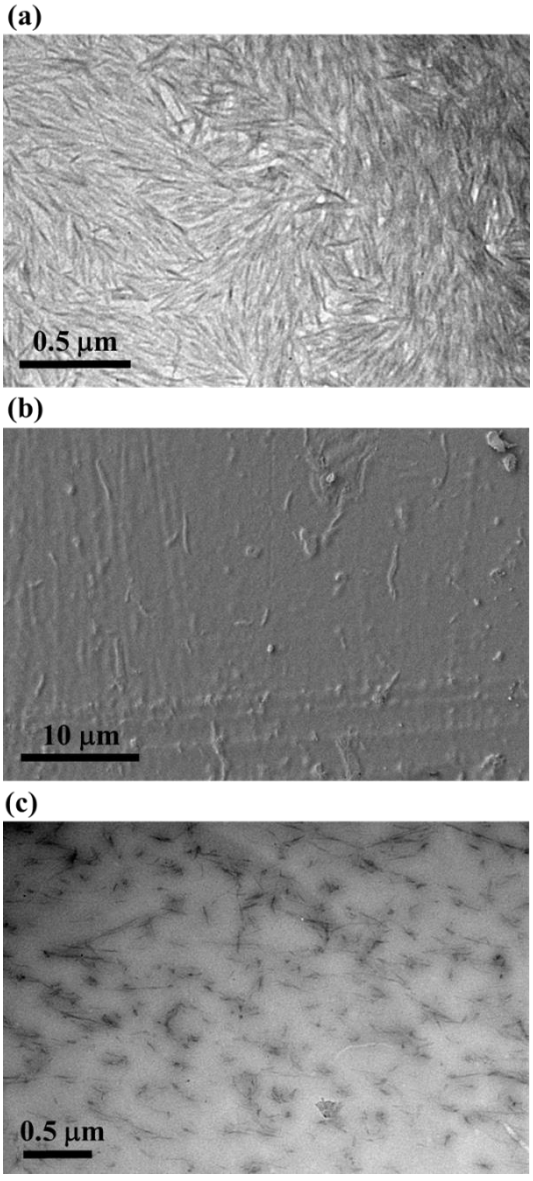

Figure 7.1: TEM image of CNC aqueous suspension (0.5 wt%) (a), SEM micrograph (b) and TEM image (c) of PLA4CNC

7.3.2 Rheology

In time-sweep experiments performed over 15 min, all samples showed stable rheological properties with changes less than 2%. Figure 7.2 illustrates the loss, G'', and storage, G', moduli and loss tangent, tan δ, where δ is the phase angle, versus frequency, ω, of the neat PLA and PLA-CNC nanocomposites for different CNC contents (1-6 wt%). The neat PLA exhibits a terminal zone with slopes equal to 1 and 2 on the log-log plot of G'' and G', respectively, versus ω (Fig. 7.2a). For PLA containing 1 wt% CNC (PLA1CNC), G'' and G' increase by 1 and 4 orders of magnitude and for higher concentrations of CNCs further increases up to 3 and 6 orders of magnitude, respectively, are observed, compared to the neat PLA (Fig. 7.2a). Figure 7.2b reports a frequency-dependent behavior for tan δ of the neat PLA and the composites. For the neat PLA, as expected, tan δ increases as the frequency decreases reflecting its Newtonian character at low frequencies. However, with the incorporation of the CNCs tan δ significantly decreases for the whole range of frequency and is almost frequency independent, showing that the nanocomposites become more elastic compared to the neat PLA. The drastic decreases of tan δ and the observations that G'' and G' tend towards plateaus at low frequencies are clear indications of the formation of a network that causes the transition from liquid- to solid-like or gel-like behavior. Similar rheological behavior in SAOS has been reported for other polymer nanocomposites containing CNCs, clays or carbon nanotubes and attributed to the efficient dispersion of the nanoparticles in polymer matrices [10, 17, 33-35]. The rheological properties reported in this section confirm the efficiency of the solution mixing to disperse the CNCs with the consequent formation of an interconnected network of CNCs within the PLA matrix.

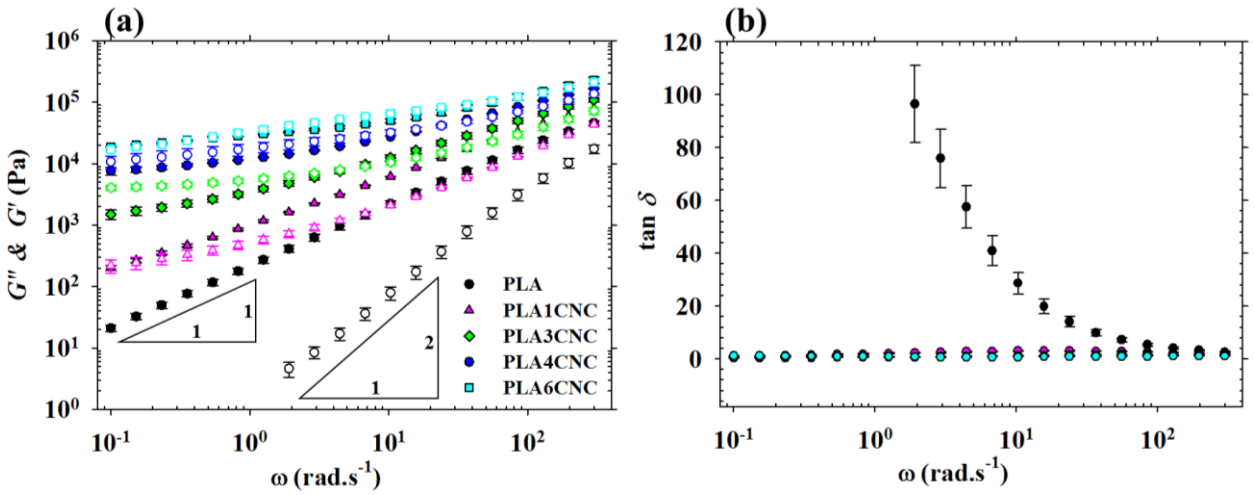

Figure 7.2: SAOS data for the neat PLA and PLA-CNC nanocomposites at 170 °C (strain = 0.05): G'', filled symbols, and G', open symbols, (a) and tan δ (b) vs ω

7.3.3 Mechanical and thermal properties

7.3.3.1 Tensile

Figure 7.3 compares the Young modulus, tensile strength and strain at break of the nanocomposites with those of the neat PLA. The Young modulus increases up to 23% for PLA6CNC (Fig. 7.3a). In Figure 7.3b, the tensile strength of the nanocomposites does not show any significant enhancement relative to the neat PLA. A similar tensile behavior with an enhanced Young modulus but unchanged tensile strength has been observed for other nanocomposites [11, 31, 36, 37] and ascribed to the lack of stress transfer from the matrix to the filler. This occurs usually when the polarity of the matrix and the filler is different, which would interfere with the stress distribution throughout the composite when a load is applied [38]. Figure 7.3c reports that the strain at break does not decrease significantly when CNCs are added to PLA, although the neat PLA is already brittle. Decreased strains at break were also reported in other investigations on polymer-CNC systems [10, 11, 31, 36].

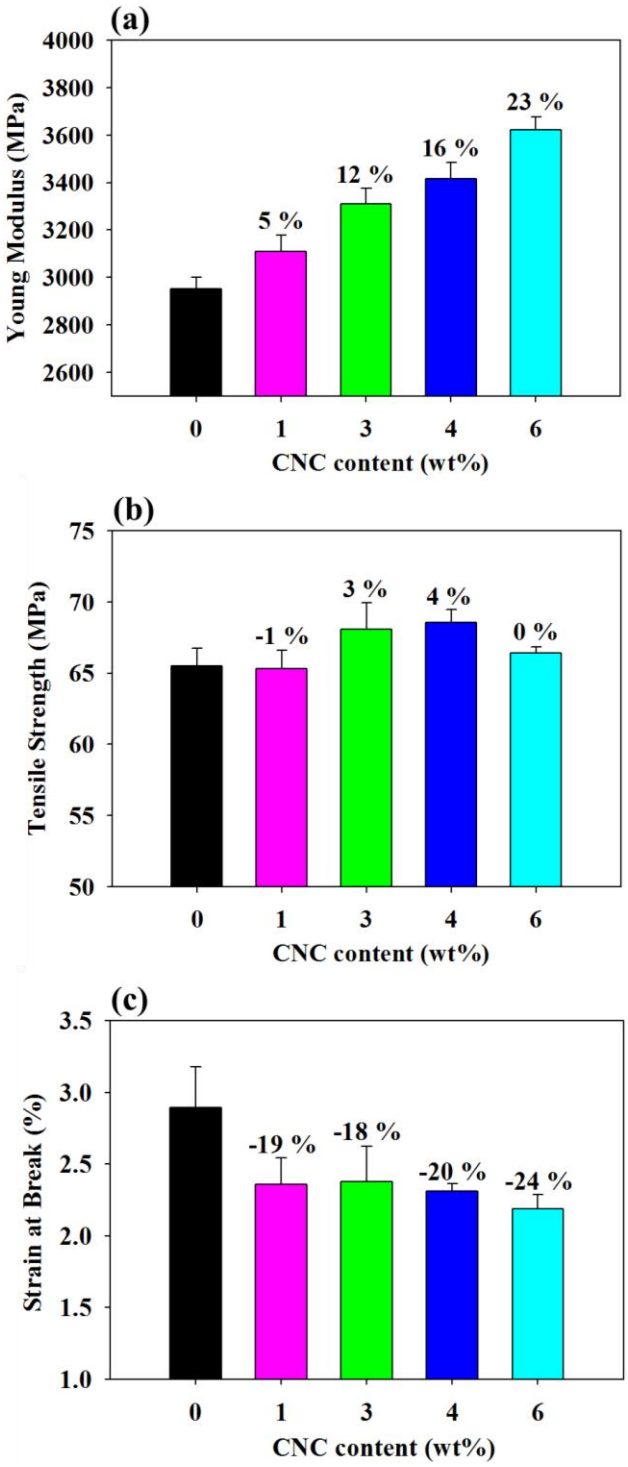

Figure 7.3: Comparison of the tensile properties of the samples: Young modulus (a), tensile strength (b) and strain at break (c). The numbers above the bars represent the changes in percentage with respect to the neat PLA

For fiber-reinforced composites the Young modulus of the composite, E, can be described by models developed by Halpin-Tsai [39, 40]. For 3D random orientation of fibers with length l and diameter d, the modulus of a composite based on the Halpin-Tsai model is given by [39]

$$E = E_m(1 + \xi\eta\varphi_f)/(1 - \eta\varphi_f) \qquad (7.1)$$

where

$$\eta = (\alpha E_f/E_m - 1)/(\alpha E_f/E_m + \xi) \quad (7.2)$$

and E_m and E_f are the Young moduli of the matrix and the fibers, respectively, $\xi = 2l/d$ is a shape parameter, φ_f is the fiber volume fraction and α is the orientation factor, which is equal to 1/6 for 3D random orientation (note that for 2D orientation α is equal to 1/3 [39]). For the calculation of E, the following values were considered: E_m= 2.95 GPa, E_f = 150 GPa, ρ_m = 1.25 g/cm^3, ρ_f = 1.58 g/cm^3, d = 16 nm, l = 90 nm and $\xi = 12$. Figure 7.4 compares the predictions of Eq. 7.1 to the experimental data. Very good agreement between the predictions and experimental data is observed.

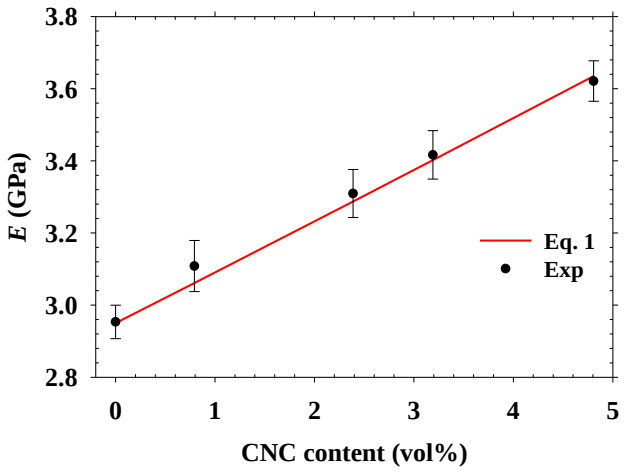

Figure 7.4: Comparison of the predictions of the Halpin-Tsai model (Eq. 7.1) with experimental data of the Young modulus for the PLA/CNC nanocomposites

7.3.3.2 DMTA

Figure 7.5 displays the DMTA results for the storage modulus, E', and tan δ of the samples over a wide range of temperature. Figure 7.5a shows that the storage modulus of PLA is significantly

enhanced by the addition of the CNCs. This improvement is much larger at temperatures higher than T_g (i.e. rubbery region). In fact, a higher content of the CNCs made the material stiffer, with a higher modulus. The characteristic peaks in tan δ curves (Fig. 7.5b) correspond to the glass transition temperature (T_g) of the samples. According to the position of the peaks, T_g of PLA is not affected significantly by the addition of the CNCs. However, the area under the peak of T_g, which is strongly related to the extent of damping or energy dissipation due to the segmental motion of the polymer chains at T_g, is significantly decreased by the CNCs. This reduction is more important as the CNC concentration in the nanocomposite samples is large. Larger contents of the filler, as long as this does not significantly affect the quality of the dispersion of the filler, provide larger interfacial interactions, which restrict more the polymer chains [10].

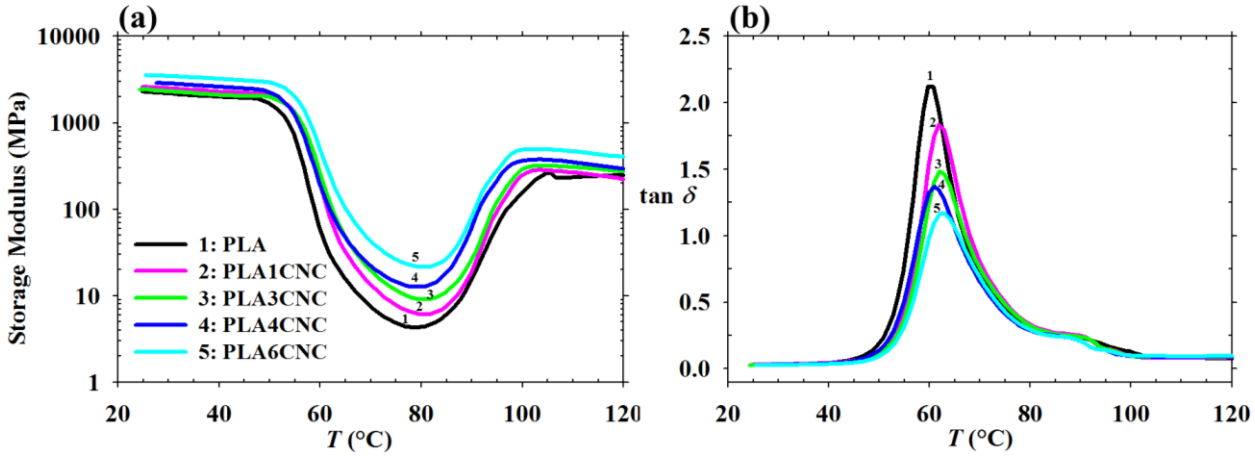

Figure 7.5: DMTA data for the various samples over a wide range of temperature: storage modulus (a) and tan δ (b)

Figure 7.6 helps to better compare the values of the storage modulus of the samples at 25 °C (glassy region) and 70 °C (rubbery region). The storage modulus of the PLA sample containing 6 wt% CNCs is enhanced by ca. 74% at room temperature and by ca. 490% at 70 °C. When PLA goes through the rubbery region its modulus decreases significantly and the reinforcement effect of the CNCs becomes more evident. This huge enhancement in the rubbery region can extend the applications of PLA, particularly for products exposed to high temperature. Kamal and Khoshkava [17] reported much lower values for PLA-CNC composites; relative to the neat PLA, the storage modulus increased up to ca. 27% in the glassy region and up to ca. 20% in the rubbery region for PLA containing 7 wt% CNCs. Bagheriasl et al. [10] reported a 60% increase for the rubbery-region modulus of polypropylene (PP) with the addition of 5 wt% CNCs.

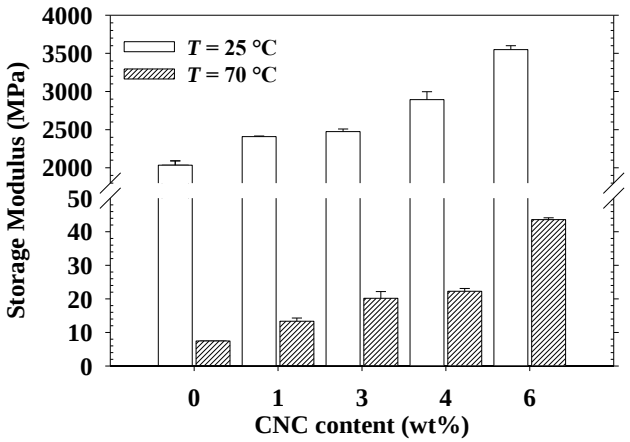

Figure 7.6: Comparison of the storage modulus of the neat PLA and PLA-CNC nanocomposites with different CNC loadings in the glassy and rubbery regions

7.3.3.3 DSC

Figure 7.7 reports the crystallization temperature and crystalline contents of PLA and the nanocomposites during heating and cooling cycles. The crystalline contents of the samples (Fig. 7a) were calculated from the enthalpies of melting, ΔH_m, and cold crystallization, ΔH_{cc}, for the heating cycles and from the enthalpy of crystallization for the cooling cycles, ΔH_c, according to the following equations [29]

$$X_c^{heating} = (\Delta H_m - \Delta H_{cc}) \times 100/(w_{PLA}\Delta H_m^0) \qquad (6.3)$$

$$X_c^{cooling} = \Delta H_c \times 100/(w_{PLA}\Delta H_m^0) \quad (6.4)$$

where w_{PLA} is the weight fraction of the PLA phase and ΔH_m^0 is the heat of fusion of 100% crystalline PLA (93 J/g) [41].

In the crystallization of polymers in presence of nanoparticles, two competing phenomena take place: the nanoparticles act as nuclei tending to increase the total crystalline content of the polymer, whereas the mobility of polymer chains decreases, which tends to lower the crystalline content. Therefore, depending on which effect is stronger the total crystalline content of the matrix can increase or decrease; sometimes no significant changes are observed with the addition of nanoparticles. Here, the addition of the CNCs does not change the total crystalline content of

PLA in the heating cycles. As the specimens for DSC measurements were cut from the dumbbell samples used for tensile tests and no significant changes in the total crystalline content of these samples were observed in the heating cycle, we can conclude that the enhancement of the mechanical properties with the addition of CNCs was entirely due to the reinforcement effect of the CNCs. However, in the cooling cycles, the crystalline content of the nanocomposites increases from ca. 37% for the neat PLA to ca. 45 and 49% for the PLA containing 1 and 6 wt% CNC, respectively. This suggests that annealing could improve the properties of the PLA-CNC composites. Slow crystallization rate is one of the drawbacks of PLA and fast cooling from the melt to solid state usually results in low crystalline contents. Thus, by slow cooling or annealing in the presence of the CNCs larger crystalline contents and, consequently, improved properties will be achieved. Figure 7.7b compares the onset temperature of crystallization of samples in cooling cycles, T_c, which is drastically shifted to higher values as soon as 1 wt% CNCs are added to the PLA matrix and, then, increases slightly by adding more CNCs. This shift from ca. 111 °C for the neat PLA to ca. 132 °C for PLA containing 1 wt% CNC and up to ca. 135 °C for larger CNC loadings, together with the enhanced crystallinity (i.e. 20-30% larger relative to the PLA) in cooling cycles can be definitely ascribed to the nucleation effect of the CNCs on the crystallization of PLA. Similar results have been reported in our previous work where compatibilized CNCs were added into a polypropylene [10].

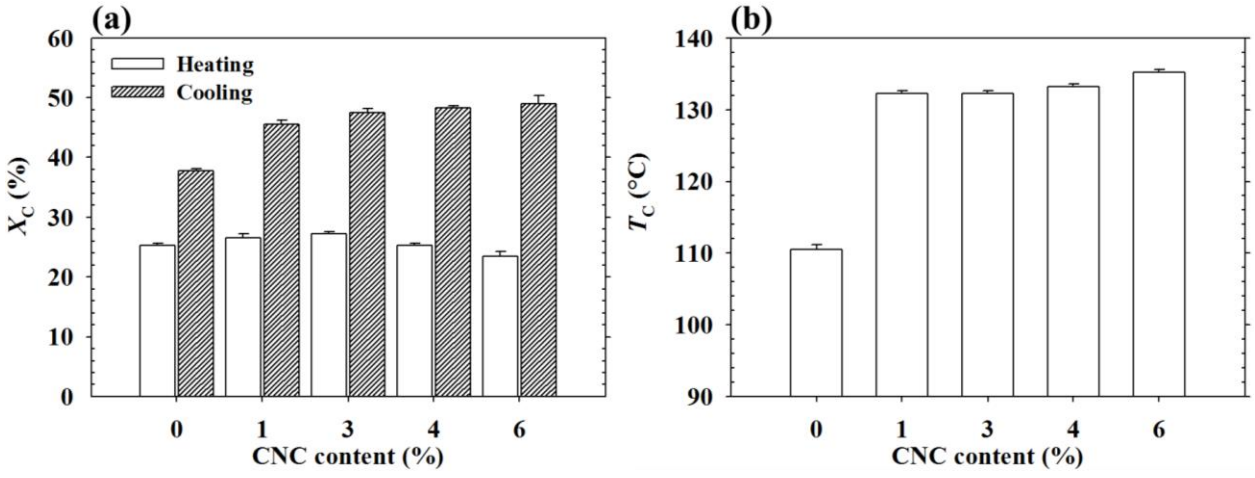

Figure 7.7: Crystalline contents of the samples calculated based on the data obtained in the heating and cooling cycles (Eqs. 7.3 and 7.4), and comparison of the onset of crystallization temperature of the samples during cooling cycles

7.4 Concluding remarks

In this work the effect of dispersed CNCs on the rheological, mechanical and thermal properties of polylactide was investigated. The addition of CNCs into the PLA matrix via a simple solution based preparation method and utilizing a water-bath sonicator to fully disperse the CNCs resulted in huge increases in the loss and storage moduli in molten state; we observed an enhancement in the Young modulus at room temperature up to a 23% and increases up to 74 and 490% for the storage modulus in DMTA at $T = 25\,℃$ and $T = 70\,℃$, respectivley. The Halpin-Tsai model was used to predict the Young moduli of nanocomposites and good agreement with the experimental data was observed. Furthermore, the nucleation effect of the CNCs on the crystallization of PLA was observed in DSC measurements by shifts of the crystallization temperature to higher values as well as increased crystalline contents during cooling cycles. SEM micrographs showed the presence of few very fine agglomerates as small as 1-3 μm. Also, TEM images showed that most of the nanoparticles were fully dispersed into the PLA. These results confirm that the simple solution preparation method used in this work was very efficient to disperse the hydrophilic CNCs within the PLA phase. This led to the formation of a network of the CNCs within the PLA matrix and, consequently, enhanced thermal and mechanical properties of PLA, without the need of compatibilization or modification of the CNCs. The results presented in this work demonstrate that the incorporation of CNCs can be a successful way to extend the applications of PLA to the packaging and automotive industries by enhancing its thermal stability, crystallinity and mechanical properties over a wide range of temperatures, while maintaining its biobased nature.

7.5 Acknowledgments

The authors acknowledge the financial support from the Natural Sciences and Engineering Research Council of Canada (NSERC). The authors are also grateful to FPInnovations for providing the CNCs. The authors wish to thank Dr. Wadood Y. Hamad for helpful discussion.

7.6 References

[1] Klemm D, Kramer F, Moritz S, Lindstrom T, Ankerfors M, Gray D, et al. Nanocelluloses: a new family of nature-based materials. Angewandte Chemie. 2011;50(24):5438-5466.

[2] Klemm D, Heublein B, Fink HP, Bohn A. Cellulose: fascinating biopolymer and sustainable raw material. Angewandte Chemie. 2005;44(22):3358-3393.

[3] Favier V, Chanzy H, Cavaille JY. Polymer Nanocomposites Reinforced by Cellulose Whiskers. Macromolecules. 1995;28(18):6365-6367.

[4] Peresin MS, Habibi Y, Zoppe JO, Pawlak JJ, Rojas OJ. Nanofiber Composites of Polyvinyl Alcohol and Cellulose Nanocrystals: Manufacture and Characterization. Biomacromolecules. 2010;11(3):674-681.

[5] Zhang W, He X, Li C, Zhang X, Lu C, Zhang X, et al. High performance poly (vinyl alcohol)/cellulose nanocrystals nanocomposites manufactured by injection molding. Cellulose. 2014;21(1):485-494.

[6] Abitbol T, Johnstone T, Quinn TM, Gray DG. Reinforcement with cellulose nanocrystals of poly(vinyl alcohol) hydrogels prepared by cyclic freezing and thawing. Soft Matter. 2011;7(6):2373-2379.

[7] Park W-I, Kang M, Kim H-S, Jin H-J. Electrospinning of Poly(ethylene oxide) with Bacterial Cellulose Whiskers. Macromolecular Symposia. 2007;249-250(1):289-294.

[8] Siqueira G, Abdillahi H, Bras J, Dufresne A. High reinforcing capability cellulose nanocrystals extracted from Syngonanthus nitens (Capim Dourado). Cellulose. 2010;17(2):289-298.

[9] Bendahou A, Kaddami H, Dufresne A. Investigation on the effect of cellulosic nanoparticles' morphology on the properties of natural rubber based nanocomposites. European Polymer Journal. 2010;46(4):609-620.

[10] Bagheriasl D, Carreau PJ, Dubois C, Riedl B. Properties of polypropylene and polypropylene/poly(ethylene-co-vinyl alcohol) blend/CNC nanocomposites. Composites Science and Technology. 2015;117:357-363.

[11] Siqueira G, Bras J, Dufresne A. Cellulose Whiskers versus Microfibrils: Influence of the Nature of the Nanoparticle and its Surface Functionalization on the Thermal and Mechanical Properties of Nanocomposites. Biomacromolecules. 2009;10(2):425-432.

[12] Goffin AL, Raquez JM, Duquesne E, Siqueira G, Habibi Y, Dufresne A, et al. Poly(ε-caprolactone) based nanocomposites reinforced by surface-grafted cellulose nanowhiskers via extrusion processing: Morphology, rheology, and thermo-mechanical properties. Polymer. 2011;52(7):1532-1538.

[13] Goffin AL, Raquez JM, Duquesne E, Siqueira G, Habibi Y, Dufresne A, et al. From interfacial ring-opening polymerization to melt processing of cellulose nanowhisker-filled polylactide-based nanocomposites. Biomacromolecules. 2011;12(7):2456-2465.

[14] Raquez JM, Murena Y, Goffin AL, Habibi Y, Ruelle B, DeBuyl F, et al. Surface-modification of cellulose nanowhiskers and their use as nanoreinforcers into polylactide: A sustainably-integrated approach. Composites Science and Technology. 2012;72(5):544-549.

[15] Siqueira G, Bras J, Follain N, Belbekhouche S, Marais S, Dufresne A. Thermal and mechanical properties of bio-nanocomposites reinforced by Luffa cylindrica cellulose nanocrystals. Carbohydrate Polymers. 2013;91(2):711-717.

[16] Morandi G, Heath L, Thielemans W. Cellulose nanocrystals grafted with polystyrene chains through surface-initiated atom transfer radical polymerization (SI-ATRP). Langmuir : the ACS journal of surfaces and colloids. 2009;25(14):8280-8286.

[17] Kamal MR, Khoshkava V. Effect of cellulose nanocrystals (CNC) on rheological and mechanical properties and crystallization behavior of PLA/CNC nanocomposites. Carbohydr Polym. 2015;123:105-114.

[18] Frone AN, Berlioz S, Chailan JF, Panaitescu DM. Morphology and Thermal Properties of PLA-Cellulose Nanofibers Composites. Carbohydr Polym. 2013;91(1):377-384.

[19] Suryanegara L, Nakagaito AN, Yano H. The Effect of Crystallization of PLA on the Thermal and Mechanical Properties of Microfibrillated Cellulose-Reinforced PLA Composites. Compos Sci Technol. 2009;69(7-8):1187-1192.

[20] Odelius K, Höglund A, Kumar S, Hakkarainen M, Ghosh AK, Bhatnagar N, et al. Porosity and Pore Size Regulate the Degradation Product Profile of Polylactide. Biomacromolecules. 2011;12(4):1250-1258.

[21] Frone A, Berlioz S, Chailan JF, Panaitescu D, Donescu D. Cellulose Fiber-Reinforced Polylactic Acid. Polym Compos. 2011;32(6):976-985.

[22] Jonoobi M, Harun J, Mathew AP, Oksman K. Mechanical Properties of Cellulose Nanofiber (CNF) Reinforced Polylactic Acid (PLA) Prepared by Twin Screw Extrusion. Compos Sci Technol. 2010;70(12):1742-1747.

[23] Nakagaito AN, Fujimura A, Sakai T, Hama Y, Yano H. Production of Microfibrillated Cellulose (MFC)-Reinforced Polylactic Acid (PLA) Nanocomposites from Sheets Obtained by a Papermaking-Like Process. Compos Sci Technol. 2009;69(7–8):1293-1297.

[24] Sanchez-Garcia M, Lagaron J. On the use of plant cellulose nanowhiskers to enhance the barrier properties of polylactic acid. Cellulose. 2010;17(5):987-1004.

[25] Kale G, Auras R, Singh SP. Degradation of Commercial Biodegradable Packages under Real Composting and Ambient Exposure Conditions. Journal of Polymers and the Environment. 2006;14(3):317-334.

[26] Goffin AL, Habibi Y, Raquez JM, Dubois P. Polyester-grafted cellulose nanowhiskers: a new approach for tuning the microstructure of immiscible polyester blends. ACS applied materials & interfaces. 2012;4(7):3364-3371.

[27] Bitinis N, Verdejo R, Bras J, Fortunati E, Kenny JM, Torre L, et al. Poly(lactic acid)/natural rubber/cellulose nanocrystal bionanocomposites part I. Processing and morphology. Carbohydr Polym. 2013;96(2):611-620.

[28] Bitinis N, Fortunati E, Verdejo R, Bras J, Kenny JM, Torre L, et al. Poly(lactic acid)/natural rubber/cellulose nanocrystal bionanocomposites. Part II: properties evaluation. Carbohydr Polym. 2013;96(2):621-627.

[29] Pei A, Zhou Q, Berglund LA. Functionalized cellulose nanocrystals as biobased nucleation agents in poly(l-lactide) (PLLA) – Crystallization and mechanical property effects. Composites Science and Technology. 2010;70(5):815-821.

[30] Fortunati E, Luzi F, Puglia D, Petrucci R, Kenny JM, Torre L. Processing of PLA nanocomposites with cellulose nanocrystals extracted from Posidonia oceanica waste: Innovative reuse of coastal plant. Industrial Crops and Products. 2015;67:439-447.

[31] Arias A, Heuzey M-C, Huneault M, Ausias G, Bendahou A. Enhanced dispersion of cellulose nanocrystals in melt-processed polylactide-based nanocomposites. Cellulose. 2015;22(1):483-498.

[32] Fortunati E, Peltzer M, Armentano I, Torre L, Jiménez A, Kenny JM. Effects of modified cellulose nanocrystals on the barrier and migration properties of PLA nano-biocomposites. Carbohydrate Polymers. 2012;90(2):948-956.

[33] Abbasi S, Carreau PJ, Derdouri A, Moan M. Rheological properties and percolation in suspensions of multiwalled carbon nanotubes in polycarbonate. Rheologica Acta. 2009;48(9):943-959.

[34] Du F, Scogna RC, Zhou W, Brand S, Fischer JE, Winey KI. Nanotube Networks in Polymer Nanocomposites: Rheology and Electrical Conductivity. Macromolecules. 2004;37(24):9048-9055.

[35] Ghanbari A, Heuzey MC, Carreau PJ, Ton-That MT. A novel approach to control thermal degradation of PET/organoclay nanocomposites and improve clay exfoliation. Polymer. 2013;54(4):1361-1369.

[36] Habibi Y, Goffin A-L, Schiltz N, Duquesne E, Dubois P, Dufresne A. Bionanocomposites based on poly(ε-caprolactone)-grafted cellulose nanocrystals by ring-opening polymerization. Journal of Materials Chemistry. 2008;18(41):5002-5010.

[37] Junior de Menezes A, Siqueira G, Curvelo AAS, Dufresne A. Extrusion and characterization of functionalized cellulose whiskers reinforced polyethylene nanocomposites. Polymer. 2009;50(19):4552-4563.

[38] Kim T-W, Lee S-Y, Chun S-J, Doh G-H, Paik K-H. Effect of silane coupling on the fundamental properties of wood flour reinforced polypropylene composites. Journal of Composite Materials. 2011;45(15):1595-1605.

[39] Gómez-del Río T, Poza P, Rodríguez J, García-Gutiérrez MC, Hernández JJ, Ezquerra TA. Influence of Single-Walled Carbon Nanotubes on the Effective Elastic Constants of Poly(ethylene terephthalate). Compos Sci Technol. 2010;70(2):284-290.

[40] Coleman JN, Khan U, Blau WJ, Gun'ko YK. Small but strong: A review of the mechanical properties of carbon nanotube–polymer composites. Carbon. 2006;44(9):1624-1652.

[41] Ambrosio-Martín J, Fabra MJ, Lopez-Rubio A, Lagaron JM. Melt polycondensation to improve the dispersion of bacterial cellulose into polylactide via melt compounding: enhanced barrier and mechanical properties. Cellulose. 2015;22(2):1201-1226.

CHAPTER 8 GENERAL DISCUSSION

The first problem we encountered to do this research was to get the appropriate information from the literature. At that time, there were several nomenclatures for CNCs. Cellulose whisker (CW), cellulose nano whisker (CNW), nanocrystalline cellulose (NCC), microcrystalline cellulose (MCC) are all referred to as the crystalline parts of cellulose chains. In most of the cases, CNCs are extracted from different cellulose sources in laboratories, resulting in different aspect ratios from ca. 2 to ca. 170. Therefore, the comparison of the efficiency of different compatibilization treatments reported is difficult.

One of the biggest challenges in preparing polymer-CNC nanocomposites originates from the fact that commonly used polymers, such as polypropylene, polyethylene, polystyrene, polyethylene terephthalate and biopolymers such as polylactide are hydrophobic whereas CNCs are strongly hydrophilic. Therefore, a poor compatibility between these polymers with unmodified CNCs systems usually results in poor dispersion and no property enhancement. Thus, the challenge is producing polymer nanocomposites loaded with CNCs at low concentration with enhanced mechanical properties. Due to the high hydrophilicity nature of CNCs and strong inter-particle interactions, CNCs form agglomerates, as large as few tens of microns, when they are introduced into hydrophobic matrices. Consequently, obtaining enhanced mechanical properties of the resultant nanocomposites requires surface modification of CNCs or use of a compatibilizer. Another point that is important in case of incorporation of CNCs into polymers is to verify their interfacial tension at the temperature of melt compounding. Since, the surface energy of CNCs decreases at high temperatures and the interfacial tension between polymer and CNCs also decreases, the chance of compatibility increases.

With surface modification of CNCs, stable suspensions in non polar solvents such as toluene and cyclohexane can be obtained but the mechanical properties of the resultant nanocomposites may remain unchanged or even reduced [33, 39, 53]. The possible reasons could be either desulfonation of sulfonate groups during the processing conditions or a thermal degradation of the modified CNCs during the nanocomposite preparation [54]. Another explanation is that when the CNCs are modified with a surfactant or by grafting, a hydrophobic tail will be added to the surface of CNCs, which makes them partially or completely hydrophobic, depending on the substitution ratio. These types of modification are conducted mostly in aqueous suspension of

CNCs, while for the addition to polymers they should be dried. Upon drying, CNCs stack together and form agglomerates. Then in the final step when they are introduced into polymers in molten state re-dispersion down to the individual particles may not happen if the degree of substitution is low or the interfacial tension between the modified CNC and the matrix is still high. Moreover, sometimes re-dispersion occurs, lack of strong physical entanglements between polymer matrix chains and short-length chains grafted onto the surface of CNC results in a plasticization effect that compromizes property enhancement; however, it can make the material less brittle.

Polymer chain restriction caused by CNCs can increase the rheological properties and enhance the mechanical properties of polymer-CNC systems, relative to the unfilled matrix. This can happen when one of the following occurs: strong polymer-CNC interactions, strong interconnected network of CNCs or strong physical interactions between polymer chains and CNCs. The first case usually happens only in hydrophilic polymers such as polyvinyl alcohol and polyethylene oxide due to strong hydrogen bonds. However, the hydrogen bonds may not be effective at high temperatures of the melt compounding and that may hamper CNC dispersion even in hydrophilic polymers. Therefore, in this case the best way for nanocomposite preparation remains via solution preparation in water. The second case happens in our research where a simple and novel method of preparation was employed. The third case usually is expected to happen when a functionalized polymer/copolymer is used as a compatibilizer or *in-situ* polymerization where long polymer chains can be grafted to the surface of the CNCs. The former will add a third component to the system that should be compatible with both polymer and CNCs.

Another problem arises when the use of a compatibilizer is necessary. For example, we have a defined polymer and we want to reinforce it with CNCs. By adding a third component as a compatibilizer, we may have some undesired effects caused by the compatibilizer that change the initial properties of that polymer. Plasticization, change in the clarity and toughness can be considered as such effects.

Several attempts to disperse cellulose nanocrystals in hydrophobic matrices have been reported in the literature. However, just a few could achieve a dispersed structure with improved melt and solid properties. The novel and simple preparation methods explored in this project offer feasible ways to adequately disperse CNCs into hydrophobic matrices and enhance their properties.

Moreover, our results suggest that there is no need of any modification or compatibilization when the matrix is PLA. This can be extended to all polymers that can be dissolved in dimethyl sulfoxide (DMSO) and DMF. If CNCs can be dispersed in the solvent of the desired polymer matrix by means of sonication, then there is no need of modification or compatibilization and the same procedure as described in Chapters 6 and 7 can be used to prepare nanocomposites with a dispersed structure.

Another concern in this research that may limit its applicability in large scale production is the use of DMF which is a toxic solvent. Although the results of thermal gravimetry analysis (TGA) did not show any trace of the solvent greater than 100 ppm, even this small quantity of solvent may not be acceptable for some applications. To solve this issue, DMF can be replaced with a less toxic solvent with almost the same effect such as DMSO. DMF and DMSO are both dipolar solvents and can dissolve PLA and poly(ethylene-co-vinyl alcohol). Moreover, by sonication stable CNC suspensions can be achieved. However, the problem of using DMSO is its high boiling temperature, ca. 190 °C. This will make the solvent evaporation step longer at higher temperature and more tedious. Therefore, for PLA that is sensitive to storage at high temperature, this can cause thermal degradation, which is not desirable.

One of the problems that may limit using CNC as reinforcing agent in industry is its availability. In most of the researches conducted so far, CNCs were prepared at a laboratory scale from paper, tunicin and other sources of cellulose, with low yield, less than 20 %. However, in the future if the number of companies producing CNCs increases, these particles can be easily available for use at a much lower cost. Moreover, simple melt-compounding to produce polymer-CNC nanocomposites cannot be employed in most of the cases, which is not desirable for industrial applications. This problem can be solved by masterbatch production so that it can be used thereafter for melt-compounding.

CHAPTER 9 CONCLUSIONS AND RECOMMENDATIONS

9.1 Conclusions

This research focused on the possibility to utilize cellulose nanocrystals as reinforcing agents to enhance the properties of non water-soluble polymers. To do so, polypropylene, which is one of the most commonly used polymers, and polylactide, which is the most common biopolymer that has been commercialized and found many applications, are employed as matrices. In the first phase of this research the use of CNCs in PP was studied. Due to the lack of compatibility between the two, a copolymer with polar and no polar parts was utilized to favor the dispersion of CNCs within the system. To prepare the nanocomposites two copolymer-CNC masterbatches were prepared, one via solvent casting and the other via melt compounding. Thereafter, the masterbatches were introduced into PP in molten state and melt compounded to yield the final nanocomposites. For sake of comparison uncompatibilized system and blend of PP and copolymer were also produced. The following conclusions can be drawn from the results of the first phase of this research:

1. Melt mixing of compatibilized CNCs and PP results in finer aggregates compared to the uncompatibilized CNCs.
2. Both solution and melt prepared masterbatches could increase the rheological and mechanical properties of PP.
3. The solution prepared masterbatch was more efficient to enhance the properties of PP.
4. A portion of the enhancement in mechanical properties was due to the increased crystalline content caused by the CNCs.
5. CNCs can act as nucleating agents by increasing the crystalline content and pushing the crystallization temperature to higher values.

The second phase of this research focused on the incorporation of the CNCs in PLA. To do so, a simple and novel single-step preparation method was utilized. Initially the CNCs were dispersed in DMF by means of sonication and then the PLA was added and the mixing continued until the complete dissolution of PLA. Then, the solvent was evaporated to obtain the final nanocomposites. The nanocomposites were characterized in melt and solid states to study the

effect of the CNCs on rheological behavior and mechanical performance of the PLA. The following findings are the main conclusions from this phase of the research:

1. The initial dispersion of the CNCs in DMF was preserved after solvent evaporation due to the barrier effect of PLA, therefore there is no need of CNC modification or use of a compatibilizer to achieve a dispersed structure of CNCs within PLA.
2. Dispersed CNCs can form a strong interconnected network within the PLA and this network was stronger for larger CNC concentrations.
3. The formation of such a network could significantly affect the melt behavior of the PLA so that the transition from liquid- to solid-like behavior was observed for PLA-CNC nanocomposites with 1wt% CNC and for larger concentrations.
4. A thixotropic behavior was observed for the PLA-CNC systems.
5. The rheological properties increased by the addition of CNCs up to 6 wt%, but decreased for 7 wt % CNC, mainly due to the agglomeration formation.
6. The structure in PLA-CNC nanocomposites could build up faster for larger concentrations after breaking down the structure in shear flow fields. The Brownian motion could play an important role in the structure reformation at rest after the structure break down in shear flows.
7. The storage modulus of PLA in both glassy and rubbery regions was significantly improved, especially in the rubbery region. This revealed the potentials of CNCs as reinforcing agents to enhance the mechanical properties of PLA in a wide range of temperature. Therefore, one of the drawbacks of PLA that has been limiting its applications, i.e. low modulus at high temperature, was solved by incorporating the CNCs.
8. CNC acts as nucleating agents by increasing the crystalline content and crystallization temperature of PLA to higher values.

9.2 Original Contributions

In the first phase of this research, poly(ethylene-co-vinyl alcohol) was used as a compatibilizer to favor a better dispersion and wetting of hydrophilic CNCs within the hydrophobic polypropylene (PP) matrix via two different masterbatch preparation methods, in molten and solution states.

Development of PP-CNC nanocomposites with enhanced mechanical properties at low CNC loadings using a masterbatch preparation method is an original contribution of the project.

Neat PLA exhibits slow crystallization, low heat resistance (low storage modulus at high temperature) and thermal stability. All these characteristics are drawbacks for many applications. To overcome these drawbacks, we employed CNCs to improve the mechanical and thermal properties of PLA while maintaining its unique properties such as biocompatibility, biodegradability and transparency without the use of compatibilizer or need to CNC modification, which is happening for the first time.

The formation of an interconnect network of particles plays an important role on the rheological behavior of a nanocomposite system that can reveal whether the preparation method is efficient in leading to nano dispersions. Therefore, in this research we employed rheology as a powerful tool to understand the interactions between the components of PLA-CNC bionanocomposites.

Our objective in the second phase of this research was first to develop fully biobased and biodegradable PLA-CNC nanocomposites with a dispersed structure via a simple method without the need of CNC modification or use of any compatibilizer or change in the microstructure of the CNC. To the best of our knowledge, this is the first time that this is achieved.

Moreover, to the best of our knowledge, this is the first time that the rheological behavior of polymer-CNC nanocomposites in different shear flow fields is systematically reported. Also, there is no report in the literature on transient and structure build-up tests performed on polymer-CNC systems.

9.3 Recommendations

This research provides great insights about the effect of a dispersed structure of CNCs on the properties of the polymers in both melt and solid states. However, there are some aspects that have not been explored in this research and are recommended in future studies:

1. In the first phase of this research only one copolymer to CNC ratio (equal to 3) was selected. Different ratios can be selected to optimize the results. Moreover, larger CNC concentrations can also be employed.
2. Since, in the second phase of this study it was demonstrated that without any modification or compatibilization CNCs can form a network within PLA and enhance its properties,

this idea can be employed in the case of PP or other non water-soluble polymers. To do this, initially the CNCs should be dispersed in a solvent and then the polymer should be added and by solvent casting the final composite will be obtained. The key challenge would be the choice of the solvent in which the CNCs should be dispersed by means of sonication and the polymer matrix should be dissolved. For instance, toluene can be used as the solvent; however, solvent exchange from water to acetone and from acetone to toluene may be required.

3. It would be greatly helpful to perform other mechanical tests such as heat deflection temperature (HDT) and impact to obtain more information about the solid-state properties. This will help to extend the applicability of PLA.
4. Since the CNCs act as nucleating agents, annealing should be carried out to obtain high crystallinity and enhanced synergistic effects on the mechanical properties.
5. Polymer-CNC nanocomposites show potential applications in the automotive and packaging industry. Therefore, polymer-CNC films and injection-molded products can be produced via film blowing and injection molding, respectively, and characterized regarding their physical and mechanical properties.

LIST OF REFERENCES

[1] Favier V, Chanzy H, Cavaille JY. Polymer Nanocomposites Reinforced by Cellulose Whiskers. Macromolecules. 1995;28(18):6365-6367.

[2] Klemm D, Kramer F, Moritz S, Lindstrom T, Ankerfors M, Gray D, et al. Nanocelluloses: a new family of nature-based materials. Angewandte Chemie. 2011;50(24):5438-5466.

[3] Peresin MS, Habibi Y, Zoppe JO, Pawlak JJ, Rojas OJ. Nanofiber Composites of Polyvinyl Alcohol and Cellulose Nanocrystals: Manufacture and Characterization. Biomacromolecules. 2010;11(3):674-681.

[4] Zhang W, He X, Li C, Zhang X, Lu C, Zhang X, et al. High performance poly (vinyl alcohol)/cellulose nanocrystals nanocomposites manufactured by injection molding. Cellulose. 2014;21(1):485-494.

[5] Abitbol T, Johnstone T, Quinn TM, Gray DG. Reinforcement with cellulose nanocrystals of poly(vinyl alcohol) hydrogels prepared by cyclic freezing and thawing. Soft Matter. 2011;7(6):2373-2379.

[6] Park W-I, Kang M, Kim H-S, Jin H-J. Electrospinning of Poly(ethylene oxide) with Bacterial Cellulose Whiskers. Macromolecular Symposia. 2007;249-250(1):289-294.

[7] Siqueira G, Abdillahi H, Bras J, Dufresne A. High reinforcing capability cellulose nanocrystals extracted from Syngonanthus nitens (Capim Dourado). Cellulose. 2010;17(2):289-298.

[8] Bendahou A, Kaddami H, Dufresne A. Investigation on the effect of cellulosic nanoparticles' morphology on the properties of natural rubber based nanocomposites. European Polymer Journal. 2010;46(4):609-620.

[9] Bagheriasl D, Carreau PJ, Dubois C, Riedl B. Properties of polypropylene and polypropylene/poly(ethylene-co-vinyl alcohol) blend/CNC nanocomposites. Composites Science and Technology. 2015;117:357-363.

[10] Siqueira G, Bras J, Dufresne A. Cellulose Whiskers versus Microfibrils: Influence of the Nature of the Nanoparticle and its Surface Functionalization on the Thermal and Mechanical Properties of Nanocomposites. Biomacromolecules. 2009;10(2):425-432.

[11] Goffin AL, Raquez JM, Duquesne E, Siqueira G, Habibi Y, Dufresne A, et al. Poly(ε-caprolactone) based nanocomposites reinforced by surface-grafted cellulose nanowhiskers via extrusion processing: Morphology, rheology, and thermo-mechanical properties. Polymer. 2011;52(7):1532-1538.

[12] Goffin AL, Raquez JM, Duquesne E, Siqueira G, Habibi Y, Dufresne A, et al. From interfacial ring-opening polymerization to melt processing of cellulose nanowhisker-filled polylactide-based nanocomposites. Biomacromolecules. 2011;12(7):2456-2465.

[13] Raquez JM, Murena Y, Goffin AL, Habibi Y, Ruelle B, DeBuyl F, et al. Surface-modification of cellulose nanowhiskers and their use as nanoreinforcers into polylactide: A sustainably-integrated approach. Composites Science and Technology. 2012;72(5):544-549.

[14] Siqueira G, Bras J, Follain N, Belbekhouche S, Marais S, Dufresne A. Thermal and mechanical properties of bio-nanocomposites reinforced by Luffa cylindrica cellulose nanocrystals. Carbohydrate Polymers. 2013;91(2):711-717.

[15] Morandi G, Heath L, Thielemans W. Cellulose nanocrystals grafted with polystyrene chains through surface-initiated atom transfer radical polymerization (SI-ATRP). Langmuir : the ACS journal of surfaces and colloids. 2009;25(14):8280-8286.

[16] Joshi SV, Drzal LT, Mohanty AK, Arora S. Are natural fiber composites environmentally superior to glass fiber reinforced composites? Composites Part A: Applied Science and Manufacturing. 2004;35(3):371-376.

[17] Peng BL, Dhar N, Liu HL, Tam KC. Chemistry and applications of nanocrystalline cellulose and its derivatives: A nanotechnology perspective. The Canadian Journal of Chemical Engineering. 2011;89(5):1191-1206.

[18] Hasani M, Cranston ED, Westman G, Gray DG. Cationic surface functionalization of cellulose nanocrystals. Soft Matter. 2008;4(11):2238.

[19] Zimmermann T, Bordeanu N, Strub E. Properties of nanofibrillated cellulose from different raw materials and its reinforcement potential. Carbohydrate Polymers. 2010;79(4):1086-1093.

[20] Lavoine N, Desloges I, Dufresne A, Bras J. Microfibrillated cellulose - its barrier properties and applications in cellulosic materials: a review. Carbohydr Polym. 2012;90(2):735-764.

[21] Saeidlou S, Huneault MA, Li H, Park CB. Poly(lactic acid) crystallization. Progress in Polymer Science. 2012;37(12):1657-1677.

[22] Dechy-Cabaret O, Martin-Vaca B, Bourissou D. Controlled ring-opening polymerization of lactide and glycolide. Chemical reviews. 2004;104(12):6147-6176.

[23] Garlotta D. A Literature Review of Poly(Lactic Acid). Journal of Polymers and the Environment. 2001;9(2):63-84.

[24] Malpass DB, Band E. Introduction to Industrial Polypropylene : Properties, Catalysts, Processes. Somerset, NJ, USA: John Wiley & Sons; 2012.

[25] Nakatani H, Iwakura K, Miyazaki K, Okazaki N, Terano M. Effect of chemical structure of silane coupling agent on interface adhesion properties of syndiotactic polypropylene/cellulose composite. Journal of Applied Polymer Science. 2011;119(3):1732-1741.

[26] Couturaud B, Baldo A, Mas A, Robin JJ. Improvement of the interfacial compatibility between cellulose and poly(l-lactide) films by plasma-induced grafting of l-lactide: The evaluation of the adhesive properties using a peel test. Journal of colloid and interface science. 2015;448:427-436.

[27] Belgacem MN, Bataille P, Sapieha S. Effect of corona modification on the mechanical properties of polypropylene/cellulose composites. Journal of Applied Polymer Science. 1994;53(4):379-385.

[28] Braun B, Dorgan JR. Single-Step Method for the Isolation and Surface Functionalization of Cellulosic Nanowhiskers. Biomacromolecules. 2009;10(2):334-341.

[29] Montanari S, Roumani M, Heux L, Vignon MR. Topochemistry of Carboxylated Cellulose Nanocrystals Resulting from TEMPO-Mediated Oxidation. Macromolecules. 2005;38(5):1665-1671.

[30] Salajková M, Berglund LA, Zhou Q. Hydrophobic cellulose nanocrystals modified with quaternary ammonium salts. Journal of Materials Chemistry. 2012;22(37):19798-19805.

[31] Hamad WY, Miao C. Nanocomposite biomaterials of nanocrystalline cellulose (ncc) and polylactic acid (pla). FPINNOVATIONS, Pointe-Claire, CA; 2011.

[32] Habibi Y, Goffin A-L, Schiltz N, Duquesne E, Dubois P, Dufresne A. Bionanocomposites based on poly(ε-caprolactone)-grafted cellulose nanocrystals by ring-opening polymerization. Journal of Materials Chemistry. 2008;18(41):5002-5010.

[33] Junior de Menezes A, Siqueira G, Curvelo AAS, Dufresne A. Extrusion and characterization of functionalized cellulose whiskers reinforced polyethylene nanocomposites. Polymer. 2009;50(19):4552-4563.

[34] Johnson RK. Tempo-oxidized nanocelluloses: surface modification and use as additives in cellulosic nanocomposites. Virginia Polytechnic Institute & State University, Macromolecular Science and Engineering, 2010.

[35] Kim T-W, Lee S-Y, Chun S-J, Doh G-H, Paik K-H. Effect of silane coupling on the fundamental properties of wood flour reinforced polypropylene composites. Journal of Composite Materials. 2011;45(15):1595-1605.

[36] Kargarzadeh H, M. Sheltami R, Ahmad I, Abdullah I, Dufresne A. Cellulose nanocrystal: A promising toughening agent for unsaturated polyester nanocomposite. Polymer. 2015;56:346-357.

[37] Lu J, Askeland P, Drzal LT. Surface modification of microfibrillated cellulose for epoxy composite applications. Polymer. 2008;49(5):1285-1296.

[38] Hamad WY, Miao C. Nanocomposite biomaterials of nanocrystalline cellulose (NCC) and polylactic acid (PLA). FPInnovations, Pointe-Claire, Quebec (CA); 2014.

[39] Ljungberg N, Bonini C, Bortolussi F, Boisson C, Heux L, Cavaille JY. New Nanocomposite Materials Reinforced with Cellulose Whiskers in Atactic Polypropylene: Effect of Surface and Dispersion Characteristics. Biomacromolecules. 2005;6(5):2732-2739.

[40] Ljungberg N, Cavaillé JY, Heux L. Nanocomposites of isotactic polypropylene reinforced with rod-like cellulose whiskers. Polymer. 2006;47(18):6285-6292.

[41] Bahar E, Ucar N, Onen A, Wang Y, Oksüz M, Ayaz O, et al. Thermal and mechanical properties of polypropylene nanocomposite materials reinforced with cellulose nano whiskers. Journal of Applied Polymer Science. 2012;125(4):2882-2889.

[42] Hassanabadi HM, Alemdar A, Rodrigue D. Polypropylene reinforced with nanocrystalline cellulose: Coupling agent optimization. Journal of Applied Polymer Science. 2015;132(34):n/a-n/a.

[43] Khoshkava V, Kamal MR. Effect of cellulose nanocrystals (CNC) particle morphology on dispersion and rheological and mechanical properties of polypropylene/CNC nanocomposites. ACS applied materials & interfaces. 2014;6(11):8146-8157.

[44] Kamal MR, Khoshkava V. Effect of cellulose nanocrystals (CNC) on rheological and mechanical properties and crystallization behavior of PLA/CNC nanocomposites. Carbohydr Polym. 2015;123:105-114.

[45] Pei A, Zhou Q, Berglund LA. Functionalized cellulose nanocrystals as biobased nucleation agents in poly(l-lactide) (PLLA) – Crystallization and mechanical property effects. Composites Science and Technology. 2010;70(5):815-821.

[46] Fortunati E, Luzi F, Puglia D, Petrucci R, Kenny JM, Torre L. Processing of PLA nanocomposites with cellulose nanocrystals extracted from Posidonia oceanica waste: Innovative reuse of coastal plant. Industrial Crops and Products. 2015;67:439-447.

[47] Arias A, Heuzey M-C, Huneault M, Ausias G, Bendahou A. Enhanced dispersion of cellulose nanocrystals in melt-processed polylactide-based nanocomposites. Cellulose. 2015;22(1):483-498.

[48] Abbasi S, Carreau PJ, Derdouri A, Moan M. Rheological properties and percolation in suspensions of multiwalled carbon nanotubes in polycarbonate. Rheologica Acta. 2009;48(9):943-959.

[49] Hu G, Zhao C, Zhang S, Yang M, Wang Z. Low percolation thresholds of electrical conductivity and rheology in poly(ethylene terephthalate) through the networks of multi-walled carbon nanotubes. Polymer. 2006;47(1):480-488.

[50] Gupta RK, Pasanovic-Zujo V, Bhattacharya SN. Shear and extensional rheology of EVA/layered silicate-nanocomposites. Journal of Non-Newtonian Fluid Mechanics. 2005;128(2–3):116-125.

[51] Letwimolnun W, Vergnes B, Ausias G, Carreau PJ. Stress overshoots of organoclay nanocomposites in transient shear flow. Journal of Non-Newtonian Fluid Mechanics. 2007;141(2–3):167-179.

[52] Mobuchon C, Carreau P, Heuzey M-C. Effect of flow history on the structure of a non-polar polymer/clay nanocomposite model system. Rheologica Acta. 2007;46(8):1045-1056.

[53] Nair KG, Dufresne A. Crab Shell Chitin Whiskers Reinforced Natural Rubber Nanocomposites. 3. Effect of Chemical Modification of Chitin Whiskers. Biomacromolecules. 2003;4(6):1835-1842.

[54] Roman M, Winter WT. Effect of Sulfate Groups from Sulfuric Acid Hydrolysis on the Thermal Degradation Behavior of Bacterial Cellulose. Biomacromolecules. 2004;5(5):1671-1677.